AD_____

Award Number: W81XWH-09-1-0029

TITLE: Exploring the role of genetic modifiers in DNA repair and breast cancer

PRINCIPAL INVESTIGATOR: Brian D. Piening

CONTRACTING ORGANIZATION: Fred Hutchinson Cancer Research Center
Seattle, WA 96109

REPORT DATE: September 2013

TYPE OF REPORT: Annual Summary

PREPARED FOR: U.S. Army Medical Research and Materiel Command
Fort Detrick, Maryland 21702-5012

REPORT DOCUMENTATION PAGE

Form Approved
OMB No. 0704-0188

1. REPORT DATE *(DD-MM-YYYY)*	2. REPORT TYPE	3. DATES COVERED *(From - To)*
September 2013	Annual Summary	1 September 2009 - 31 August 2013

4. TITLE AND SUBTITLE
Exploring the Role of Genetic Modifiers in DNA Repair and Breast Cancer

5a. CONTRACT NUMBER

5b. GRANT NUMBER
W81XWH-09-1-0029

5c. PROGRAM ELEMENT NUMBER

6. AUTHOR(S)
Brian D. Piening

E-Mail: bpiening@fhcrc.org

5d. PROJECT NUMBER

5e. TASK NUMBER

5f. WORK UNIT NUMBER

7. PERFORMING ORGANIZATION NAME(S) AND ADDRESS(ES)
Fred Hutchinson Cancer Research Center
Seattle, WA 96109

8. PERFORMING ORGANIZATION REPORT NUMBER

9. SPONSORING / MONITORING AGENCY NAME(S) AND ADDRESS(ES)
U.S. Army Medical Research and Materiel Command
Fort Detrick, Maryland 21702-5012

10. SPONSOR/MONITOR'S ACRONYM(S)

11. SPONSOR/MONITOR'S REPORT NUMBER(S)

12. DISTRIBUTION / AVAILABILITY STATEMENT
Approved for public release; distribution is unlimited.

13. SUPPLEMENTARY NOTES

14. ABSTRACT

In this study, I have performed a genome-wide screen for gene-gene interactions which cause sensitivity to DNA damage in the yeast Saccharomyces cerevisiae in an attempt to identify genetic factors which cause predisposition to breast cancer. I have identified 13 TEL1 (ATM ortholog) interactions which cause enhanced sensitivity to the DNA damaging agent MMS. Surprisingly, many of these interactions confer a significant defect in telomere metabolism.Restoration of normal telomere lengths in the tel1 xxx double mutants results in only minor suppression of the DNA damage sensitivity, demonstrating that the sensitivity of these mutants must also involve mechanisms independent of telomere length. In support of a model for increased replication stress in the tel1 xxx double mutants, I show that depletion of dNTP pools through pre-treatment with hydroxyurea renders tel1 cells (but not wild-type) MMS-sensitive, demonstrating that under certain conditions, Tel1p does indeed play a critical role in the DDR.

15. SUBJECT TERMS
Breast cancer, DNA damage, Mutagenesis

16. SECURITY CLASSIFICATION OF:			17. LIMITATION OF ABSTRACT	18. NUMBER OF PAGES	19a. NAME OF RESPONSIBLE PERSON
a. REPORT	b. ABSTRACT	c. THIS PAGE			USAMRMC
U	U	U	UU	52	19b. TELEPHONE NUMBER *(include area code)*

Table of Contents

Page

I. INTRODUCTION

Despite prior successes in identifying individual highly-penetrant breast cancer susceptibility loci such as *BRCA1* and *BRCA2* (Miki et al., 1994; Wooster et al., 1995), these cases represent a minority of breast cancer incidence. While twin and family studies reveal a strong genetic component for risk to so-called "common" forms of breast cancer (Peto and Mack, 2000), large-scale GWAS efforts to map out this missing genetic component have been largely unsuccessful. While work is currently being undertaken to pursue exceedingly rare variants using next-generation sequencing-based approaches, an alternative hypothesis is that the genetic component underlying cancer susceptibility is due to gene-gene interactions, either due to the cumulative effect of additive interactions of perhaps many mutant alleles or due to a strong synergistic effect between a small number of alleles (Manolio et al., 2009). Due to the combinatorial problem of accounting for two or more interacting variants genome-wide, even the large sample sizes associated with current GWAS and next-gen studies are ill-suited to this approach. The goal of the completed research and training program has been to identify low-penetrant, epistatic alleles utilizing a novel, cross-species investigation of DNA repair defects in the budding yeast *S. cerevisiae.* Specifically, I have focused on the discovery and characterization of novel interactions with the yeast *ATM* ortholog *TEL1* that cause severe DNA damage sensitivity. From this I propose that mutant alleles corresponding to the interactions identified as potential risk factors for breast cancer.

II. BODY

My research and training over the funding period has followed the approved timeline detailed in the Statement of Work for this training grant. I have applied for and received a no-cost extension (Amendment P00001, 24-Aug-2012), during which I have completed and defended my dissertation. I have also completed experiments and revisions in response to the peer reviews of my *TEL1* manuscript. This work has recently been published in the journal *Genetics* (see Reportable Outcomes below as well as the Appendix). Moreover, during this time I have made significant contributions to a related study on chronic low-dose MMS treatment. This study has recently been published as well in the journal *Molecular and Cellular Biology* (also see Appendix) and I have thanked the BCRP for support in the acknowledgements for both these recent publications.

As a recap of my work during the period of funding, I have successfully:

- Completed the proposed coursework in molecular biology, genetics, and statistics (cumulative GPA 3.8).
- Assembled a world-class graduate committee with expertise in oncology and genetics (Dr. Amanda Paulovich), breast cancer genetics (Dr. Mary-Claire King), yeast genetics (Drs. Daniel Gottschling and Trisha Davis), DNA repair (Dr. Toshi Taniguchi), and statistical genetics (Dr. Pei Wang).
- Successfully completed the General Examination.

- Learned laboratory techniques in genetics that are critical to my project by contributing to a related screen for interactions with a *BRCA1* homolog (see reference in Reportable Outcomes below, as well as in the appendix).
- Authored a manuscript detailing the results of the *TEL1* (ATM ortholog) screen; this report describes a novel connection between DNA damage sensitivity and telomere defects (see Reportable Outcomes and Appendix).
- Co-authored a manuscript describing novel key differences between the cellular responses to low-dose vs. high dose DNA damage (see Reportable Outcomes and Appendix).
- Successfully defended my dissertation.
- I have accepted a postdoctoral position in the laboratory of Dr. Michael Snyder in the Genetics Department at Stanford University. The training and research conducted under Dr. Paulovich during the training period were critical to my securing this position.

Research Accomplishments to Date

In Year 1 of this grant I successfully constructed a yeast *tel1*Δ *xxx*Δ genome-wide double-deletion library that was screened for sensitivity to DNA damaging agents. From this screen, I identified 13 genetic interactions that caused enhanced sensitivity to methylmethanesulfonate (MMS) and/or ionizing radiation (IR) (Piening *et al.* 2013 Figure 1). A reference table detailing these results as well as subsequent follow-up work for each interaction is included in the Appendix (Piening *et al.* 2013, Table 2). In order to elucidate the mechanism(s) by which these interactions cause DNA damage sensitivity, I performed a series of genetic and biochemical assays measuring defects in DNA repair or metabolism. Notably from these measurements, a number of *tel1*Δ *xxx*Δ mutants exhibited significantly higher rates of MMS-induced gross chromosomal rearrangements (GCR) (Piening *et al.* 2013, Figure 7), which is measured as loss of the end of chromosome V (Chen and Kolodner, 1999). As *TEL1* and the GCR positive mutants (*RAD24, DDC1, RAD17, RAD27,* and *NUP60*) have been previously implicated in telomere maintenance, I hypothesized that the loss of genetic information at the chromosome end may be due to an inability to maintain proper telomeres. Indeed, upon examination of telomere lengths by Southern blotting, I observed that many of the *tel1*Δ *xxx*Δ interactions also display extremely shortened telomeres (Piening *et al.* 2013, Figure 3). This is a novel result, as a number of the identified genes play no known role in telomere metabolism nor do most single mutants exhibit telomere defects.

Based on the previous results linking *TEL1* interactions to telomere shortening and chromosomal rearrangements, I hypothesized that telomere shortening in these double mutants renders cells susceptible to telomere erosion and de-protection due to MMS-induced DNA damage at the telomere. Telomere erosion due to DNA damage has been described previously to occur spontaneously at low rates (Chang et al., 2007) however it has not yet been shown to be induced upon MMS treatment. Based on this hypothesis, I predicted that the inactivation of telomerase would cause MMS sensitivity but only after a period of telomere shortening. To test this prediction, I sporulated yeast cells heterozygous for a mutation in *TLC1*, a telomerase subunit. The *TLC1* and *tlc1* progeny were cultured over a period of 3 days to shorten telomeres, and cells were tested for MMS sensitivity on each day. As expected, the telomerase-deficient *tlc1* cells

exhibited a progressive increase in MMS sensitivity over the three day period while the *TLC1* cells remained MMS-resistant (Piening *et al.* 2013, Figure 2). From this I conclude that telomere shortening is a cause for MMS sensitivity in yeast.

Additionally, I predicted that if I could restore telomeres to normal lengths in my *tel1Δ xxxΔ* interaction mutants, it would suppress the MMS sensitivity of these strains. In order to test this, I transformed cells with a plasmid containing a fusion of the Est2 subunit of telomerase to the telomere end capping protein Cdc13; this construct has been shown to restore normal telomere lengths to *tel1*Δ cells (Evans and Lundblad, 1999; Tsukamoto et al., 2001). As expected, the addition of the fusion plasmid elongated telomeres in both wildtype and mutant strains (Piening *et al.* 2013, Figure 5). For a subset of interactions (*rad24Δ tel1Δ* and *rad17Δ tel1Δ*) the addition of the plasmid caused a partial suppression of MMS sensitivity (Piening *et al.* 2013, Figure 5) and suppressed the GCR rate (Piening *et al.* 2013, Figure 7). From this I conclude that telomere shortening is a cause for MMS sensitivity in *tel1Δ* interactions. However it is not the sole cause as not all interactions exhibited a suppression of MMS sensitivity (Piening *et al.* 2013, Table 2) nor was the sensitivity of the *9-1-1Δ tel1Δ* interactions completely abolished.

As prior studies have shown that a subset of genes identified in this screen are required for efficient deoxyribonucleotide (dNTP) production (Mulder et al., 2005; Traven et al., 2005; Westmoreland et al., 2004; Woolstencroft et al., 2006; Zhao et al., 2001), I hypothesized that a decrease in dNTP pools may be an additional cause for MMS sensitivity for *tel1-Δ* interactions. Supporting this, I used the common chemotherapy agent hydroxyurea (which depletes dNTP pools) to show that *tel1-Δ* cells (and not wild type) are specifically sensitive to MMS after pretreatment with hydroxyurea (Piening *et al.* 2013, Figure 8). In total, I demonstrate that *tel1-Δ* cells are rendered sensitive to MMS by increased replication stress or exacerbation of the short telomere phenotype. As such, human orthologs for the yeast genes identified here represent potential breast cancer risk susceptibility genes.

III. KEY RESEARCH ACCOMPLISHMENTS

- I have performed the first ever genome-wide damage sensitivity screen for interactions with the *TEL1* gene (ortholog of the human tumor suppressor gene *ATM*).
- I have identified 13 novel genetic interactions with *tel1Δ* that cause enhanced sensitivity to MMS and/or IR.
- I have shown that many of the *tel1Δ* interactions confer novel genomic defects; 11 of the 13 exhibit short telomeres and 5 of the 13 exhibit increased genome instability (GCR).
- For a subset of these interactions, the DNA damage sensitivity and genome instability can be suppressed by elongating telomeres through bypass of the *TEL1* pathway.
- While a *tel1-Δ* single-mutant strain is relatively insensitive to MMS, the prior depletion of dNTPs through pretreatment with hydroxyurea renders *tel1-Δ* cells (and not wild type) MMS-sensitive.

- By tracking DNA damage sensitivity and telomere lengths following the inactivation of telomerase, I show that yeast cells exhibit progressive and dose-dependent MMS sensitivity as telomeres shorten.

IV. REPORTABLE OUTCOMES

- **B.D. Piening**, D. Huang and A.G. Paulovich. Novel Connections Between DNA Replication, Telomere Homeostasis, and the DNA Damage Response Revealed by a Genome-Wide Screen for *TEL1/ATM* Interactions in *Saccharomyces cerevisiae*. Genetics 193 (2013) 1117-33.
- D. Huang, **B.D. Piening**, and A.G. Paulovich. The Preference for Error-Free or Error-Prone Postreplication Repair in *Saccharomyces cerevisiae* Exposed to Low-Dose Methyl Methanesulfonate Is Cell Cycle Dependent. Molecular and Cellular Biology 33 (2013) 1515-27.
- **B.D. Piening**, D. Huang, H.M. Hu, U. Voytovich, A. Murakami-Sekimata, S. Wang, P. Wang and A.G. Paulovich. A cross-species approach for the discovery of genetic interactions in the DNA damage response and breast cancer (Poster). 2011 Era of Hope Conference, Orlando FL.
- **B.D. Piening**, D. Huang, H.M. Hu, S. Wang, A. Murakami-Sekimata, P. Wang and A.G. Paulovich. A cross-species approach for the discovery of genetic interactions in the DNA damage response (Platform talk). 2010 Environmental Mutagen Society Annual Meeting, Fort Worth TX.
- Murakami-Sekimata, D. Huang, **B.D. Piening**, C. Bangur and A.G. Paulovich. The *Saccharomyces cerevisiae RAD9, RAD17* and *RAD24* genes are required for suppression of mutagenic post-replicative repair during chronic DNA damage. DNA Repair (Amst) 9 (2010) 824-834.
- **B.D. Piening**, D. Huang, A. Murakami-Sekimata, C. Bangur, A.G. Paulovich. The *Saccharomyces cerevisiae RAD9* gene is required for suppression of mutagenic translesion synthesis during chronic DNA damage (Poster). 2010 Yeast Genetics and Molecular Biology Meeting. July 2010, Vancouver BC Canada.
- Ph.D. earned in Molecular and Cellular Biology, University of Washington, 2013.
- Employment as a Postdoctoral Research Associate in the laboratory of Dr. Michael Snyder, Department of Genetics, Stanford University (May 2013).

V. CONCLUSION

Genome-wide screening for interactions with the budding yeast *ATM* ortholog reveals multiple interactions that cause enhanced sensitivity to DNA damage. Many of these mutants cause little or no DNA damage sensitivity on their own, which highlights the utility of this approach for identifying novel potential tumor suppressor genes. The striking fact that many of these interactions also confer telomere defects and that MMS resistance can be restored by bypassing Tel1's role in telomere metabolism indicates that alleles associated with shortened telomeres may contribute to tumorigenesis.

VI. REFERENCES

Chang, M., Arneric, M., and Lingner, J. (2007). Telomerase repeat addition processivity is increased at critically short telomeres in a Tel1-dependent manner in Saccharomyces cerevisiae. Genes Dev *21*, 2485-2494.

Chen, C., and Kolodner, R.D. (1999). Gross chromosomal rearrangements in Saccharomyces cerevisiae replication and recombination defective mutants. Nat Genet *23*, 81-85.

Evans, S.K., and Lundblad, V. (1999). Est1 and Cdc13 as comediators of telomerase access. Science *286*, 117-120.

Manolio, T.A., Collins, F.S., Cox, N.J., Goldstein, D.B., Hindorff, L.A., Hunter, D.J., McCarthy, M.I., Ramos, E.M., Cardon, L.R., Chakravarti, A.*, et al.* (2009). Finding the missing heritability of complex diseases. Nature *461*, 747-753.

Miki, Y., Swensen, J., Shattuck-Eidens, D., Futreal, P.A., Harshman, K., Tavtigian, S., Liu, Q., Cochran, C., Bennett, L.M., Ding, W.*, et al.* (1994). A strong candidate for the breast and ovarian cancer susceptibility gene BRCA1. Science *266*, 66-71.

Mulder, K.W., Winkler, G.S., and Timmers, H.T. (2005). DNA damage and replication stress induced transcription of RNR genes is dependent on the Ccr4-Not complex. Nucleic Acids Res *33*, 6384-6392.

Peto, J., and Mack, T.M. (2000). High constant incidence in twins and other relatives of women with breast cancer. Nat Genet *26*, 411-414.

Traven, A., Hammet, A., Tenis, N., Denis, C.L., and Heierhorst, J. (2005). Ccr4-not complex mRNA deadenylase activity contributes to DNA damage responses in Saccharomyces cerevisiae. Genetics *169*, 65-75.

Tsukamoto, Y., Taggart, A.K., and Zakian, V.A. (2001). The role of the Mre11-Rad50-Xrs2 complex in telomerase- mediated lengthening of Saccharomyces cerevisiae telomeres. Curr Biol *11*, 1328-1335.

Westmoreland, T.J., Marks, J.R., Olson, J.A., Jr., Thompson, E.M., Resnick, M.A., and Bennett, C.B. (2004). Cell cycle progression in G1 and S phases is CCR4 dependent following ionizing radiation or replication stress in Saccharomyces cerevisiae. Eukaryot Cell *3*, 430-446.

Woolstencroft, R.N., Beilharz, T.H., Cook, M.A., Preiss, T., Durocher, D., and Tyers, M. (2006). Ccr4 contributes to tolerance of replication stress through control of CRT1 mRNA poly(A) tail length. J Cell Sci *119*, 5178-5192.

Wooster, R., Bignell, G., Lancaster, J., Swift, S., Seal, S., Mangion, J., Collins, N., Gregory, S., Gumbs, C., and Micklem, G. (1995). Identification of the breast cancer susceptibility gene BRCA2. Nature *378*, 789-792.

Zhao, X., Chabes, A., Domkin, V., Thelander, L., and Rothstein, R. (2001). The ribonucleotide reductase inhibitor Sml1 is a new target of the Mec1/Rad53 kinase cascade during growth and in response to DNA damage. EMBO J *20*, 3544-3553.

Novel Connections Between DNA Replication, Telomere Homeostasis, and the DNA Damage Response Revealed by a Genome-Wide Screen for *TEL1/ATM* Interactions in *Saccharomyces cerevisiae*

Brian D. Piening,*,† Dongqing Huang,* and Amanda G. Paulovich*,[1]
*Fred Hutchinson Cancer Research Center, Seattle, Washington 98109, and †Molecular and Cellular Biology Program, University of Washington, Seattle, Washington 98195

ABSTRACT Tel1 is the budding yeast ortholog of the mammalian tumor suppressor and DNA damage response (DDR) kinase ATM. However, *tel1-Δ* cells, unlike *ATM*-deficient cells, do not exhibit sensitivity to DNA-damaging agents, but do display shortened (but stably maintained) telomere lengths. Neither the extent to which Tel1p functions in the DDR nor the mechanism by which Tel1 contributes to telomere metabolism is well understood. To address the first question, we present the results from a comprehensive genome-wide screen for genetic interactions with *tel1-Δ* that cause sensitivity to methyl methanesulfonate (MMS) and/or ionizing radiation, along with follow-up characterizations of the 13 interactions yielded by this screen. Surprisingly, many of the *tel1-Δ* interactions that confer DNA damage sensitivity also exacerbate the short telomere phenotype, suggesting a connection between these two phenomena. Restoration of normal telomere length in the *tel1-Δ xxx-Δ* mutants results in only minor suppression of the DNA damage sensitivity, demonstrating that the sensitivity of these mutants must also involve mechanisms independent of telomere length. In support of a model for increased replication stress in the *tel1-Δ xxx-Δ* mutants, we show that depletion of dNTP pools through pretreatment with hydroxyurea renders *tel1-Δ* cells (but not wild type) MMS-sensitive, demonstrating that, under certain conditions, Tel1p does indeed play a critical role in the DDR.

THE ATM tumor suppressor kinase is a major signaling component of the DNA damage response (DDR) pathway, and patients with homozygous *ATM* mutations are afflicted with the cancer-prone disorder ataxia telangiectasia (AT) (Savitsky *et al.* 1995; Shiloh 2003). *ATM*-deficient cell lines are sensitive to DNA damage, exhibit pronounced checkpoint and double-strand break (DSB) repair defects (Painter and Young 1980; Kastan *et al.* 1992; Kuhne *et al.* 2004), and exhibit significantly reduced phosphorylation levels of DDR targets (Canman *et al.* 1998). Cells from AT patients exhibit accelerated telomere shortening (Metcalfe *et al.* 1996), and ATM is thought to play a role in telomere length regulation through interactions with telomere binding proteins (Wu *et al.* 2007).

doi: 10.1534/genetics.113.149849
Manuscript received September 20, 2012; accepted for publication January 29, 2013
Supporting information is available online at http://www.genetics.org/lookup/suppl/doi:10.1534/genetics.113.149849/-/DC1.
[1]Corresponding author: Fred Hutchinson Cancer Research Center, 1100 Fairview Ave. N., P.O. Box 19024, Seattle, WA 98109-1024. E-mail: apaulovi@fhcrc.org

The *Saccharomyces cerevisiae* ortholog for mammalian *ATM* is *TEL1* (Greenwell *et al.* 1995; Morrow *et al.* 1995; Mallory and Petes 2000). Tel1p is recruited to DSBs via an interaction with the Mre11-Rad50-Xrs2 (MRX; MRN in mammals) DNA-binding complex (Nakada *et al.* 2003), and Tel1 both facilitates efficient end resection through an unknown mechanism and participates in phosphorylation of downstream DDR substrates (Mantiero *et al.* 2007). Following DSB resection, the related kinase Mec1 [ATR in mammals (Cimprich *et al.* 1996)] recognizes RPA-coated, single-strand DNA (ssDNA) at ssDNA–double-strand DNA (dsDNA) junctions via an interaction with Ddc2, and the DNA damage checkpoint is activated (Paciotti *et al.* 2000). The distinct sensing of double-strand and single-strand damaged DNA structures by Tel1p and Mec1p bears a striking resemblance to the different roles of their ATM and ATR counterparts in mammalian cells (Zou and Elledge 2003; Lee and Paull 2007). However, while the loss of *MEC1* results in severe sensitivity to DNA-damaging agents (Weinert *et al.* 1994), Tel1p is not functionally required for checkpoint activation

in response to intrachromosomal DSBs, and the loss of *TEL1* does not significantly sensitize cells to DNA-damaging agents (Greenwell *et al.* 1995; Morrow *et al.* 1995). Despite this, a *mec1 tel1* double mutant is more sensitive to DNA damage than the *mec1* single mutant. These results demonstrate that, although *MEC1* plays the predominant role at intrachromosomal DSBs, *TEL1* does play some role in response to DNA damage in a *mec1* background (Morrow *et al.* 1995).

While Mec1p appears to be the primary responder to DNA damage (with Tel1p functioning in a back-up role), the respective roles of Mec1p and Tel1p are reversed at telomeres. In *S. cerevisiae*, the telomerase enzyme preferentially associates with short telomeres for elongation through an interaction with Cdc13, and this preferential association is dependent on *TEL1* and the MRX complex (Sabourin *et al.* 2007). MRX recruits Tel1p to DNA ends (Fukunaga *et al.* 2011), at which Tel1p phosphorylates one or more substrates to facilitate telomerase recruitment by Cdc13 via an as-yet poorly understood mechanism (Gao *et al.* 2010; Martina *et al.* 2012). *tel1* mutant cells exhibit a decreased frequency of telomere elongation events and decreased telomerase processivity at telomeres (Arneric and Lingner 2007; Chang *et al.* 2007) that leads to progressive telomere shortening (Greenwell *et al.* 1995; Mallory and Petes 2000). Telomeres in *tel1* cells are shortened but are stably maintained; this depends on *MEC1* (Ritchie *et al.* 1999). Telomere erosion in a *mec1 tel1* mutant leads to aneuploidy, senescence, and cell death (Craven *et al.* 2002; Vernon *et al.* 2008; McCulley and Petes 2010). Despite the requirement for *MEC1* in telomere homeostasis in the absence of *TEL1*, Mec1p is not detected at telomeres in wild-type or *tel1-Δ* cells, and the specific role that Mec1p plays in facilitating telomere maintenance in the absence of *TEL1* is not yet understood (McGee *et al.* 2010).

For Tel1p's role in both the DDR and telomere metabolism, significant questions remain. While the kinase was once thought to be functionally redundant with Mec1p in the DDR, recent studies have identified distinct Mec1-independent roles for Tel1p in checkpoint signaling (Mantiero *et al.* 2007), replication fork stability (Doksani *et al.* 2009), and the suppression of genome rearrangements (Lee *et al.* 2008). None of the mechanisms underlying these roles are well understood. At telomeres, the straightforward model consisting of Tel1p phosphorylation of Cdc13 leading to a conformational change that allows for recruitment of the Est1 subunit of telomerase has recently given way to a model of more complex interactions potentially involving multiple kinases, rates of telomere end resection, and other, possibly novel intermediates (Gao *et al.* 2010; Martina *et al.* 2012; Wu *et al.* 2013). Moreover, the mechanism(s) by which MRX and Tel1 are targeted to short telomeres is poorly understood but likely involves constituents of the shelterin complex (Marcand *et al.* 1997; Teixeira *et al.* 2004).

Despite recent characterizations of Mec1-independent roles for Tel1p in the DDR, these roles are apparently either nonessential, infrequently utilized, or redundant with other pathways as the fact remains that the loss of *TEL1* alone does not confer sensitivity to DNA-damaging agents. To comprehensively characterize the contexts by which Tel1p fits into the DNA damage response, we performed genome-wide screens for *TEL1* genetic interactions that cause sensitivity to two different genotoxic agents, methyl methanesulfonate (MMS) and ionizing radiation (IR). From these screens, we have identified a diverse set of mutant backgrounds for which *TEL1* is required for survival upon exposure to DNA damage. We report that, despite the diversity of *tel1-Δ* interactions identified here, most share an additional common phenotype of an exacerbated telomere defect.

Materials and Methods

Media and growth conditions

Yeast-extract-peptone-dextrose (YEPD) and dropout media have been previously described (Paulovich *et al.* 1998). MMS and hydroxyurea (HU) were purchased from Sigma. YEPD and synthetic plates containing MMS were freshly prepared ~15 hr prior to use.

Yeast strains and plasmids

S. cerevisiae strains used in this study are listed in Table 1. Strain BY4741 and the haploid yeast knockout collection were purchased from Open Biosystems. Plasmid p4339 and strain Y7092 were gifts from Charles Boone and Brenda Andrews. Strain SLY60 was a gift from Sang Eun Lee; strain UCC3508 and plasmid pRS313-Y′ were a gift from Daniel Gottschling, and plasmid pVL1107 was a gift from Vicki Lundblad. All gene disruptions were achieved by homologous recombination at their chromosomal loci by standard polymerase chain reaction (PCR)-based methods (Brachmann *et al.* 1998). Briefly, a deletion cassette with a 0.5-kb region flanking the target ORF was amplified by PCR from the corresponding *xxx*::*kanMX* strain of the deletion array (Open Biosystems) and transformed into the target strain for gene knockout. The primers used in the gene disruptions were designed using 20- to 23-bp sequences that are 0.5 kb upstream and downstream of the target gene. A list of primer sequences for all knockouts used in this study is available upon request from the authors.

tel1-Δ double-deletion library construction and screening

The synthetic genetic array (SGA) approach was used to construct a *tel1-Δ* double-deletion library following the protocol described in Tong and Boone (2006). Library replication was performed using floating-pin manual replicators (VP Scientific). For the IR screen, the library was pin-replicated onto fresh YEPD plates and exposed to gamma irradiation using a Mark II ^{137}Cs irradiator (JL Shepherd & Associates) operated at varying dose rates. Plates were analyzed by manual inspection at 24 and 36 hr following IR. For the MMS screen, the library was pin-replicated onto plates

Table 1 *S. cerevisiae* strains

Strain	Genotype	Source
BY4741	*MATa his3Δ1 leu2Δ0 met15Δ0 ura3Δ0*	Open Biosystems
Y7092	MATα *can1Δ::STE2pr-Sp_his5 lyp1Δ his3Δ1 leu2delta0 ura3Δ0 met15Δ0*	Tong and Boone (2006)
UCC3508	*MATa/MATα ura3-52/ura3-52 lys2-801/lys2-801 ade2-101/ade2-101 his3-Δ200/his3-Δ200 trp1-Δ1/TRP1 leu2-Δ1/leu2-Δ1 adh4::URA3-TEL/adh4::URA3-TEL DIA5-1/DIA5-1 ppr1::HIS3/ppr1::LYS2 TLC1/tlc1:LEU2*	Singer *et al*. (1998)
SLY60	*MATΔ3′:intron:ura3Δ5′ hoΔ hmlΔ:ADE1 hmrΔ:ADE1 ade1-100 leu2-3,112 lys5 trp1:hisG ura3Δ3′:intron:HOcs ade3:GAL:HO*	Lee *et al.* (2008)
yBP1020-22	*MATα can1Δ::STE2pr-Sp_his5 lyp1Δ his3Δ1 leu2delta0 ura3Δ0 met15Δ0 tel1::natMX*	This study
yBP1406-08	*MATa his3Δ1 leu2Δ0 met15Δ0 ura3Δ0 hxt3::URA3*	This study
yBP1416-18	*MATΔ3′:intron:ura3Δ5′ hoΔ hmlΔ:ADE1 hmrΔ:ADE1 ade1-100 leu2-3,112 lys5 trp1:hisG ura3Δ3′:intron:HOcs ade3:GAL:HO tel1:natMX*	This study
yBP1423	*MATa his3Δ1 leu2Δ0 met15Δ0 ura3Δ0 hxt3::URA3 tel1::natMX*	This study
yBP1490-91	*MATa his3Δ1 leu2Δ0 met15Δ0 ura3Δ0 hxt3::URA3 pop2::kanMX*	This study
yBP1502-04	*MATa his3Δ1 leu2Δ0 met15Δ0 ura3Δ0 hxt3::URA3 sap30::kanMX*	This study
yBP1505-07	*MATΔ3′:intron:ura3Δ5′ hoΔ hmlΔ:ADE1 hmrΔ:ADE1 ade1-100 leu2-3,112 lys5 trp1:hisG ura3Δ3′:intron:HOcs ade3:GAL:HO tel1::natMX rad17::kanMX*	This study
yBP1508-10	*MATΔ3′:intron:ura3Δ5′ hoΔ hmlΔ:ADE1 hmrΔ:ADE1 ade1-100 leu2-3,112 lys5 trp1:hisG ura3Δ3′:intron:HOcs ade3:GAL:HO tel1::natMX ddc1::kanMX*	This study
yBP1511-13	*MATΔ3′:intron:ura3Δ5′ hoΔ hmlΔ:ADE1 hmrΔ:ADE1 ade1-100 leu2-3,112 lys5 trp1:hisG ura3Δ3′:intron:HOcs ade3:GAL:HO tel1::natMX nup60::kanMX*	This study
yBP1517-19	*MATΔ3′:intron:ura3Δ5′ hoΔ hmlΔ:ADE1 hmrΔ:ADE1 ade1-100 leu2-3,112 lys5 trp1:hisG ura3Δ3′:intron:HOcs ade3:GAL:HO tel1::natMX nup133::kanMX*	This study
yBP1520-21	*MATΔ3′:intron:ura3Δ5′ hoΔ hmlΔ:ADE1 hmrΔ:ADE1 ade1-100 leu2-3,112 lys5 trp1:hisG ura3Δ3′:intron:HOcs ade3:GAL:HO tel1::natMX lsm7::kanMX*	This study
yBP1524-26	*MATΔ3′:intron:ura3Δ5′ hoΔ hmlΔ:ADE1 hmrΔ:ADE1 ade1-100 leu2-3,112 lys5 trp1:hisG ura3Δ3′:intron:HOcs ade3:GAL:HO tel1::natMX sap30::kanMX*	This study
yBP1527-29	*MATΔ3′:intron:ura3Δ5′ hoΔ hmlΔ:ADE1 hmrΔ:ADE1 ade1-100 leu2-3,112 lys5 trp1:hisG ura3Δ3′:intron:HOcs ade3:GAL:HO tel1::natMX hda3::kanMX*	This study
yBP1550-52	*MATa his3Δ1 leu2Δ0 met15Δ0 ura3Δ0 hxt3::URA3 rad17::kanMX*	This study
yBP1553-55	*MATa his3Δ1 leu2Δ0 met15Δ0 ura3Δ0 hxt3::URA3 nup60::kanMX*	This study
yBP1558-60	*MATa his3Δ1 leu2Δ0 met15Δ0 ura3Δ0 hxt3::URA3 tel1::natMX rad17::kanMX*	This study
yBP1564-66	*MATa his3Δ1 leu2Δ0 met15Δ0 ura3Δ0 hxt3::URA3 tel1::natMX nup60::kanMX*	This study
yBP1576-78	*MATa his3Δ1 leu2Δ0 met15Δ0 ura3Δ0 hxt3::URA3 tel1::natMX sap30::kanMX*	This study
yBP1585-87	*MATa his3Δ1 leu2Δ0 met15Δ0 ura3Δ0 hxt3::URA3 tel1::natMX hda3::kanMX*	This study
yBP1608-10	*MATa his3Δ1 leu2Δ0 met15Δ0 ura3Δ0 hxt3::URA3 nup133::kanMX*	This study
yBP1611-13	*MATa his3Δ1 leu2Δ0 met15Δ0 ura3Δ0 hxt3::URA3 tel1::natMX nup133::kanMX*	This study
yBP1622-23	*MATΔ3′:intron:ura3Δ5′ hoΔ hmlΔ:ADE1 hmrΔ:ADE1 ade1-100 leu2-3,112 lys5 trp1:hisG ura3Δ3′:intron:HOcs ade3:GAL:HO tel1::natMX pop2::kanMX*	This study
yBP1630-32	*MATa his3Δ1 leu2Δ0 met15Δ0 ura3Δ0 hxt3::URA3 rad26::kanMX*	This study
yBP1633-35	*MATa his3Δ1 leu2Δ0 met15Δ0 ura3Δ0 hxt3::URA3 tel1::natMX rad26::kanMX*	This study
yBP1636-38	*MATΔ3′:intron:ura3Δ5′ hoΔ hmlΔ:ADE1 hmrΔ:ADE1 ade1-100 leu2-3,112 lys5 trp1:hisG ura3Δ3′:intron:HOcs ade3:GAL:HO tel1::natMX rad26::kanMX*	This study
yBP1669-71	*MATa his3Δ1 leu2Δ0 met15Δ0 ura3Δ0 hxt3::URA3 ccr4::kanMX*	This study
yBP1672-74	*MATa his3Δ1 leu2Δ0 met15Δ0 ura3Δ0 hxt3::URA3 tel1::natMX ccr4::kanMX*	This study
yBP1681-83	*MATa his3Δ1 leu2Δ0 met15Δ0 ura3Δ0 hxt3::URA3 lsm7::kanMX*	This study
yBP1684-86	*MATa his3Δ1 leu2Δ0 met15Δ0 ura3Δ0 hxt3::URA3 tel1::natMX lsm7::kanMX*	This study
yBP1714-16	*MATa his3Δ1 leu2Δ0 met15Δ0 ura3Δ0 hxt3::URA3 hda3::kanMX*	This study
yBP1717-19	*MATa his3Δ1 leu2Δ0 met15Δ0 ura3Δ0 hxt3::URA3 ddc1::kanMX*	This study
yBP1720-22	*MATa his3Δ1 leu2Δ0 met15Δ0 ura3Δ0 hxt3::URA3 tel1::natMX ddc1::kanMX*	This study
yBP1738-40	*MATa his3Δ1 leu2Δ0 met15Δ0 ura3Δ0 hxt3::URA3 tel1::natMX pop2::kanMX*	This study
yBP1787-89	*MATa his3Δ1 leu2Δ0 met15Δ0 ura3Δ0 hxt3::URA3 fyv4::kanMX*	This study
yBP1790-92	*MATa his3Δ1 leu2Δ0 met15Δ0 ura3Δ0 hxt3::URA3 tel1::natMX fyv4::kanMX*	This study
yBP1793-95	*MATa his3Δ1 leu2Δ0 met15Δ0 ura3Δ0 hxt3::URA3 yku80::kanMX*	This study
yBP1796-98	*MATa his3Δ1 leu2Δ0 met15Δ0 ura3Δ0 hxt3::URA3 tel1::natMX yku80::kanMX*	This study
yBP1799-1801	*MATa his3Δ1 leu2Δ0 met15Δ0 ura3Δ0 hxt3::URA3 rad27::kanMX*	This study
yBP1802-04	*MATa his3Δ1 leu2Δ0 met15Δ0 ura3Δ0 hxt3::URA3 tel1::natMX rad27::kanMX*	This study
yBP1805-07	*MATa his3Δ1 leu2Δ0 met15Δ0 ura3Δ0 hxt3::URA3 rad24::kanMX*	This study
yBP1808-10	*MATa his3Δ1 leu2Δ0 met15Δ0 ura3Δ0 hxt3::URA3 tel1::natMX rad24::kanMX*	This study
yBP1838-40	*MATΔ3′:intron:ura3Δ5′ hoΔ hmlΔ:ADE1 hmrΔ:ADE1 ade1-100 leu2-3,112 lys5 trp1:hisG ura3Δ3′:intron:HOcs ade3:GAL:HO tel1::natMX ccr4::kanMX*	This study
yBP1841-43	*MATΔ3′:intron:ura3Δ5′ hoΔ hmlΔ:ADE1 hmrΔ:ADE1 ade1-100 leu2-3,112 lys5 trp1:hisG ura3Δ3′:intron:HOcs ade3:GAL:HO yku80::kanMX*	This study

(continued)

Table 1, *continued*

Strain	Genotype	Source
yBP1844-46	*MATΔ3′:intron:ura3Δ5′ hoΔ hmlΔ::ADE1 hmrΔ::ADE1 ade1-100 leu2-3,112 lys5 trp1:hisG ura3Δ3′:intron:HOcs ade3:GAL:HO tel1::natMX yku80::kanMX*	This study
yBP1847-49	*MATΔ3′:intron:ura3Δ5′ hoΔ hmlΔ::ADE1 hmrΔ::ADE1 ade1-100 leu2-3,112 lys5 trp1:hisG ura3Δ3′:intron:HOcs ade3:GAL:HO rad27::kanMX*	This study
yBP1850-52	*MATΔ3′:intron:ura3Δ5′ hoΔ hmlΔ::ADE1 hmrΔ::ADE1 ade1-100 leu2-3,112 lys5 trp1:hisG ura3Δ3′:intron:HOcs ade3:GAL:HO tel1::natMX rad27::kanMX*	This study
yBP1859-61	*MATΔ3′:intron:ura3Δ5′ hoΔ hmlΔ::ADE1 hmrΔ::ADE1 ade1-100 leu2-3,112 lys5 trp1:hisG ura3Δ3′:intron:HOcs ade3:GAL:HO rad24::kanMX*	This study
yBP1862-64	*MATΔ3′:intron:ura3Δ5′ hoΔ hmlΔ::ADE1 hmrΔ::ADE1 ade1-100 leu2-3,112 lys5 trp1:hisG ura3Δ3′:intron:HOcs ade3:GAL:HO tel1::natMX rad24::kanMX*	This study

containing 0.01% and 0.03% MMS, grown for 2 days at 30°, and analyzed by visual inspection.

MMS/IR spot and colony assays

For serial-dilution spot assays, log-phase cells were serially diluted in PBS and spotted onto YEPD or YEPD + MMS plates using a pin replicator. A subset of the plates was immediately irradiated using the conditions described above. Plates were incubated at 30° and analyzed by visual inspection at 24 and 36 hr.

For colony-based survival assays, three independent transformants were analyzed for each mutant, along with wild-type and *tel1-Δ* controls. Log-phase cells ($\sim 5 \times 10^7$ cells) were sonicated and counted using a Beckman-Dickinson Coulter counter. Cells were serially diluted in PBS and plated onto YEPD or YEPD + MMS plates. For analyzing radiation sensitivity, cells were spread on YEPD plates and the plates were subsequently irradiated as described above. Viability was determined by plating serial dilutions of cultures onto YEPD and scoring the number of colony-forming units (CFU) after 3–4 days at 30°. Viability was calculated as CFU/total cells. For experiments utilizing a low dose rate (0.9 Gy/min), cells were irradiated in 5-ml liquid cultures over a 7.5-hr period prior to plating on YEPD to assess colony-based survival. In experiments in which a HU pretreatment was used, cells were incubated in liquid YEPD media +/− HU (Sigma) at the indicated times. Following the incubation period, cells were washed twice with PBS, counted by Coulter counter, serially diluted, and plated onto YEPD or YEPD + MMS plates.

Gross chromosomal rearrangement and translocation assays

For the measurement of gross chromosomal rearrangement (GCR) frequencies, log-phase cells grown at 30° in YEPD were harvested, sonicated, and counted using a Coulter counter. Cells (1×10^8) were resuspended in 20 ml YEPD and YEPD + 0.003% MMS and grown at 30° overnight. At 15 hr, cells were washed in 5% Na_2SO_3, sonicated, and counted using a Coulter counter. Cells (1×10^9) were plated onto C-Arg-Ser + canavanine + 5-fluororotic acid (FOA) to measure GCR events, and serial dilutions were plated onto YEPD to measure cell viability. GCR plates were incubated for 4–5 days at 30°. Viability was calculated as CFU/total cells, and MMS-induced GCR frequencies were normalized to GCR frequencies from untreated cells.

The *HO*-inducible translocation assay was performed according to Lee *et al.* (2008). Briefly, log-phase cells were sonicated, cell number was determined using a Coulter counter (Beckman Dickinson), and serial dilutions were plated on C-Ura dropout plates containing galactose to induce *HO* expression. Strain growth and translocations in the absence of *HO*-induced DSBs were measured on synthetic complete media and C-Ura plates containing glucose.

Southern blotting

Southern blotting for telomere lengths was carried out using a previously described DNA probe targeting telomeric Y′ regions (Singer *et al.* 1998). DIG-labeled probe synthesis was carried out by PCR using the Roche DIG Probe Synthesis Kit following the manufacturer's instructions. Genomic DNA was prepared using a Yeastar genomic DNA kit (Zymo Research). Genomic DNA preparations were digested overnight with *Xho*I (Invitrogen) and separated on 1% gels. Separated DNA molecules were transferred onto nylon membranes via blot sandwich overnight in 20× SSC buffer. DNA molecules were crosslinked onto the membrane using a UV crosslinker (Fisher Scientific) at 60 mJ/cm^2, and the membrane was incubated with the Y′ telomeric DIG-labeled probe overnight. Antibody detection of the DIG probe was performed using the DIG luminescent detection kit (Roche), and blots were imaged on a ChemiDoc XRS system (Bio-Rad).

Results

Synthetic genetic array screen for interactions with tel1-Δ in response to MMS and IR

To better understand the extent of Tel1p's role in the DDR, we sought to characterize mutant backgrounds in which *TEL1* is required for survival in response to MMS and/or ionizing radiation. To achieve this, we constructed a genome-wide double-deletion library by mating a *MATα tel1-Δ* strain to the *MAT*a haploid deletion library (Winzeler *et al.* 1999) using the SGA procedure developed by Tong *et al.* (2001) and Tong and Boone (2006). The *tel1-Δ xxx-Δ*

double-deletion library was screened for survival on YEPD plates containing either 0.01% or 0.03% MMS. Plates were examined after 24 and 48 hr by visual inspection for double mutants that exhibited MMS sensitivity. Double-mutant strains exhibiting sensitivity were subsequently spotted in 10-fold serial dilutions along with the parental single-mutant strains on YEPD + MMS to confirm the interaction. As an additional verification step, we remade each single and double mutant by PCR-mediated transformation in a new BY4741 parental haploid strain. These new double-deletion mutants were then retested by serial-dilution spot assay on MMS plates and scored by visual inspection. Interactions passing this second criterion were then subjected to colony survival analyses to quantify the degree of interaction with *tel1-Δ* on MMS plates. After validation, 13 gene deletions showed enhanced sensitivity to MMS when paired with *tel1-Δ* (Figure 1A). These genes include multiple subunits of the 9-1-1 checkpoint clamp (*RAD17*, *DDC1*; ~400-fold) as well as the 9-1-1 clamp loader *RAD24* (deletion of the third subunit *mec3-Δ* grows poorly in BY4741 and could not be evaluated in the SGA screen) and members of the CCR4-NOT deadenylase complex (*CCR4* and *POP2*; 6- to 130-fold). Additional interactions exhibiting >10-fold increases in MMS sensitivity were between *TEL1* and the base excision repair endonuclease *RAD27* (~30-fold) and the histone deacetylase (HDAC) subunit *HDA3* (~30-fold). Additional genes exhibiting <10-fold interactions with *tel1-Δ* consisted of two nucleoporins (*NUP60* and *NUP133*), the nonhomologous end-joining (NHEJ) repair factor *YKU80*, a second HDAC subunit (*SAP30*), the *RAD26* ATPase, and a member of the Sm-like mRNA decay family (*LSM7*). We note that, in the initial and confirmative screens, an additional *tel1-Δ* interaction with the uncharacterized *FYV4* gene exhibited a growth defect with *tel1-Δ* as well as a >10-fold increase in MMS sensitivity. However, the *FYV4* ORF is located ~200 bp upstream of the transcription start site of the essential mediator subunit *MED6*. Transforming the *fyv4-Δ tel1-Δ* strain with a plasmid containing the *MED6* gene and its promoter completely abolished the growth defect and MMS sensitivity of this strain (data not shown), leading us to conclude that the *fyv4-Δ* gene replacement exerts an off-target effect on the essential *MED6* gene. Due to these complications, the *FYV4/MED6* candidate was removed from further consideration in this study.

As our MMS screen revealed a diverse set of interactions that cause enhanced MMS sensitivity with *tel1-Δ*, we asked whether a different set of mutants would interact with *tel1-Δ* in response to a different DNA-damaging agent, γ-irradiation. To test for genetic interactions with *tel1-Δ* in ionizing radiation, the *tel1-Δ xxx-Δ* double-deletion library was plated onto YEPD and exposed to either 200 or 400 Gy of ionizing radiation. In contrast to the MMS screen, only the 9-1-1 checkpoint genes *rad17-Δ*, *ddc1-Δ*, and *rad24-Δ* exhibited interactions with *tel1-Δ* in response to IR, and these interactions were minor (<10-fold) in comparison to the *9-1-1-Δ tel1-Δ* interactions in MMS (>100-fold) (Figure 1B). To confirm that the *tel1-Δ xxx-Δ* interactions identified in the MMS sensitivity screen were indeed not also sensitive to IR, we tested each of the 13 MMS-sensitive *tel1-Δ xxx-Δ* strains for IR sensitivity. Consistent with the screen results, only the *9-1-1-Δ tel1-Δ* double mutants exhibited enhanced IR sensitivity (Figure 1B).

As MMS is often referred to as a "radiomimetic" agent, the finding that many of the MMS interactions were not recapitulated using IR was unexpected. One possible explanation for this is that the 400 Gy of IR was delivered as a pulse over a short period of time (8 Gy/min), while for MMS treatment cells were grown continuously in 0.03% MMS. [DNA damage phenotypes can differ significantly when the agent is delivered as a pulse or chronic treatment (Murakami-Sekimata *et al.* 2010).] To test this hypothesis, three of the *tel1-Δ xxx-Δ* double mutants identified in our screen (*ccr4-Δ tel1-Δ*, *hda3-Δ tel1-Δ*, and *rad17-Δ tel1-Δ*) were examined for sensitivity to the same 400-Gy cumulative dose of IR (as in Figure 1B), but this time delivered chronically over a period of 7.5 hr (0.9 Gy/min). As seen in Figure 1C, the total IR sensitivity for wild-type and single-mutant strains was increased somewhat in the chronic exposure relative to the pulse of 400 Gy (Figure 1B); however, no additional (*i.e.*, aside from 9-1-1) interactions with *tel1-Δ* were observed, and the *rad17-Δ tel1-Δ* interaction was reduced. From this, we conclude that, unlike the MMS case, *tel1-Δ* interactions in IR are limited to mutations in the 9-1-1 pathway.

Loss of telomerase is associated with a progressive increase in MMS sensitivity

Mammalian cells with shortened telomeres exhibit increased sensitivity to DNA-damaging agents via an as-yet-unknown mechanism (Goytisolo *et al.* 2000; Wong *et al.* 2000; Gonzalez-Suarez *et al.* 2003; Nakamura *et al.* 2005; Agarwal *et al.* 2008; Soler *et al.* 2009; Drissi *et al.* 2011; Woo *et al.* 2012). Based on this precedent, we hypothesized that resistance to DNA-damaging agents in yeast would also be tightly linked to telomere length and that yeast cells would become more sensitive to DNA damage in a progressive manner as telomeres shorten. To evaluate this possibility, we employed a heterozygous diploid *tlc1* strain, which, upon sporulation into haploid progeny, exhibits progressive telomere shortening that leads to eventual replicative senescence (Singer and Gottschling 1994). After inducing sporulation, we subcultured *TLC1* and *tlc1* haploid progeny over a series of days, and each day we removed an aliquot of cells for testing of survival on YEPD or YEPD + MMS plates. In the absence of MMS, *tlc1* strains exhibited progressive telomere shortening over the 3-day period, while telomere lengths in the *TLC1* strains remained unchanged over the same period (data not shown). When tested for viability on plates containing either 0.01% or 0.03% MMS, *TLC1* strains showed minimal MMS sensitivity that was unchanged over the course of the experiment (Figure 2). In contrast, the *tlc1* mutant strains exhibited a progressive and dose-dependent

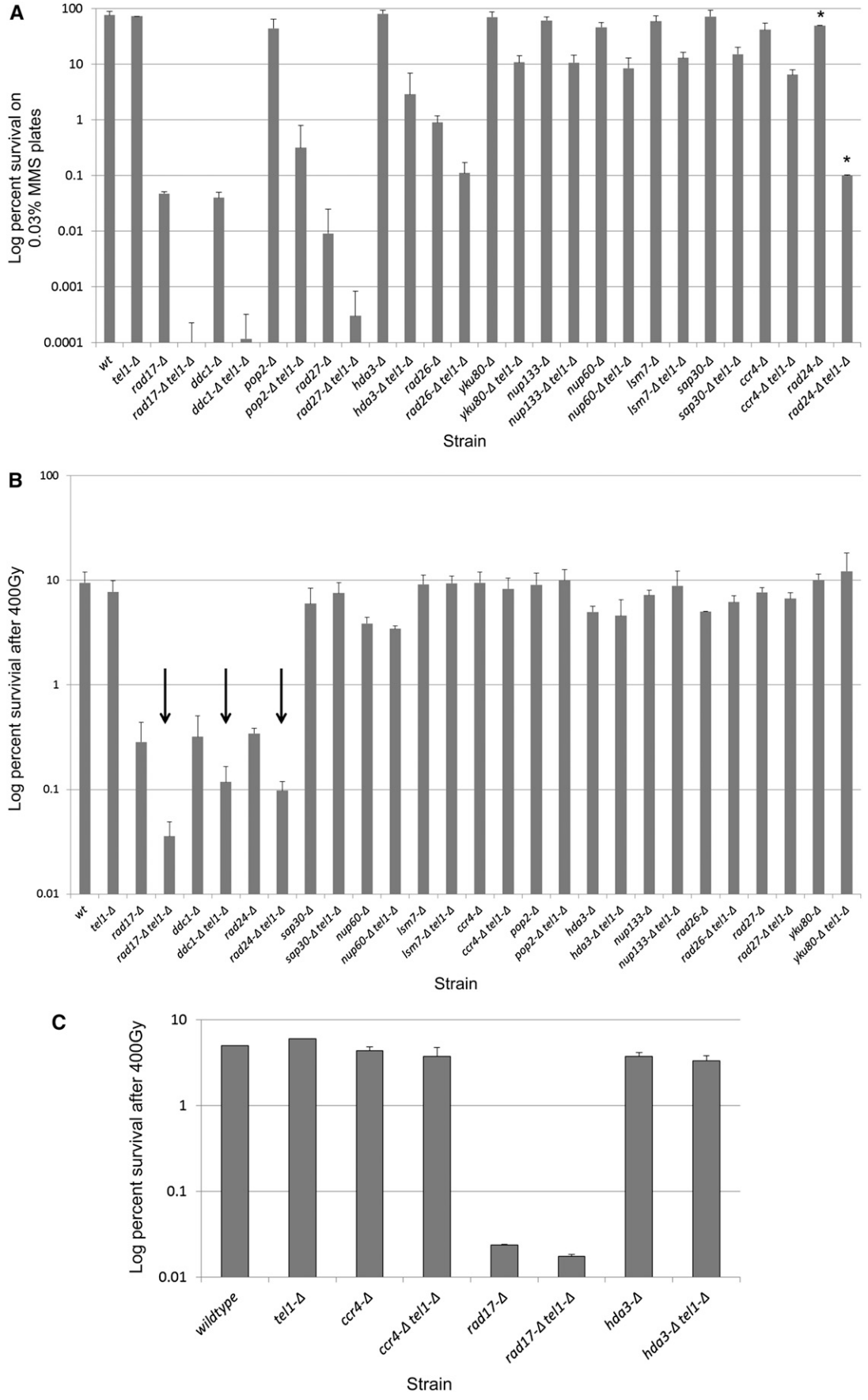
A
Log percent survival on 0.03% MMS plates
100
10
1
0.1
0.01
0.001
0.0001
*
*
wt
tel1-Δ
rad17-Δ
rad17-Δ tel1-Δ
ddc1-Δ
ddc1-Δ tel1-Δ
pop2-Δ
pop2-Δ tel1-Δ
rad27-Δ
rad27-Δ tel1-Δ
hda3-Δ
hda3-Δ tel1-Δ
rad26-Δ
rad26-Δ tel1-Δ
yku80-Δ
yku80-Δ tel1-Δ
nup133-Δ
nup133-Δ tel1-Δ
nup60-Δ
nup60-Δ tel1-Δ
lsm7-Δ
lsm7-Δ tel1-Δ
sap30-Δ
sap30-Δ tel1-Δ
ccr4-Δ
ccr4-Δ tel1-Δ
rad24-Δ
rad24-Δ tel1-Δ
Strain
B
Log percent survivial after 400Gy
100
10
1
0.1
0.01
wt
tel1-Δ
rad17-Δ
rad17-Δ tel1-Δ
ddc1-Δ
ddc1-Δ tel1-Δ
rad24-Δ
rad24-Δ tel1-Δ
sap30-Δ
sap30-Δ tel1-Δ
nup60-Δ
nup60-Δ tel1-Δ
lsm7-Δ
lsm7-Δ tel1-Δ
ccr4-Δ
ccr4-Δ tel1-Δ
pop2-Δ
pop2-Δ tel1-Δ
hda3-Δ
hda3-Δ tel1-Δ
nup133-Δ
nup133-Δ tel1-Δ
rad26-Δ
rad26-Δ tel1-Δ
rad27-Δ
rad27-Δ tel1-Δ
yku80-Δ
yku80-Δ tel1-Δ
Strain
C
Log percent survival after 400Gy
10
1
0.1
0.01
wildtype
tel1-Δ
ccr4-Δ
ccr4-Δ tel1-Δ
rad17-Δ
rad17-Δ tel1-Δ
hda3-Δ
hda3-Δ tel1-Δ
Strain

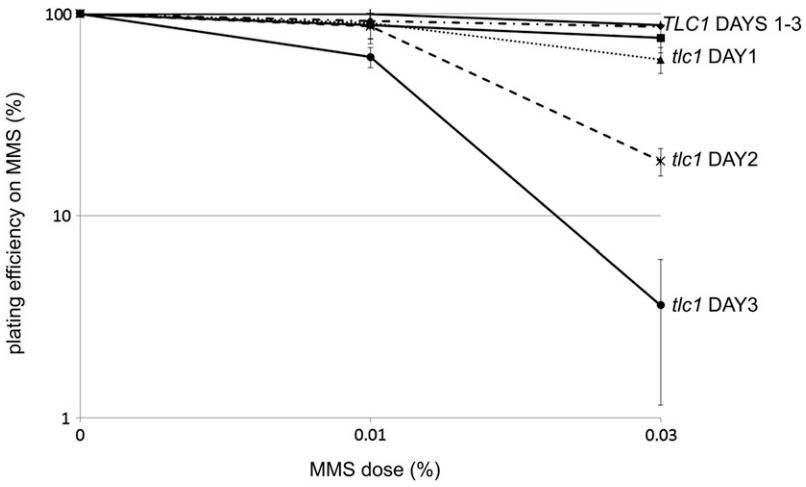

Figure 2 Telomerase-null cells exhibit a progressive increase in MMS sensitivity. *TLC1* and *tlc1* haploid spores from freshly dissected tetrads were subcultured in YEPD over multiple days. Each day, an aliquot was removed and assayed for MMS sensitivity by colony-forming assay. Error bars represent the standard deviation of values from three independent spores.

increase in MMS sensitivity that was most pronounced by day 3 on 0.03% MMS plates (survival rates in MMS were normalized to rates on YEPD alone to correct for MMS-independent loss of viability). As the half-life of telomerase RNA is a few hours (Chapon *et al.* 1997) and the MMS sensitivity manifests after *days*, we conclude that MMS sensitivity is telomere length-dependent in *tlc1* cells, rather than due to *TLC1* loss alone. These results raised the interesting possibility that the DNA damage sensitivity exhibited by the identified *tel1-Δ xxx-Δ* interactions results from an exacerbation of the well-known telomere length defect caused by loss of *TEL1*.

Many of the tel1-Δ MMS interactions exhibit shortened telomeres

As cellular sensitivity to MMS increases progressively with telomere shortening (Figure 2), we hypothesized that some or all of the interactions identified in the *tel1-Δ* screen exacerbate the *tel1*-mediated telomere length defect and that this may be a cause for DNA damage sensitivity in these cells. Thus we asked whether any of the *tel1-Δ xxx-Δ* double mutants exhibited telomere lengths that were significantly shorter than either corresponding single mutant. To answer this question, we isolated genomic DNA from single and double mutants for each of the 13 *tel1-Δ xxx-Δ* interactions and analyzed *Xho*I fragments by Southern blotting with a Y′ subtelomeric probe (Singer *et al.* 1998). As expected (Lustig and Petes 1986; Greenwell *et al.* 1995; Morrow *et al.* 1995), the *tel1-Δ* single mutant exhibited shorter telomere lengths relative to a wild-type strain (Figure 3). Additionally, a number of the other single mutants exhibited shorter telomere lengths relative to the wild type, including *yku80-Δ*, *rad27-Δ*, and *sap30-Δ*, with the *yku80-Δ* mutant being the only single mutant exhibiting a shorter telomere length than *tel1-Δ* (Figure 3). Notably, the 9-1-1 mutants *ddc1-Δ* and *rad17-Δ* were shown in a previous study to exhibit a minor telomere defect (Longhese *et al.* 2000). However, we did not observe discernible shortening of these mutants relative to the wild type (Figures 3 and 4); this may reflect differences in the strain background used in these studies. Notably, the *9-1-1-Δ tel1-Δ* double mutants (*rad24-Δ tel1-Δ*, *rad17-Δ tel1*, and *ddc1-Δ tel1-Δ*) exhibited very short telomeres relative to *tel1-Δ*, and a second class consisting of *sap30-Δ tel1-Δ*, *ccr4-Δ tel1-Δ*, *pop2-Δ tel1-Δ*, *hda3-Δ tel1-Δ*, *nup133-Δ tel1-Δ*, *nup60-Δ tel1-Δ*, *rad27-Δ tel1-Δ*, and *yku80-Δ tel1-Δ* also exhibited shorter telomeres relative to *tel1-Δ*. The *rad26-Δ tel1-Δ* and *lsm7-Δ tel1-Δ* double mutants exhibited telomere lengths that were identical to *tel1-Δ*. Our finding that 11 of the 13 *tel1-Δ xxx-Δ* interactions exhibited decreased telomere lengths relative to *tel1-Δ* is unexpected, since many of identified genes play no known role in telomere metabolism. To exclude the possibility that the *tel1-Δ xxx-Δ* short telomere phenotype was not merely an artifact due to a previously characterized phenotypic lag for *tel1* telomeres

Figure 1 Quantitative survival analysis for *tel1* interactions in MMS and IR via colony-forming assay. (A) Quantitative survival analysis in MMS. Log-phase cultures for three independent transformants of each single and double mutant were serially diluted in PBS and spread onto YEPD or YEPD + 0.03% MMS plates (asterisks indicate that screening was done in 0.015% MMS due to extreme MMS sensitivity). Viable cells were determined by the number of CFU after 3 days at 30°. (B) Quantitative survival analysis in IR. Log-phase cultures for three independent transformants of each single and double mutant were serially diluted in PBS and spread onto YEPD plates and irradiated at 400 Gy at 8 Gy/min. Viable cells were determined by the number of CFU after 3 days at 30°. Arrows indicate interactions identified in the genome-wide screen. Error bars represent the standard deviation of values from three independent transformants. (C) Quantitative survival analysis using continuous low-dose-rate IR. Log-phase cultures for two independent transformants of each single and double mutant were diluted in YEPD in 15-ml tubes and irradiated with 400 Gy delivered at a continuous dose rate of 0.9 Gy/min over 7.5 hr. Following delivery of IR, cells were counted, serially diluted, and plated for colony survival analysis. Error bars show the range of values for two independent transformants.

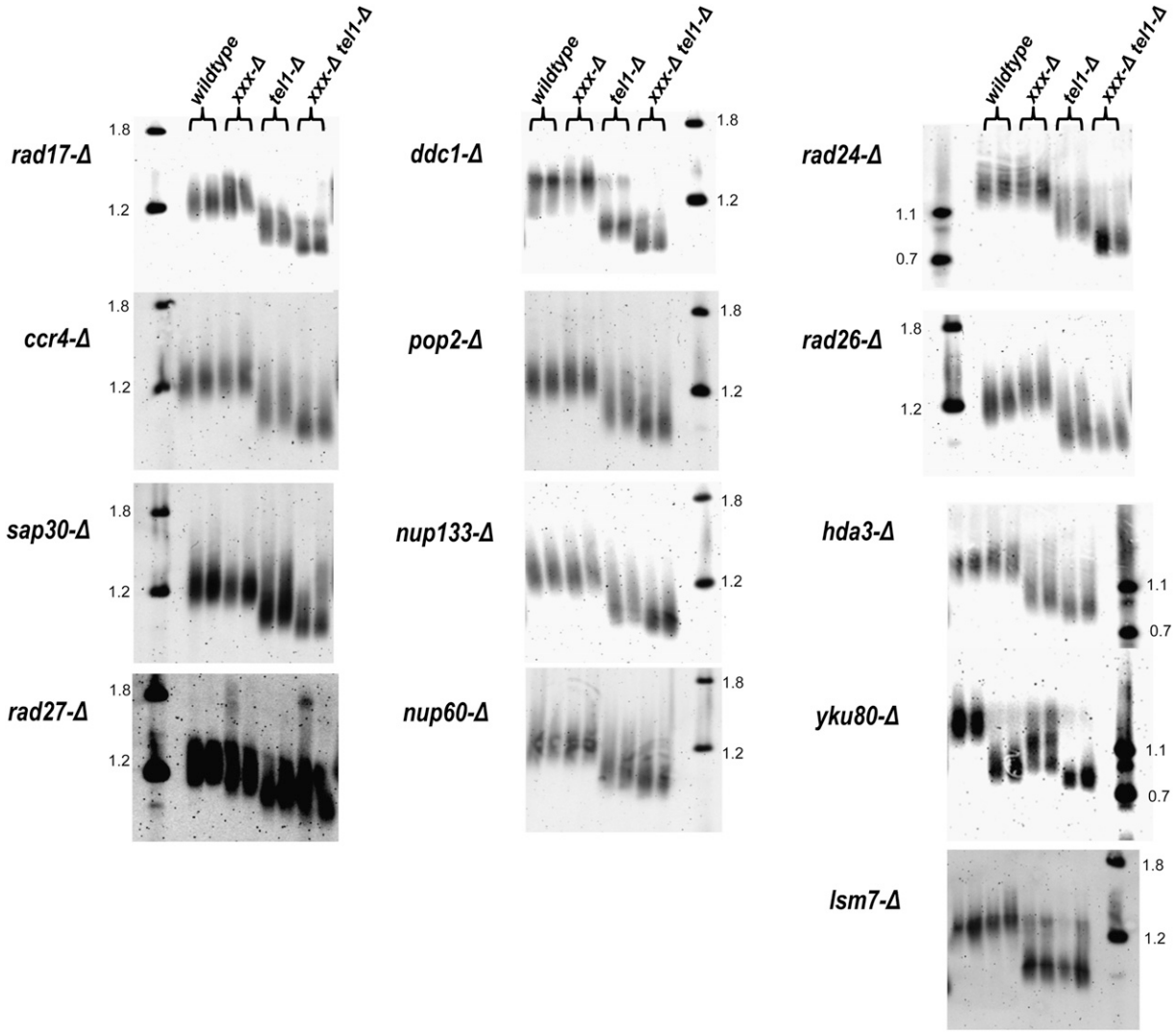

Figure 3 Telomere lengths for *tel1*-Δ MMS-sensitive interactions. For each strain, *Xho*I-digested DNA was analyzed by Southern blot using a probe complementary to the Y′ subtelomere. Each *xxx-Δ* mutant is listed to the left of each corresponding blot, and duplicates representing independent transformants for each strain are loaded side by side (duplicates are indicated by the brackets above). DNA ladders (in kb) are indicated in the far left or right lane of each blot.

[∼150 generations (Lustig and Petes 1986)], we examined telomere lengths for a selection of single and double mutants over additional subculturing for a period of 5 days. During the repeated subculturing, we did not observe any further changes in telomere length by Southern blot (Figure 4). From these data, we conclude that the majority of *tel1-Δ* interactions identified in the MMS sensitivity screen also confer shorter telomeres, suggesting a possible connection between the two phenotypes.

Artificial elongation of telomeres in tel1-Δ 9-1-1-Δ mutants partially suppresses MMS sensitivity

As telomere shortening was shown to be causative for MMS sensitivity in the *tlc1* case (Figure 2), we next hypothesized that the exacerbated telomere defect exhibited by the majority of *tel1-Δ xxx-Δ* strains (Figure 3) may be causative for enhanced MMS sensitivity. Thus, reversal of the telomere length defect would also reduce the MMS sensitivity of these mutants. To test this, we transformed each of the *tel1-Δ xxx-Δ* single and double mutants with a plasmid expressing a fusion of the Cdc13 capping protein to the Est2 subunit of telomerase (Evans and Lundblad 1999). This fusion has been previously shown to alleviate the short telomere phenotype in a *tel1* mutant (Tsukamoto *et al.* 2001). A panel of *tel1-Δ xxx-Δ* mutant strains with and without the *CDC13-EST2* plasmid was screened for sensitivity by spotting cells on MMS plates (supporting information, Figure S1). Of the tested *tel1-Δ xxx-Δ* interactions, the *rad24-Δ tel1-Δ* strain exhibited a visible increase in survival on MMS plates when transformed with the *CDC13-EST2* fusion plasmid (and not the vector). None of the other *tel1-Δ xxx-Δ* interactions exhibited any change in MMS sensitivity upon transformation with *CDC13-EST2*. We confirmed the suppression of MMS sensitivity in *rad24-Δ tel1-Δ* as well as a second 9-1-1

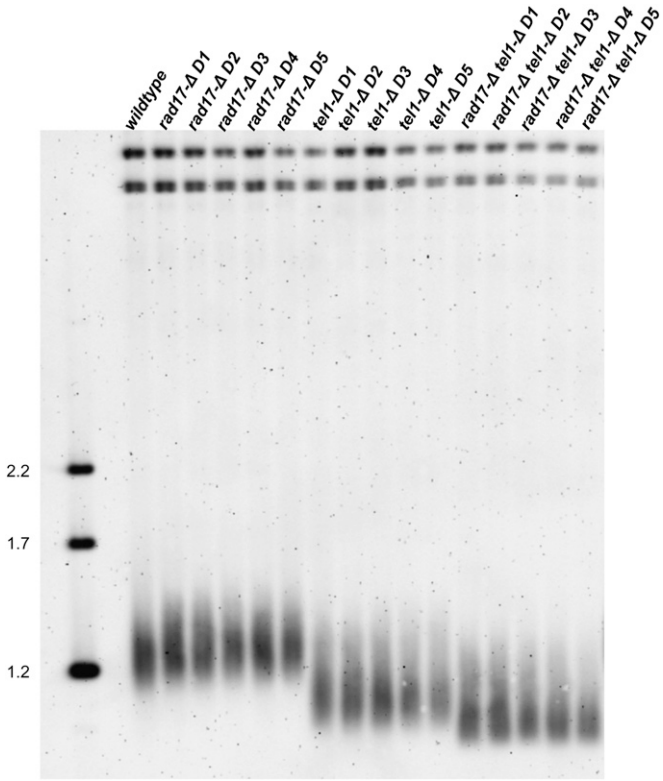

Figure 4 Repeated subculturing does not alter telomere lengths. Wild-type, *tel1-Δ*, *rad17-Δ*, and *rad17-Δ tel1-Δ* cultures were diluted in fresh YEPD media and grown overnight. Genomic DNA was harvested the following day, and a portion of the cells was diluted in fresh medium and cultured overnight. The process was repeated over a period of 5 days (D1–D5). *Xho*I-digested DNA was analyzed by gel electrophoresis and Southern blotting with a probe recognizing subtelomeric Y′ sequence. Molecular weight markers are indicated on the left (in kb).

component (*rad17-Δ tel1-*Δ) by a quantitative colony-forming assay (Figure 5, A and B), and again the fusion plasmid conferred discernible (but not total) resistance to MMS (11-fold for *rad24-Δ tel1-Δ* and 4-fold for *rad17-Δ tel1-Δ vs.* the vector). Telomeres in these strains were significantly elongated to wild-type levels by addition of the *CDC13-EST2* fusion and were hyper-elongated in wild-type and *tel1-Δ* strains (Figure 5C). (*CDC13-EST2* was able to elongate telomeres to an identical degree in other non-9-1-1-related *tel1-Δ xxx-Δ* interactions (not shown) despite having no effect on MMS resistance.) While expression of *CDC13-EST2* suppresses strong (>100-fold) MMS sensitivity in *9-1-1-Δ tel1-Δ* interactions by ~10-fold (Figure 5), the fact that this suppression is not total and that *CDC13-EST2* expression does not affect the MMS sensitivity of the other *tel1-Δ xxx-Δ* interactions suggests that there are additional telomere-length-independent defects that contribute to the MMS sensitivity of *tel1-Δ xxx-Δ* interactions.

tel1-Δ xxx-Δ interactions do not affect the frequency of NHEJ-mediated translocations

Lee *et al.* (2008) previously described an 11-fold increase in the frequency of DSB-induced, NHEJ-mediated translocations for a *tel1-Δ* mutant, reflecting a role for *TEL1* in preventing deleterious chromosomal fusions through an as-yet-undefined mechanism. That a *tel1-Δ* strain is not sensitive to DNA-damaging agents despite this defect suggests that the occurrence of these events even in the presence of DNA-damaging agents is a rarity. Thus, one possibility is that the *tel1-Δ xxx-Δ* interactions identified here may increase cellular dependence on *TEL1* to prevent deleterious chromosomal fusions. We tested this possibility by determining whether the *tel1-Δ xxx-Δ* double mutants experience enhanced frequencies (compared to *tel1*) of chromosomal translocations. We cloned each of the 13 single mutants and *tel1-Δ xxx-Δ* double mutants into a strain background harboring the translocation assay construct (Lee *et al.* 2008) that employs two *GAL*-inducible *HO* cuts on chromosomes V and VII, where each breakpoint contains a nonfunctional fragment of the *URA3* gene. Translocations are measured by the reconstitution of a functional *URA3* allele, which is dependent on Ku70/80-mediated NHEJ (Lee *et al.* 2008). We measured the frequency of translocations after the induction of *GAL-HO* for the panel of *tel1-Δ xxx-Δ* interaction strains (Figure 6). While we were able to reproduce the Ku-dependent increase in Ura^+ translocations for *tel1-Δ*, none of the other double mutants exhibited frequencies that differed from *tel1-Δ*. From this we conclude that an increased frequency of DSB-induced chromosomal translocations is unlikely to be the cause of the MMS sensitivity exhibited by *tel1-Δ xxx-Δ* interactions. This is supported by the fact that the *tel1-Δ xxx-Δ* MMS interactions were also largely insensitive to IR (Figure 1), which directly induces DSBs [whether or not MMS produces DSBs is a current source of controversy (Lundin *et al.* 2005)].

GCRs in tel1-Δ xxx-Δ strains

Kolodner and colleagues have previously shown that one double mutant identified in this screen (*rad24 tel1*) causes an increased frequency of spontaneous chromosome breakage and rearrangement involving the left arm of chromosome V (the GCR arrangement assay) (Myung and Kolodner 2002). As MMS has also been shown to induce higher GCR frequencies (Myung and Kolodner 2003; Stellwagen *et al.* 2003), we asked whether the MMS sensitivity exhibited by the *tel1-Δ xxx-Δ* double mutants may reflect an increased frequency of MMS-induced genome rearrangements. To do this, we grew single- and double-mutant strains in the presence of 0.003% MMS for 15 hr to induce GCR events, which were detected by selecting for the loss of two nearby markers (*CAN1* and *URA3*) on the left arm of chromosome V, as previously described (Chen and Kolodner 1999). The 0.003% MMS exposure resulted in an ~10-fold induction of GCR events for wild-type cells. For the *tel1-Δ xxx-Δ* double mutants, members of the 9-1-1 complex showed an ~300-fold induction of MMS-induced GCR events when combined with *tel1-Δ* (Figure 7A). The *rad27-Δ tel1-Δ* mutant and *nup60-Δ tel1-Δ* each showed a minor ~5-fold increase in MMS-induced GCR. None of

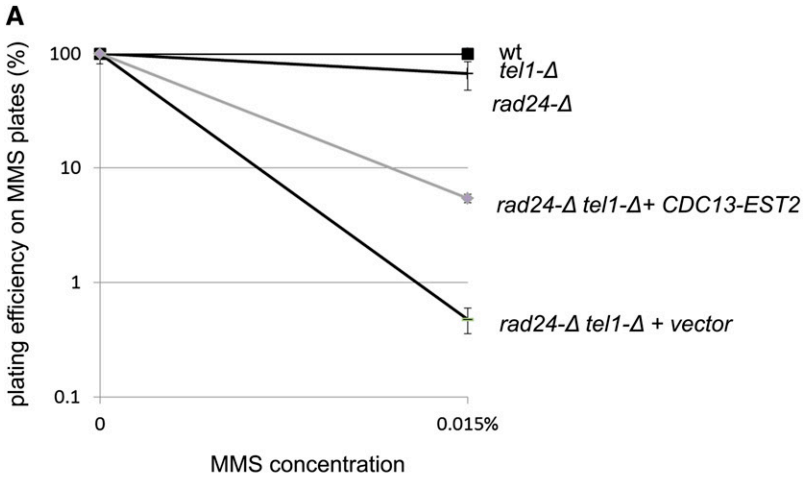

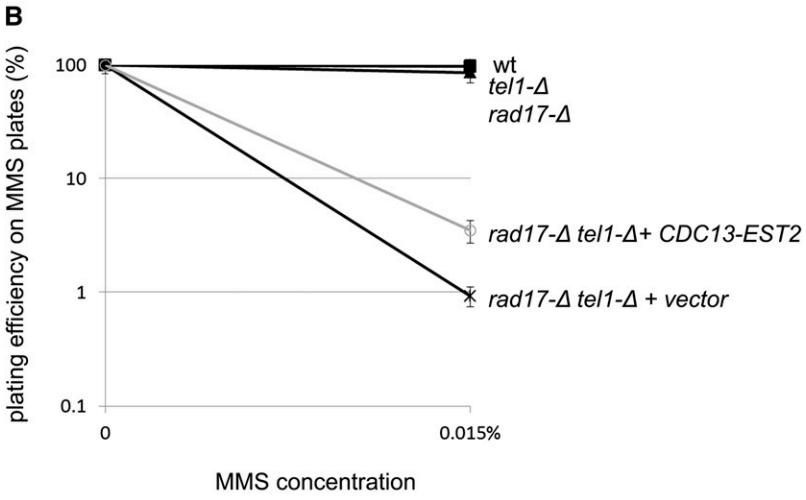

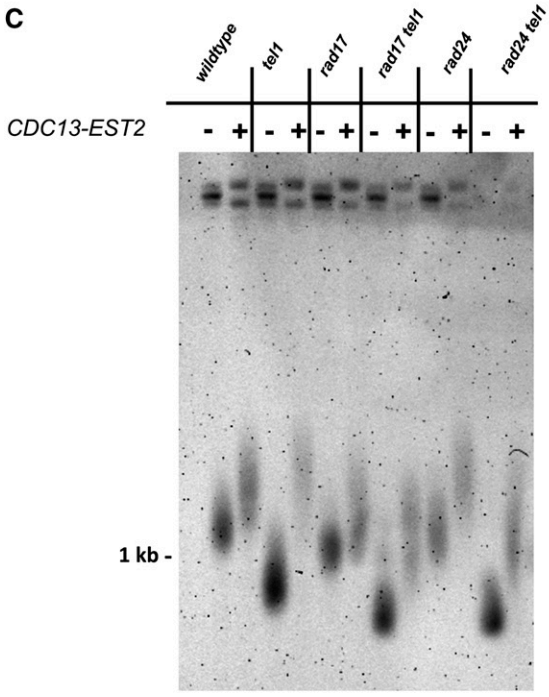

Figure 5 Suppression of MMS sensitivity in *rad24-Δ tel1-Δ* and *rad17-Δ tel1-Δ* by a *CDC13-EST2* fusion plasmid. (A and B) Strains of the indicated genotype were transformed either with an empty vector or with a *CDC13-EST*2 fusion plasmid (pVL1107) and screened for MMS sensitivity by colony-forming assay on MMS plates. Error bars represent the standard deviation of values from three independent transformants. (C) Telomere lengths for *tel1-*Δ interactions with or without the *CDC13-EST2* fusion plasmid. Cells with the *CDC13-EST2* fusion plasmid or empty vector were propagated on –Leu media and diluted in fresh rich medium overnight. Genomic DNA was harvested the following day and analyzed by electrophoresis and Southern blotting. The blot was probed with sequence complementary to a region in the Y′ subtelomeric element.

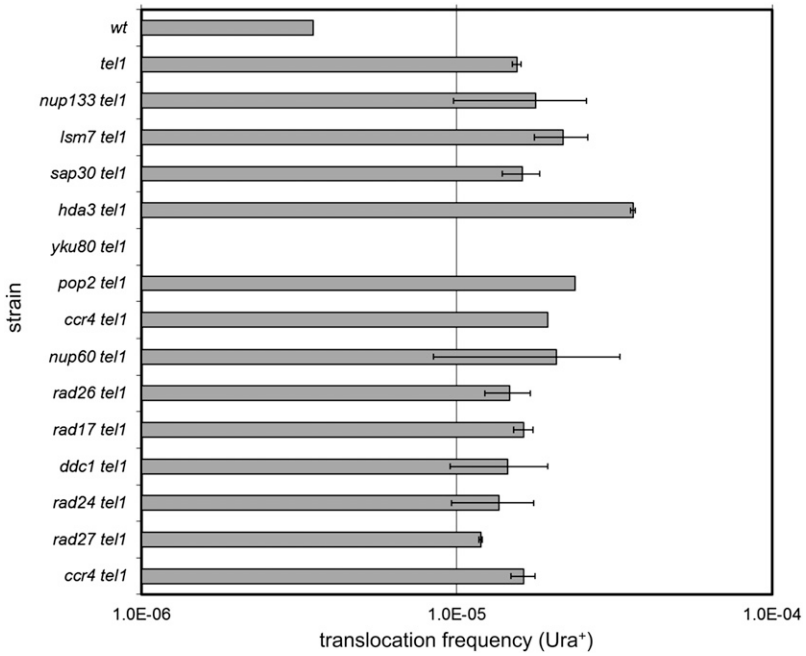

Figure 6 *HO*-induced translocation frequency for *tel1-Δ* interactions. NHEJ-mediated translocation frequency for *tel1*-Δ double mutants following *GAL-HO* induction of DSBs on chromosome V and chromosome VII. Frequencies are measured as the fraction of colonies that survive on −Ura plates. Error bars indicate the standard deviation of values from three independent transformants.

the other double mutants exhibited an increased GCR frequency (Figure 7A). From these data, we conclude that a subset of *tel1-Δ xxx-Δ* interactions (*rad17-Δ tel1-Δ*, *ddc1-Δ tel1-Δ*, *rad24-Δ tel1-Δ*, *rad27-Δ tel1-Δ*, and *nup60-Δ tel1-Δ*) exhibit increased genome instability as measured by the GCR assay.

As restoration of telomere lengths through addition of the *CDC13-EST2* fusion plasmid restored a proportion of MMS resistance to the *9-1-1-Δ tel1-Δ* mutant strains, we asked whether the *CDC13-EST2* fusion would also suppress the increased MMS-induced GCR frequency of a *9-1-1-Δ tel1-Δ* mutant as well. We tested a *rad17-Δ tel1-Δ* mutant along with the corresponding single mutants for the induction of GCR events with or without the fusion construct. As can be seen in Figure 7B, the *rad17-Δ tel1-Δ* double-mutant strain harboring the fusion plasmid had a reduced GCR frequency relative to the same strain carrying an empty vector. Consistent with a partial reduction in MMS sensitivity, the *CDC13-EST2* fusion did not completely abolish MMS-induced gross chromosomal rearrangements in the *rad17-Δ tel1-Δ* strain. From these data, we conclude that a proportion of the MMS sensitivity exhibited by *9-1-1-Δ tel1-Δ* strains is due to MMS-induced genomic instability that is caused by telomere shortening. However, much of the increased GCR in *9-1-1-Δ tel1-Δ* is unexplained by telomere length effects; thus additional mechanisms (*i.e.*, aside from altered telomere length) contribute to the sensitivity of *tel1-Δ xxx-Δ* interactions.

A tel1-Δ strain is rendered sensitive to MMS by predepletion of nucleotide pools

Prior studies have implicated both the *9-1-1* complex and the CCR4-NOT complex as key regulators of ribonucleotide reductase, and mutants in these pathways exhibit depleted nucleotide pools and are sensitive to replication stress (Zhao *et al.* 2001; Westmoreland *et al.* 2004; Mulder *et al.* 2005; Traven *et al.* 2005; Woolstencroft *et al.* 2006). Moreover, a *ccr4-Δ tel1-Δ* strain has been previously shown to exhibit enhanced sensitivity to the ribonucleotide reductase inhibitor hydroxyurea (Woolstencroft *et al.* 2006). Thus we hypothesized that a decrease in dNTP pools in *9-1-1-Δ tel1-Δ* and *ccr4-Δ/pop2-Δ tel1-Δ* may contribute to the MMS sensitivity exhibited by these strains. From this, we predicted that depletion of nucleotide pools (*e.g.*, by pretreating cells with hydroxyurea) in *tel1-Δ* cells should phenocopy deletion of *CCR4* in a *tel1-Δ* background, thus sensitizing *tel1-Δ* cells to MMS. To test this prediction, wild-type and *tel1-Δ* cells were cultured in rich medium with 0, 50, or 150 mM HU for a period of 4 hr, after which the HU was removed, and cells were plated onto MMS plates to assess viability. As expected, the MMS sensitivity of a wild-type strain does not change, regardless of whether the cells have been pretreated with HU (Figure 8). In contrast, while a *tel1-Δ* strain is insensitive to the HU pretreatment alone, when HU pretreatment is followed by plating on MMS plates, *tel1-Δ* cells exhibit enhanced MMS sensitivity in a dose-dependent manner, with the greatest MMS sensitivity observed in 150 mM HU (Figure 8). From this we conclude that depletion of nucleotide pools renders *tel1-Δ* sensitive to the DNA-damaging agent MMS, consistent with a model in which increased replication stress contributes to the MMS sensitivity exhibited by the *9-1-1-Δ tel1-Δ* and ccr4-Δ *tel1-Δ/pop2-Δ tel1-Δ* mutants (and possibly other *tel1-Δ xxx-Δ* double mutants isolated in the screen; see *Discussion*).

Discussion

Categorizing the tel1-Δ interactions

While a *tel1-Δ* mutant exhibits interactions with a diverse set of 13 mutants, we found that these interactions fell into

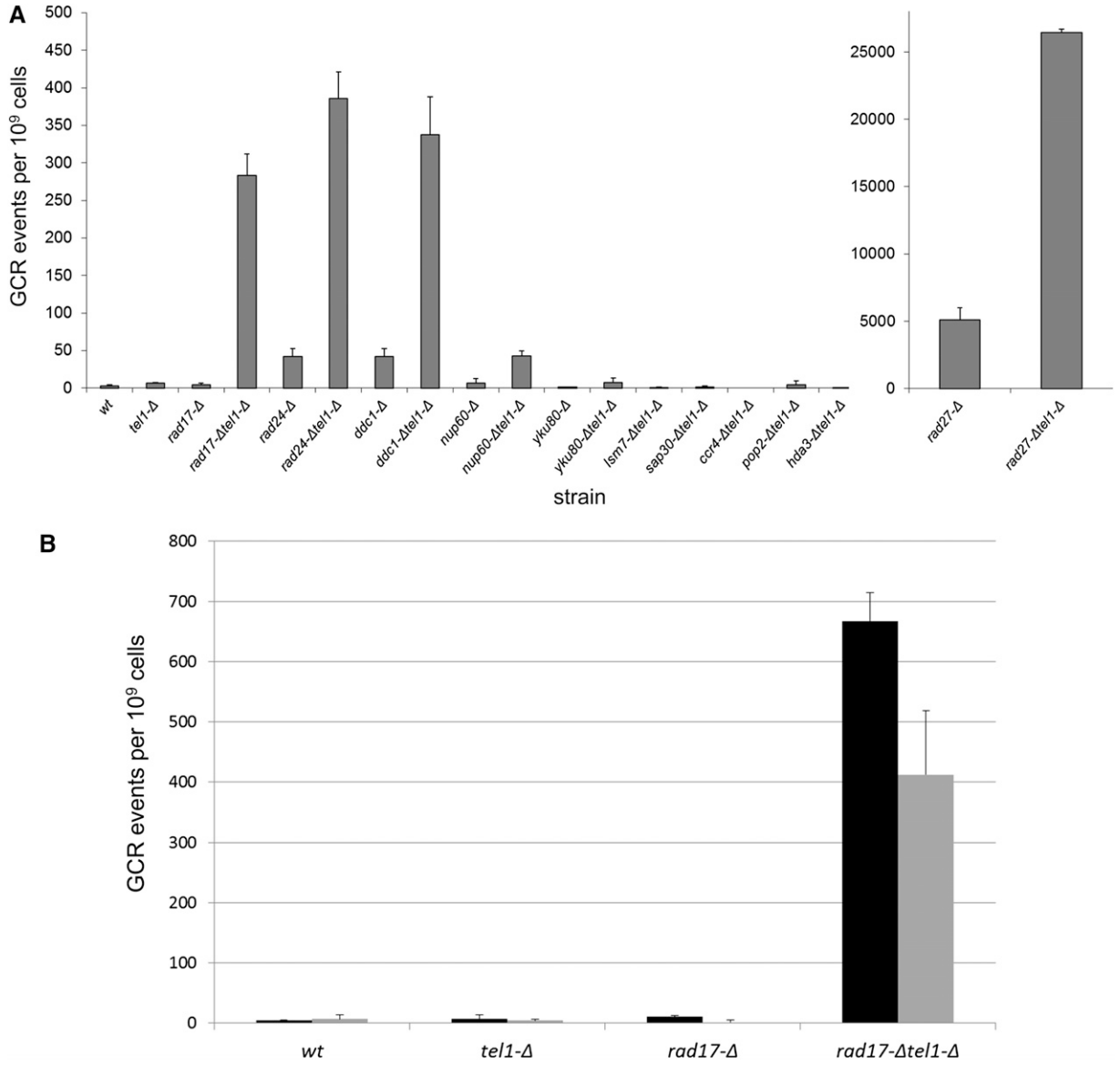

Figure 7 GCR frequency in 0.003% MMS. (A) GCR frequency for *tel1-Δ* interactions. Strains were grown in YEPD + 0.003% MMS for 15 hr and subsequently plated onto C-Arg-Ser + canavanine + 5-FOA to simultaneously select for the loss of *CAN1* and *URA3* markers on the left end of chromosome V. Error bars represent standard deviations from two independent cultures per strain, each plated two times. The *rad27-Δ* mutants are plotted separately due to scale. (B) GCR frequency in 0.003% MMS with or without the *CDC13-EST2* fusion plasmid. The indicated strains containing either an empty vector (black bars) or the *CDC13-EST2* fusion (gray bars) were grown in YEPD + 0.003% MMS for 15 hr and subsequently plated onto C-Arg-Ser + canavanine + 5-FOA to select for simultaneous loss of *CAN1* and *URA3* markers. Error bars represent standard deviations from two independent cultures per strain, each plated two times.

three phenotypic classes based upon our follow-up characterizations (Table 2). The first class is composed of mutants in the 9-1-1 complex (*rad17-Δ* and *ddc1-Δ*) and the 9-1-1 clamp loader (*rad24-Δ*); these *tel1-Δ* interactions conferred a rather large (>100-fold) increase in MMS sensitivity (Figure 1A), cross-sensitivity to IR (Figure 1, B and C), a pronounced telomere defect (Figure 3), and a synergistic increase in GCR events (Figure 7). For this class, the DNA damage sensitivity and the increase in GCR frequencies were partially suppressed by elongating telomeres using the *CDC13-EST2* fusion construct (Figures 5 and 7B). The second class of interactions comprises *ccr4-Δ*, *pop2-Δ*, *sap30-Δ*, *hda3-Δ*, *yku80-Δ*, *rad27-Δ*, *nup133-Δ*, and *nup60-Δ* (Table 2); these exhibited a somewhat milder interaction with *tel1-Δ* in MMS and no cross-sensitive interactions to IR, but exhibited a discernible telomere length defect with *tel1-Δ* (Figure 3). The third class of mutants, *rad26-Δ* and *lsm7-Δ*, showed similar characteristics to class 2, but did not exhibit any discernible telomere length defect (Figure 3). There is likely some overlap between these classes in the mechanism that causes their interactions with *tel1-Δ* (discussed below).

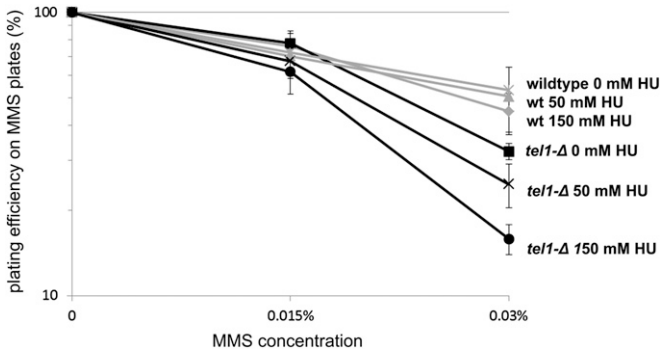

Figure 8 MMS sensitivity following pretreatment with HU. The indicated strains were grown in the presence of the indicated dose of HU for 4 hr to deplete nucleotide pools. Cells were then washed two times and plated onto MMS plates to assay MMS sensitivity by colony-forming assay. The error bars indicate the standard deviation of values from three independent cultures.

A replication defect underlies sensitivity to MMS in multiple classes of tel1-Δ interactions

While the *tel1-Δ* interactions composing classes 1 and 2 (Table 2) exhibit shortened telomeres relative to the corresponding single mutants, only in the class 1 case is MMS sensitivity suppressed by telomere elongation (Figure 5), and even in this class of double mutants the suppression is modest. While it is formally possible that telomere elongation due to the expression of the *CDC13-EST2* fusion creates a structure that is somehow physiologically different from a natural telomere and thus is not a good substitute, a more straightforward model is that only a minor proportion of MMS sensitivity is directly caused by telomere shortening in class 1 mutants, while the majority of MMS sensitivity in these and other *tel1-Δ xxx-Δ* interactions reflects an underlying replication defect that manifests a dual-pronged effect on telomere metabolism and MMS resistance.

Our data (and other studies) support a model in which increased replication stress, combined with a *tel1-Δ*-mediated defect in replication fork stability, causes both MMS sensitivity and telomere shortening in *tel1-Δ xxx-Δ* interactions. First, aside from a modest effect in the class 1 mutants, none of the identified in *tel1-Δ xxx-Δ* interactions exhibit cross-sensitivity to ionizing radiation, regardless of whether the IR was administered as a pulse (Figure 1B) or as chronic treatment (Figure 1C). Unlike MMS treatment, IR does not induce detectable replication fork stalling (Merrick *et al.* 2004), so while there is a minor IR interaction in *tel1-Δ 9-1-1-Δ* cells (Figure 1, B and C) (likely through an additive defect in Mec1/Tel1 DSB sensing), replication fork stalling/collapse is the likely major lethal lesion in *tel1-Δ xxx-Δ* interactions. Additionally, recent studies have uncovered a *TEL1*-dependent role in the preservation of fork stability through the prevention of fork reversion and degradation into abnormal cruciform structures (Doksani *et al.* 2009). Consistent with this, Kaochar *et al.* (2010) showed that *tel1-Δ* exhibits an increased frequency of dicentric chromosomes due to the fusion of inverted repeats likely due to fork reversion. As the reason why *tel1-Δ* cells exhibit short telomeres is poorly understood, it is formally possible that a failure to preserve fork stability in telomeric regions in *tel1-Δ* cells is causative for the short telomere phenotype [telomeres are enriched for replication pause sites such as G-quadruplex structures (Ivessa *et al.* 2002; Bochman *et al.* 2012)].

Many of the *tel1-Δ* interactions identified in the MMS screen fit a model for increased replication stress. Members of class 1 (9-1-1 components) (Table 2) are required for the *MEC1*-dependent degradation of the ribonucleotide reductase inhibitor Sml1 following MMS treatment (Zhao *et al.* 2001; Chabes *et al.* 2003); the resultant increase in dNTP production following this process is thought to facilitate DNA synthesis at stalled forks to prevent fork collapse (Fasullo *et al.* 2010). In addition, members of class 2 (*CCR4* and *POP2*, members of the CCR4-NOT deadenylation complex) are known regulators of ribonucleotide reductase, and mutants in *ccr4-Δ* and *pop2-Δ* are sensitive to replication inhibitors such as HU (Westmoreland *et al.* 2004; Mulder *et al.* 2005; Traven *et al.* 2005; Woolstencroft

Table 2 Tabulation of phenotypes for *tel1-Δ* interactions identified in the MMS screen

	Strain	MMS interaction	IR interaction	GCR	Short telomere	*CDC13-EST2* rescue	Description
Class 1	*rad24-Δtel1-Δ*	++	+	++	++	+/−	9-1-1 complex
	rad17-Δtel1-Δ	++	+	++	++	+/−	9-1-1 complex
	ddc1-Δtel1-Δ	++	+	++	++	+/−	9-1-1 complex
Class 2	*nup60-Δtel1-Δ*	+	—	+	+	—	Nucleoporin
	rad27-Δtel1-Δ	+	—	+	+	—	Flap endonuclease
	sap30-Δtel1-Δ	+	—	—	+	—	Deacetylase
	pop2-Δtel1-Δ	+	—	—	+	—	Deadenylase
	ccr4-Δtel1-Δ	+	—	—	+	—	Deadenylase
	hda3-Δtel1-Δ	+	—	—	+	—	deacetylase
	yku80-Δtel1-Δ	+	—	—	+	—	NHEJ
	nup133-Δtel1-Δ	+	—	—	+	—	Nucleoporin
Class 3	*lsm7-Δtel1-Δ*	+	—	—	—	—	mRNA decap
	rad26-Δtel1-Δ	+	—	—	—	—	TCR

For each of the *tel1-Δ xxx-Δ* genetic interactions identified in the MMS screen a "+" indicates whether a double mutant exhibited a positive result in each of the assays tested (*e.g.*, increased GCR frequency, shorter telomere, etc.); a "++" indicates a more severe phenotype; and a "+/−" indicates partial suppression. TCR, transcription-coupled repair.

et al. 2006). As telomere shortening has recently been shown to occur upon dNTP depletion (Gupta *et al.* 2013), it is likely that the short telomeres in CCR4-NOT and 9-1-1 mutants are at least partially due to this mechanism. Consistent with a model for increased replication stress in *tel1-Δ xxx-Δ* cells, depleting nucleotide pools by pretreatment with HU (effectively phenocopying the loss of *9-1-1* or *CCR4/POP2*) sensitizes *tel1-Δ* cells to MMS in a dose-dependent manner, whereas a wild-type strain is unaffected by the HU pretreatment (Figure 8).

Other mutants composing class 2 are also linked to preventing replication stress via counteracting fork regression [*RAD27* (Kang *et al.* 2010)] or stabilizing sites of active transcription [*NUP60/NUP133* (Palancade *et al.* 2007; Bermejo *et al.* 2011)]. Additionally, the mutants composing class 3 (Table 2) are linked to increased replication stress due to defects in histone regulation [*LSM7* (Herrero and Moreno 2011; Tkach *et al.* 2012)] or through defective targeting of transcription-coupled repair [*RAD26* (Kapitzky *et al.* 2010; Malik *et al.* 2010)].

Progressive telomere shortening is a cause for MMS sensitivity

Recently, numerous studies have described a connection between short telomeres and enhanced sensitivity to DNA-damaging agents across a variety of organisms (Wong *et al.* 2000; Lin *et al.* 2009; Soler *et al.* 2009; Drissi *et al.* 2011); the reason for this relationship is poorly understood. Here, we show that, in yeast, cellular sensitivity to MMS progressively increases as telomeres shorten (Figure 2), suggesting that the progressive loss of telomere protection renders cells sensitive to MMS. In concordance with this, a proportion of MMS sensitivity and genome instability can be suppressed in *9-1-1-Δ tel1-Δ* mutants by alleviating the short telomere phenotype in these cells (Figures 5 and 7B).

There are multiple possible mechanisms for how short telomeres cause MMS sensitivity. Loss of telomeric protection can render telomeres as targets for the DDR, and the loss of telomerase activity is associated with a gradual increase in constitutive Rad53 phosphorylation (Grandin *et al.* 2005); accordingly, in telomerase-deficient cells telomeres are enriched for DDR proteins while nontelomeric DSBs exhibit reduced binding of DDR factors (Lin *et al.* 2009). Thus, the recruitment of DDR factors to short telomeres may interfere with the ability of the cell to cope with MMS-induced stress elsewhere in the genome. Alternatively, de-protected telomeres themselves may be problematic in the presence of MMS due to the potential for lethal chromosomal fusions with DSBs resulting from MMS-induced collapsed forks. Supporting this, a subset of GCR events can be suppressed by elongating telomeres in *9-1-1-Δ tel1-Δ* (Figure 7B), and a previous study has shown that a *9-1-1-Δ tel1-Δ* double mutant exhibits an increased frequency of spontaneous telomere–telomere fusions that can also be suppressed by elongating telomeres (Mieczkowski *et al.* 2003).

For the other identified interactions (class 2, Table 2), despite a lack of MMS suppression by *CDC13-EST2*, the telomere defect in these cells may still be a cause of MMS sensitivity. For example, an increase in ssDNA at telomeres would create a structure that is more susceptible to MMS-induced lesions [fork-blocking lesions occur predominantly in ssDNA in MMS (Shrivastav *et al.* 2010)]. Accordingly, a *rad27* mutant is associated with abnormally large regions of ssDNA in telomeres (Parenteau and Wellinger 1999). As DNA damage in telomeres has recently been shown to be uniquely irreparable (Fumagalli *et al.* 2012), it is likely that telomeres exhibiting abnormal structures are both more susceptible to MMS-induced damage and less able to survive it.

Implications of the tel1-Δ screen for mammalian cells

From this study, we show that *tel1-Δ* cells are rendered sensitive to MMS by increased replication stress or exacerbation of the short telomere phenotype. Thus, targeting these mechanisms may be an effective strategy for killing tumor cells that have lost ATM activity. Intriguingly, a recent study found that the specific combination of an *ATM* (*TEL1* ortholog) inhibitor drug combined with a telomerase inhibitor rendered tumor cells extremely sensitive to the chemotherapy agent etoposide (Tamakawa *et al.* 2010). Furthermore, based on the replication stress model described above, targeting ATM for inhibition, combined with agents such as MMS, would be expected to confer a synergistic effect in cells experiencing oncogene-induced replication stress.

Acknowledgments

We thank Brenda Andrews, Charles Boone, Daniel Gottschling, Vicki Lundblad, and Sang Eun Lee for strains and plasmids used in this study and Mary Ellard-Ivey for access to equipment. We thank members of the Brewer/Raghuraman and Gottschling labs and Wenyi Feng and Lindsey Williams for helpful discussions related to this study. We thank our anonymous reviewers and the *GENETICS* Editor for helpful comments on the manuscript. B.D.P. was supported by the Fred Hutchinson Cancer Research Center Dual Mentor Program and a U.S. Department of Defense Breast Cancer Research Program predoctoral fellowship. This work was supported by National Institutes of Health grant R01 CA 129604.

Literature Cited

Agarwal, M., S. Pandita, C. R. Hunt, A. Gupta, X. Yue *et al.*, 2008 Inhibition of telomerase activity enhances hyperthermia-mediated radiosensitization. Cancer Res. 68: 3370–3378.

Arneric, M., and J. Lingner, 2007 Tel1 kinase and subtelomere-bound Tbf1 mediate preferential elongation of short telomeres by telomerase in yeast. EMBO Rep. 8: 1080–1085.

Bermejo, R., T. Capra, R. Jossen, A. Colosio, C. Frattini *et al.*, 2011 The replication checkpoint protects fork stability by releasing transcribed genes from nuclear pores. Cell 146: 233–246.

Bochman, M. L., K. Paeschke, and V. A. Zakian, 2012 DNA secondary structures: stability and function of G-quadruplex structures. Nat. Rev. Genet. 13: 770–780.

Brachmann, C. B., A. Davies, G. J. Cost, E. Caputo, J. Li *et al.*, 1998 Designer deletion strains derived from *Saccharomyces cerevisiae* S288C: a useful set of strains and plasmids for PCR-mediated gene disruption and other applications. Yeast 14: 115–132.

Canman, C. E., D. S. Lim, K. A. Cimprich, Y. Taya, K. Tamai *et al.*, 1998 Activation of the ATM kinase by ionizing radiation and phosphorylation of p53. Science 281: 1677–1679.

Chabes, A., B. Georgieva, V. Domkin, X. Zhao, R. Rothstein *et al.*, 2003 Survival of DNA damage in yeast directly depends on increased dNTP levels allowed by relaxed feedback inhibition of ribonucleotide reductase. Cell 112: 391–401.

Chang, M., M. Arneric, and J. Lingner, 2007 Telomerase repeat addition processivity is increased at critically short telomeres in a Tel1-dependent manner in *Saccharomyces cerevisiae*. Genes Dev. 21: 2485–2494.

Chapon, C., T. R. Cech, and A. J. Zaug, 1997 Polyadenylation of telomerase RNA in budding yeast. RNA 3: 1337–1351.

Chen, C., and R. D. Kolodner, 1999 Gross chromosomal rearrangements in *Saccharomyces cerevisiae* replication and recombination defective mutants. Nat. Genet. 23: 81–85.

Cimprich, K. A., T. B. Shin, C. T. Keith, and S. L. Schreiber, 1996 cDNA cloning and gene mapping of a candidate human cell cycle checkpoint protein. Proc. Natl. Acad. Sci. USA 93: 2850–2855.

Craven, R. J., P. W. Greenwell, M. Dominska, and T. D. Petes, 2002 Regulation of genome stability by *TEL1* and *MEC1*, yeast homologs of the mammalian *ATM* and *ATR* genes. Genetics 161: 493–507.

Doksani, Y., R. Bermejo, S. Fiorani, J. E. Haber, and M. Foiani, 2009 Replicon dynamics, dormant origin firing, and terminal fork integrity after double-strand break formation. Cell 137: 247–258.

Drissi, R., J. Wu, Y. Hu, C. Bockhold, and J. S. Dome, 2011 Telomere shortening alters the kinetics of the DNA damage response after ionizing radiation in human cells. Cancer Prev. Res. (Phila.) 4: 1973–1981.

Evans, S. K., and V. Lundblad, 1999 Est1 and Cdc13 as comediators of telomerase access. Science 286: 117–120.

Fasullo, M., O. Tsaponina, M. Sun, and A. Chabes, 2010 Elevated dNTP levels suppress hyper-recombination in *Saccharomyces cerevisiae* S-phase checkpoint mutants. Nucleic Acids Res. 38: 1195–1203.

Fukunaga, K., Y. Kwon, P. Sung, and K. Sugimoto, 2011 Activation of protein kinase Tel1 through recognition of protein-bound DNA ends. Mol. Cell. Biol. **31:** 1959–1971.

Fumagalli, M., F. Rossiello, M. Clerici, S. Barozzi, D. Cittaro *et al.*, 2012 Telomeric DNA damage is irreparable and causes persistent DNA-damage-response activation. Nat. Cell Biol. 14: 355–365.

Gao, H., T. B. Toro, M. Paschini, B. Braunstein-Ballew, R. B. Cervantes *et al.*, 2010 Telomerase recruitment in *Saccharomyces cerevisiae* is not dependent on Tel1-mediated phosphorylation of Cdc13. Genetics 186: 1147–1159.

Gonzalez-Suarez, E., F. A. Goytisolo, J. M. Flores, and M. A. Blasco, 2003 Telomere dysfunction results in enhanced organismal sensitivity to the alkylating agent N-methyl-N-nitrosourea. Cancer Res. 63: 7047–7050.

Goytisolo, F. A., E. Samper, J. Martin-Caballero, P. Finnon, E. Herrera *et al.*, 2000 Short telomeres result in organismal hypersensitivity to ionizing radiation in mammals. J. Exp. Med. 192: 1625–1636.

Grandin, N., A. Bailly, and M. Charbonneau, 2005 Activation of Mrc1, a mediator of the replication checkpoint, by telomere erosion. Biol. Cell 97: 799–814.

Greenwell, P. W., S. L. Kronmal, S. E. Porter, J. Gassenhuber, B. Obermaier *et al.*, 1995 *TEL1*, a gene involved in controlling telomere length in *S. cerevisiae*, is homologous to the human ataxia telangiectasia gene. Cell 82: 823–829.

Gupta, A., S. Sharma, P. Reichenbach, L. Marjavaara, A. K. Nilsson *et al.*, 2013 Telomere length homeostasis responds to changes in intracellular dNTP pools. Genetics 193: 1095–1105.

Herrero, A. B., and S. Moreno, 2011 Lsm1 promotes genomic stability by controlling histone mRNA decay. EMBO J. 30: 2008–2018.

Ivessa, A. S., J. Q. Zhou, V. P. Schulz, E. K. Monson, and V. A. Zakian, 2002 *Saccharomyces* Rrm3p, a 5′ to 3′ DNA helicase that promotes replication fork progression through telomeric and subtelomeric DNA. Genes Dev. 16: 1383–1396.

Kang, M. J., C. H. Lee, Y. H. Kang, I. T. Cho, T. A. Nguyen *et al.*, 2010 Genetic and functional interactions between Mus81-Mms4 and Rad27. Nucleic Acids Res. 38: 7611–7625.

Kaochar, S., L. Shanks, and T. Weinert, 2010 Checkpoint genes and Exo1 regulate nearby inverted repeat fusions that form dicentric chromosomes in *Saccharomyces cerevisiae*. Proc. Natl. Acad. Sci. USA 107: 21605–21610.

Kapitzky, L., P. Beltrao, T. J. Berens, N. Gassner, C. Zhou *et al.*, 2010 Cross-species chemogenomic profiling reveals evolutionarily conserved drug mode of action. Mol. Syst. Biol. 6: 451.

Kastan, M. B., Q. Zhan, W. S. el-Deiry, F. Carrier, T. Jacks *et al.*, 1992 A mammalian cell cycle checkpoint pathway utilizing p53 and GADD45 is defective in ataxia-telangiectasia. Cell 71: 587–597.

Kuhne, M., E. Riballo, N. Rief, K. Rothkamm, P. A. Jeggo *et al.*, 2004 A double-strand break repair defect in *ATM*-deficient cells contributes to radiosensitivity. Cancer Res. 64: 500–508.

Lee, J. H., and T. T. Paull, 2007 Activation and regulation of ATM kinase activity in response to DNA double-strand breaks. Oncogene 26: 7741–7748.

Lee, K., Y. Zhang, and S. E. Lee, 2008 *Saccharomyces cerevisiae* ATM orthologue suppresses break-induced chromosome translocations. Nature 454: 543–546.

Lin, Y. H., C. C. Chang, C. W. Wong, and S. C. Teng, 2009 Recruitment of Rad51 and Rad52 to short telomeres triggers a Mec1-mediated hypersensitivity to double-stranded DNA breaks in senescent budding yeast. PLoS ONE 4: e8224.

Longhese, M. P., V. Paciotti, H. Neecke, and G. Lucchini, 2000 Checkpoint proteins influence telomeric silencing and length maintenance in budding yeast. Genetics 155: 1577–1591.

Lundin, C., M. North, K. Erixon, K. Walters, D. Jenssen *et al.*, 2005 Methyl methanesulfonate (MMS) produces heat-labile DNA damage but no detectable in vivo DNA double-strand breaks. Nucleic Acids Res. 33: 3799–3811.

Lustig, A. J., and T. D. Petes, 1986 Identification of yeast mutants with altered telomere structure. Proc. Natl. Acad. Sci. USA 83: 1398–1402.

Malik, S., P. Chaurasia, S. Lahudkar, G. Durairaj, A. Shukla *et al.*, 2010 Rad26p, a transcription-coupled repair factor, is recruited to the site of DNA lesion in an elongating RNA polymerase II-dependent manner in vivo. Nucleic Acids Res. 38: 1461–1477.

Mallory, J. C., and T. D. Petes, 2000 Protein kinase activity of Tel1p and Mec1p, two *Saccharomyces cerevisiae* proteins related to the human ATM protein kinase. Proc. Natl. Acad. Sci. USA 97: 13749–13754.

Mantiero, D., M. Clerici, G. Lucchini, and M. P. Longhese, 2007 Dual role for *Saccharomyces cerevisiae* Tel1 in the checkpoint response to double-strand breaks. EMBO Rep. 8: 380–387.

Marcand, S., E. Gilson, and D. Shore, 1997 A protein-counting mechanism for telomere length regulation in yeast. Science 275: 986–990.

Martina, M., M. Clerici, V. Baldo, D. Bonetti, G. Lucchini *et al.*, 2012 A balance between Tel1 and Rif2 activities regulates nucleolytic processing and elongation at telomeres. Mol. Cell. Biol. 32: 1604–1617.

McCulley, J. L., and T. D. Petes, 2010 Chromosome rearrangements and aneuploidy in yeast strains lacking both Tel1p and Mec1p reflect deficiencies in two different mechanisms. Proc. Natl. Acad. Sci. USA 107: 11465–11470.

McGee, J. S., J. A. Phillips, A. Chan, M. Sabourin, K. Paeschke *et al.*, 2010 Reduced Rif2 and lack of Mec1 target short telomeres for elongation rather than double-strand break repair. Nat. Struct. Mol. Biol. 17: 1438–1445.

Merrick, C. J., D. Jackson, and J. F. Diffley, 2004 Visualization of altered replication dynamics after DNA damage in human cells. J. Biol. Chem. 279: 20067–20075.

Metcalfe, J. A., J. Parkhill, L. Campbell, M. Stacey, P. Biggs *et al.*, 1996 Accelerated telomere shortening in ataxia telangiectasia. Nat. Genet. 13: 350–353.

Mieczkowski, P. A., J. O. Mieczkowska, M. Dominska, and T. D. Petes, 2003 Genetic regulation of telomere-telomere fusions in the yeast *Saccharomyces cerevisae*. Proc. Natl. Acad. Sci. USA 100: 10854–10859.

Morrow, D. M., D. A. Tagle, Y. Shiloh, F. S. Collins, and P. Hieter, 1995 *TEL1*, an *S. cerevisiae* homolog of the human gene mutated in ataxia telangiectasia, is functionally related to the yeast checkpoint gene *MEC1*. Cell 82: 831–840.

Mulder, K. W., G. S. Winkler, and H. T. Timmers, 2005 DNA damage and replication stress induced transcription of *RNR* genes is dependent on the Ccr4-Not complex. Nucleic Acids Res. 33: 6384–6392.

Murakami-Sekimata, A., D. Huang, B. D. Piening, C. Bangur, and A. G. Paulovich, 2010 The *Saccharomyces cerevisiae RAD9*, *RAD17* and *RAD24* genes are required for suppression of mutagenic post-replicative repair during chronic DNA damage. DNA Repair (Amst.) 9: 824–834.

Myung, K., and R. D. Kolodner, 2002 Suppression of genome instability by redundant S-phase checkpoint pathways in *Saccharomyces cerevisiae*. Proc. Natl. Acad. Sci. USA 99: 4500–4507.

Myung, K., and R. D. Kolodner, 2003 Induction of genome instability by DNA damage in *Saccharomyces cerevisiae*. DNA Repair (Amst.) 2: 243–258.

Nakada, D., K. Matsumoto, and K. Sugimoto, 2003 *ATM*-related Tel1 associates with double-strand breaks through an Xrs2-dependent mechanism. Genes Dev. 17: 1957–1962.

Nakamura, M., K. Masutomi, S. Kyo, M. Hashimoto, Y. Maida *et al.*, 2005 Efficient inhibition of human telomerase reverse transcriptase expression by RNA interference sensitizes cancer cells to ionizing radiation and chemotherapy. Hum. Gene Ther. 16: 859–868.

Paciotti, V., M. Clerici, G. Lucchini, and M. P. Longhese, 2000 The checkpoint protein Ddc2, functionally related to *S. pombe* Rad26, interacts with Mec1 and is regulated by Mec1-dependent phosphorylation in budding yeast. Genes Dev. 14: 2046–2059.

Painter, R. B., and B. R. Young, 1980 Radiosensitivity in ataxia-telangiectasia: a new explanation. Proc. Natl. Acad. Sci. USA 77: 7315–7317.

Palancade, B., X. Liu, M. Garcia-Rubio, A. Aguilera, X. Zhao *et al.*, 2007 Nucleoporins prevent DNA damage accumulation by modulating Ulp1-dependent sumoylation processes. Mol. Biol. Cell 18: 2912–2923.

Parenteau, J., and R. J. Wellinger, 1999 Accumulation of single-stranded DNA and destabilization of telomeric repeats in yeast mutant strains carrying a deletion of *RAD27*. Mol. Cell. Biol. 19: 4143–4152.

Paulovich, A. G., C. D. Armour, and L. H. Hartwell, 1998 The *Saccharomyces cerevisiae RAD9*, *RAD17*, *RAD24* and *MEC3* genes are required for tolerating irreparable, ultraviolet-induced DNA damage. Genetics 150: 75–93.

Ritchie, K. B., J. C. Mallory, and T. D. Petes, 1999 Interactions of *TLC1* (which encodes the RNA subunit of telomerase), *TEL1*, and *MEC1* in regulating telomere length in the yeast *Saccharomyces cerevisiae*. Mol. Cell. Biol. 19: 6065–6075.

Sabourin, M., C. T. Tuzon, and V. A. Zakian, 2007 Telomerase and Tel1p preferentially associate with short telomeres in *S. cerevisiae*. Mol. Cell 27: 550–561.

Savitsky, K., S. Sfez, D. A. Tagle, Y. Ziv, A. Sartiel *et al.*, 1995 The complete sequence of the coding region of the *ATM* gene reveals similarity to cell cycle regulators in different species. Hum. Mol. Genet. 4: 2025–2032.

Shiloh, Y., 2003 ATM and related protein kinases: safeguarding genome integrity. Nat. Rev. Cancer 3: 155–168.

Shrivastav, N., D. Li, and J. M. Essigmann, 2010 Chemical biology of mutagenesis and DNA repair: cellular responses to DNA alkylation. Carcinogenesis 31: 59–70.

Singer, M. S., and D. E. Gottschling, 1994 *TLC1*: template RNA component of *Saccharomyces cerevisiae* telomerase. Science 266: 404–409.

Singer, M. S., A. Kahana, A. J. Wolf, L. L. Meisinger, S. E. Peterson *et al.*, 1998 Identification of high-copy disruptors of telomeric silencing in *Saccharomyces cerevisiae*. Genetics 150: 613–632.

Soler, D., J. Pampalona, L. Tusell, and A. Genesca, 2009 Radiation sensitivity increases with proliferation-associated telomere dysfunction in nontransformed human epithelial cells. Aging Cell 8: 414–425.

Stellwagen, A. E., Z. W. Haimberger, J. R. Veatch, and D. E. Gottschling, 2003 Ku interacts with telomerase RNA to promote telomere addition at native and broken chromosome ends. Genes Dev. 17: 2384–2395.

Tamakawa, R. A., H. B. Fleisig, and J. M. Wong, 2010 Telomerase inhibition potentiates the effects of genotoxic agents in breast and colorectal cancer cells in a cell cycle-specific manner. Cancer Res. 70: 8684–8694.

Teixeira, M. T., M. Arneric, P. Sperisen, and J. Lingner, 2004 Telomere length homeostasis is achieved via a switch between telomerase-extendible and -nonextendible states. Cell 117: 323–335.

Tkach, J. M., A. Yimit, A. Y. Lee, M. Riffle, M. Costanzo *et al.*, 2012 Dissecting DNA damage response pathways by analysing protein localization and abundance changes during DNA replication stress. Nat. Cell Biol. 14: 966–976.

Tong, A. H., and C. Boone, 2006 Synthetic genetic array analysis in *Saccharomyces cerevisiae*. Methods Mol. Biol. 313: 171–192.

Tong, A. H., M. Evangelista, A. B. Parsons, H. Xu, G. D. Bader *et al.*, 2001 Systematic genetic analysis with ordered arrays of yeast deletion mutants. Science (New York, N.Y.) 294: 2364–2368.

Traven, A., A. Hammet, N. Tenis, C. L. Denis, and J. Heierhorst, 2005 Ccr4-not complex mRNA deadenylase activity contributes to DNA damage responses in *Saccharomyces cerevisiae*. Genetics 169: 65–75.

Tsukamoto, Y., A. K. Taggart, and V. A. Zakian, 2001 The role of the Mre11-Rad50-Xrs2 complex in telomerase-mediated lengthening of *Saccharomyces cerevisiae* telomeres. Curr. Biol. 11: 1328–1335.

Vernon, M., K. Lobachev, and T. D. Petes, 2008 High rates of "unselected" aneuploidy and chromosome rearrangements in *tel1 mec1* haploid yeast strains. Genetics **179:** 237–247.

Weinert, T. A., G. L. Kiser, and L. H. Hartwell, 1994 Mitotic checkpoint genes in budding yeast and the dependence of mitosis on DNA replication and repair. Genes Dev. 8: 652–665.

Westmoreland, T. J., J. R. Marks, J. A. Olson Jr., E. M. Thompson, M. A. Resnick *et al.*, 2004 Cell cycle progression in G1 and S phases is *CCR4* dependent following ionizing radiation or replication stress in *Saccharomyces cerevisiae*. Eukaryot. Cell 3: 430–446.

Winzeler, E. A., D. D. Shoemaker, A. Astromoff, H. Liang, K. Anderson *et al.*, 1999 Functional characterization of the *S. cerevisiae* genome by gene deletion and parallel analysis. Science (New York, N.Y.) 285: 901–906.

Wong, K. K., S. Chang, S. R. Weiler, S. Ganesan, J. Chaudhuri *et al.*, 2000 Telomere dysfunction impairs DNA repair and enhances sensitivity to ionizing radiation. Nat. Genet. 26: 85–88.

Woo, S. R., J. E. Park, K. M. Juhn, Y. J. Ju, J. Jeong *et al.*, 2012 Cells with dysfunctional telomeres are susceptible to reactive oxygen species hydrogen peroxide via generation of multichromosomal fusions and chromosomal fragments bearing telomeres. Biochem. Biophys. Res. Commun. 417: 204–210.

Woolstencroft, R. N., T. H. Beilharz, M. A. Cook, T. Preiss, D. Durocher *et al.*, 2006 Ccr4 contributes to tolerance of replication stress through control of *CRT1* mRNA poly(A) tail length. J. Cell Sci. 119: 5178–5192.

Wu, Y., S. Xiao, and X. D. Zhu, 2007 MRE11–RAD50–NBS1 and ATM function as co-mediators of TRF1 in telomere length control. Nat. Struct. Mol. Biol. 14: 832–840.

Wu, Y., P. A. Dimaggio Jr., D. H. Perlman, V. A. Zakian, and B. A. Garcia, 2013 Novel phosphorylation sites in the *S. cerevisiae* Cdc13 protein reveal new targets for telomere length regulation. J. Proteome Res. 12: 316–327.

Zhao, X., A. Chabes, V. Domkin, L. Thelander, and R. Rothstein, 2001 The ribonucleotide reductase inhibitor Sml1 is a new target of the Mec1/Rad53 kinase cascade during growth and in response to DNA damage. EMBO J. 20: 3544–3553.

Zou, L., and S. J. Elledge, 2003 Sensing DNA damage through ATRIP recognition of RPA-ssDNA complexes. Science 300: 1542–1548.

Communicating editor: N. M. Hollingsworth

GENETICS

Supporting Information
http://www.genetics.org/lookup/suppl/doi:10.1534/genetics.113.149849/-/DC1

Novel Connections Between DNA Replication, Telomere Homeostasis, and the DNA Damage Response Revealed by a Genome-Wide Screen for *TEL1/ATM* Interactions in *Saccharomyces cerevisiae*

Brian D. Piening, Dongqing Huang, and Amanda G. Paulovich

DOI: 10.1534/genetics.113.149849

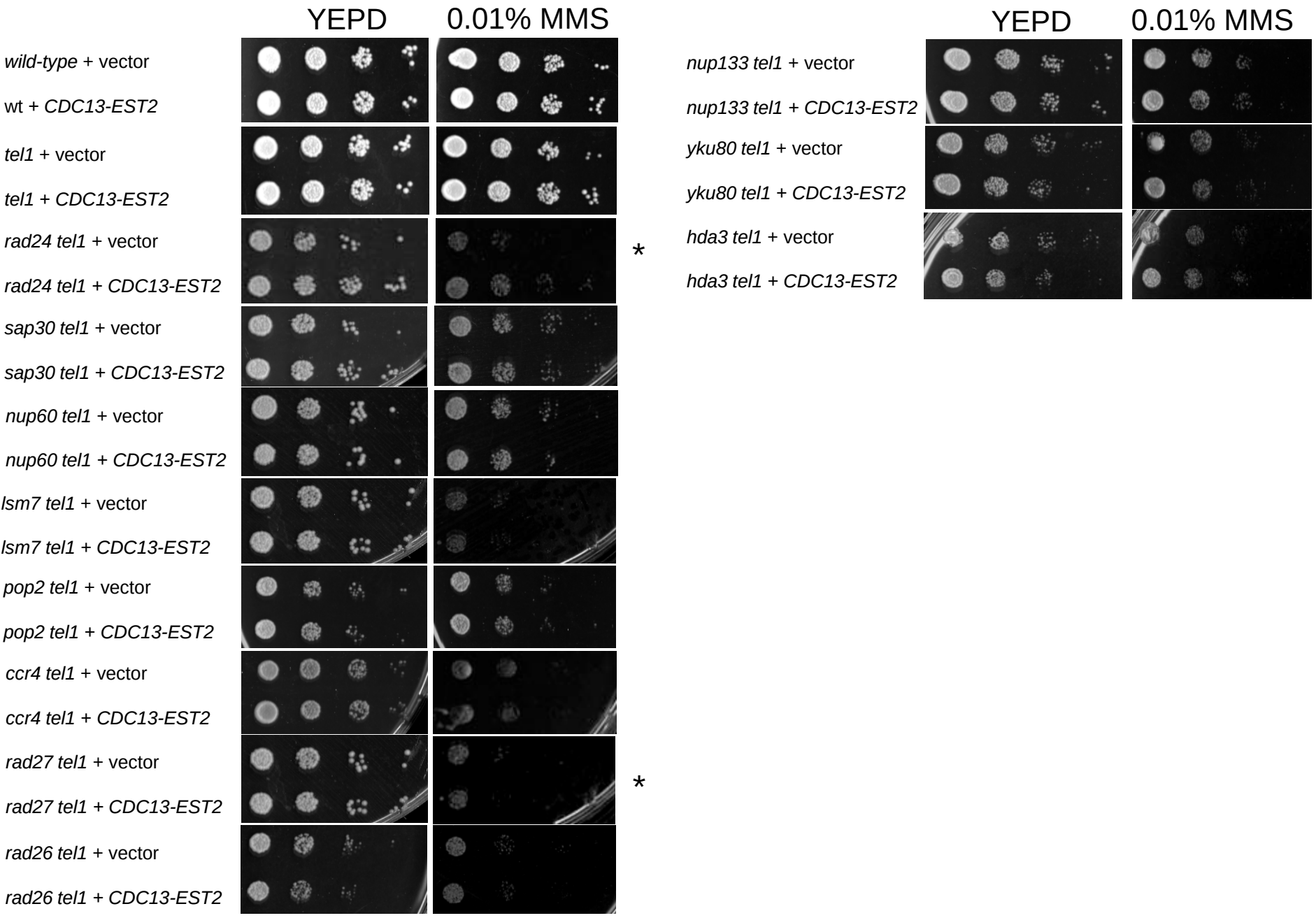

Figure S1 MMS sensitivity with or without the *CDC13-EST2* fusion construct. Strains containing either an empty vector or a *CDC13-EST2* fusion plasmid were cultured in selective media, serially diluted and spotted onto YEPD+/- MMS plates. An asterisk indicates that 0.005% MMS plates were used due to strain sensitivity.

Molecular and Cellular Biology

The Preference for Error-Free or Error-Prone Postreplication Repair in Saccharomyces cerevisiae Exposed to Low-Dose Methyl Methanesulfonate Is Cell Cycle Dependent

Dongqing Huang, Brian D. Piening and Amanda G. Paulovich

Mol. Cell. Biol. **2013, 33(8):1515. DOI: 10.1128/MCB.01392-12.**
Published Ahead of Print 4 February 2013.

MCB
Journals.ASM.org

The Preference for Error-Free or Error-Prone Postreplication Repair in *Saccharomyces cerevisiae* Exposed to Low-Dose Methyl Methanesulfonate Is Cell Cycle Dependent

Dongqing Huang,[a] Brian D. Piening,[b] Amanda G. Paulovich[a]

Fred Hutchinson Cancer Research Center, Seattle, Washington, USA[a]; Molecular and Cellular Biology Program, University of Washington, Seattle, Washington, USA[b]

Cells employ error-free or error-prone postreplication repair (PRR) processes to tolerate DNA damage. Here, we present a genome-wide screen for sensitivity to 0.001% methyl methanesulfonate (MMS). This relatively low dose is of particular interest because wild-type cells exhibit no discernible phenotypes in response to treatment, yet PRR mutants are unique among repair mutants in their exquisite sensitivity to 0.001% MMS; thus, low-dose MMS treatment provides a distinctive opportunity to study postreplication repair processes. We show that upon exposure to low-dose MMS, a PRR-defective *rad18*Δ mutant stalls into a lengthy G_2 arrest associated with the accumulation of single-stranded DNA (ssDNA) gaps. Consistent with previous results following UV-induced damage, reactivation of Rad18, even after prolonged G_2 arrest, restores viability and genome integrity. We further show that PRR pathway preference in 0.001% MMS depends on timing and context; cells preferentially employ the error-free pathway in S phase and do not require *MEC1*-dependent checkpoint activation for survival. However, when PRR is restricted to the G_2 phase, cells utilize *REV3*-dependent translesion synthesis, which requires a *MEC1*-dependent delay and results in significant hypermutability.

The DNA damage response (DDR) employs a signal transduction network to delay cell cycle progression and promote DNA repair (1). While it is well known that DNA damage checkpoints are critical for maintaining genome integrity, how the cell balances between checkpoint arrest and cell proliferation in the setting of constant endogenous and exogenous sources of DNA damage (~20,000 lesions per day per human cell) remains a critical question (2, 3). For example, cells utilize excision repair and DNA damage tolerance pathways without significant delay of the cell cycle to address low levels of DNA damage (such as spontaneous base lesions), yet when responding to a higher level of DNA damage, these processes become tightly integrated with cell cycle delay (1). For genotoxic agents, there is a dose threshold below which checkpoint activation is minimal despite measurable activity of DNA repair pathways (4, 5); this threshold may vary, depending on the damaging agent, organism, and cell type. We (6) and others (4) have described novel cellular phenotypes that manifest only in response to low doses of DNA-damaging agents; however, the field lacks a consistent definition of what constitutes a low dose. To generalize this phenomenon, we propose the definition of a "low dose" of a damaging agent as a treatment condition that does not cause discernible DNA damage sensitivity in treated wild-type cells yet manifests discernible biological effects (such as sensitivity) in mutant genetic backgrounds. While other definitions are equally valid, this definition is not agent specific and thus allows for a comparison of results spanning multiple genotoxic agents. Our use of the terms "low dose" and "high dose" in this study refers to this distinction.

DNA-alkylating agents (methyl methanesulfonate [MMS], ethylmethanesulfonate [EMS], melphalan, etc.) are of particular interest at low doses, as this class of genotoxic agents encompasses a number of natural and industrial environmental carcinogens (2). Alkylating agents induce DNA damage by transferring methyl groups to oxygen or nitrogen atoms of DNA bases, resulting in highly mutagenic DNA base lesions, such as O^6-methylguanine and N^3-methyladenine (2, 7). Use of such agents at high doses (most prominently the monofunctional agent MMS) have aided in the discovery of novel DDR genes and the elucidation of many biochemical processes underlying the DDR (8–11). While these studies have relied specifically on high doses of MMS, there is reason to believe that the cellular response to exposure to a low dose of MMS is executed differently (5, 6).

Recent work has begun to characterize the differences between low- and high-dose DNA damage responses (4, 6). In a recent study chronicling novel, low-dose-specific DDR phenotypes, Hishida et al. continuously exposed yeast cells to low-dose UV light (0.1 J/m^2/min) over a period of multiple days in order to mimic how yeast might cope with sunlight-induced UV damage in the wild (4). They tested a panel of strains defective for different components of DDR pathways, and the results were striking: only mutants comprising members of postreplicative repair (PRR) pathways exhibited any sensitivity to chronic low-dose UV treatment, and despite this, the sensitivity of these mutants was extreme. Moreover, they showed that while wild-type cells cycle normally in low-dose UV, a PRR-defective *rad18*Δ mutant rapidly synchronizes into prolonged G_2 arrest (4).

PRR facilitates the bypass (rather than the repair) of base lesions through either an error-prone polymerase switch or an error-free template switch mechanism (12–14). The polymerase switch pathway involves a switch to an error-prone translesion synthesis (TLS) polymerase that can catalyze DNA synthesis

Received 15 October 2012 Returned for modification 15 November 2012
Accepted 30 January 2013
Published ahead of print 4 February 2013
Address correspondence to Amanda G. Paulovich, apaulovi@fhcrc.org.

doi:10.1128/MCB.01392-12

across a damaged template by inserting a noncognate nucleotide (13–15). In contrast, the template switch mechanism is error free and utilizes the newly synthesized sister chromatid as a template for DNA synthesis across the damaged base (13, 14, 16). Both pathways are initiated by the Rad6/Rad18-mediated ubiquitination of PCNA; the monoubiquitination of PCNA at K164 triggers TLS; however if this site is further polyubiquitinated by Ubc13-Mms2-Rad5, the cell instead employs an error-free template switch (12). The conditions that determine PRR pathway choice are not yet understood.

While the work of Hishida et al. has chronicled the requirement for PRR for survival under chronic low-dose UV treatment conditions, significant questions remain. It is unknown whether this PRR reliance is low-dose UV specific or if it extends to low doses of other DNA-damaging agents. Moreover, Hishida et al. screened a small panel of known DNA repair mutants for low-dose UV sensitivity; it is unknown whether genes outside this panel of canonical DNA repair genes are also required for survival under low-dose conditions. If under low-dose conditions the PRR pathway is predominantly responsible for cell survival, then this genotoxic context presents a tremendous opportunity for detailed studies of PRR mechanisms with minimal competition from repair processes and without the need for additional mutations.

In order to address these outstanding questions, we performed the first genome-wide screen for mutants that cause sensitivity to low-dose MMS. We show that mutants in PRR pathways are exquisitely sensitive to 0.001% MMS, while mutants that function in end resection and homologous recombination (HR)-intermediate processing exhibit only mild sensitivity. We show that in low-dose MMS, loss of PRR function is associated with prolonged G_2 arrest that is likely due to unrepaired single-stranded DNA (ssDNA) gaps occurring during DNA replication. Reactivation of PRR during this arrest restores cell viability, restarts cell cycle progression, and restores ssDNA to intact chromosomal double-stranded DNA (dsDNA) but results in significant mutagenesis. We show that, unlike PRR during the S phase, which favors the error-free pathway, delayed PRR activation results in DNA repair predominantly by error-prone translesion synthesis. Elucidation of these phenotypes was made possible by specifically utilizing continuous low-dose MMS treatment, in which S-phase progression is unaffected and wild-type cells rely on tolerance pathways to facilitate DNA replication.

MATERIALS AND METHODS

Strains, medium, and growth conditions. The *S. cerevisiae* strains used in this study are listed in Table 1. Strain BY4741 was obtained from Open Biosystems. All of the other strains used in this study are derived from BY4741. YPD medium contains 1% yeast extract, 2% peptone, and 2% glucose. YPG medium contains a 2% concentration of galactose to induce the expression of genes under the control of the *pGAL1* promoter. MMS was purchased from Acros Organics (AC254609). YPD plates containing MMS were prepared approximately 15 h prior to use.

Gene disruptions and integrations. All gene disruptions and integrations were achieved by homologous recombination at their respective chromosomal loci by standard PCR-based methods (17). Briefly, a deletion cassette with a 0.5-kb region flanking the target open reading frame (ORF) was amplified by PCR from the corresponding *xxx*Δ::*KANMX* strain of the deletion array (Open Biosystems) and transformed into the target strain for gene knockout. The primers used in the gene disruptions were designed using 20-bp sequences that are 0.5 kb upstream and downstream of the target gene (18).

TABLE 1 *Saccharomyces cerevisiae* strains

Strain[a]	Genotype	Source
BY4741	*MATa his3Δ1 leu2Δ0 met15Δ0 ura3Δ0*	Open Biosystems
yDH125	*MATa BY4741 mec1*ΔKAN^r *sml1*ΔNAT^r	This study
yDH143	*MATa BY4741 rev3*ΔNAT^r	This study
yDH156	*MATa BY4741 rad9*ΔKAN^r *rad57*ΔNAT^r	This study
yDH157	*MATa BY4741 mag1*ΔKAN^r *rad57*ΔNAT^r	This study
yDH159	*MATa BY4741 mag1*ΔKAN^r *rad9*ΔNAT^r	This study
yDH162	*MATa BY4741 pGAL-RAD18::HIS3MX6*	This study
yDH179	*MATa BY4741 pGAL-RAD18::HIS3MX6 rad57*ΔKAN^r	This study
yDH183	*MATa BY4741 sml1*ΔNAT^r *mec1ΔHIS3MX6 mms2*ΔKAN^r	This study
yDH184	*MATa BY4741 sml1*ΔNAT^r *mec1ΔHIS3MX6 rev3*ΔKAN^r	This study
yDH215	*MATa BY4741 rad18*ΔKAN^r *pGAL-RAD57::HIS3MX6*	This study
yDH227	*MATa BY4741 rad18*ΔKAN^r	This study
yDH231	*MATa BY4741 rad18*ΔKAN^r *rad57*ΔNAT^r	This study
yDH237	*MATa BY4741 rad9*ΔNAT^r *rad18*ΔKAN^r	This study
yDH240	*MATa BY4741 rad18*ΔNAT^r *mag1*ΔKAN^r	This study
yDH253	*MATa BY4741 pGAL-RAD18::HIS3MX6 mms2*ΔKAN^r	This study
yDH254	*MATa BY4741 pGAL-RAD18::HIS3MX6 rev3*ΔKAN^r	This study
yDH341	*MATa BY4741 srs2*ΔNAT^r *rad18*ΔKAN^r *pGAL-RAD57::HIS3MX6*	This study
yDH342	*MATa BY4741 mms2*ΔKAN^r *rev3*ΔNAT^r	This study
yDH343	*MATa BY4741 mec1*ΔKAN^r *sml1*ΔNAT^r *pGAL-RAD18::HIS3MX6*	This study
yDH346	*MATa BY4741 rad6*ΔKAN^r	This study
yDH347	*MATa BY4741 rad57*ΔKAN^r	This study
yDH348	*MATa BY4741 rad52*ΔKAN^r	This study
yDH349	*MATa BY4741 mag1*ΔKAN^r	This study
yDH350	*MATa BY4741 rad9*ΔKAN^r	This study
yDH352	*MATa BY4741 top3*ΔKAN^r	This study
yDH353	*MATa BY4741 rad5*ΔKAN^r	This study
yDH354	*MATa BY4741 mre11*ΔKAN^r	This study
yDH355	*MATa BY4741 sgs1*ΔKAN^r	This study
yDH356	*MATa BY4741 esc2*ΔKAN^r	This study
yDH357	*MATa BY4741 xrs2*ΔKAN^r	This study
yDH358	*MATa BY4741 mms22*ΔKAN^r	This study
yDH359	*MATa BY4741 rad50*ΔKAN^r	This study
yDH360	*MATa BY4741 rtt101*ΔKAN^r	This study
yDH361	*MATa BY4741 rmi1*ΔKAN^r	This study
yDH362	*MATa BY4741 mms1*ΔKAN^r	This study
yDH363	*MATa BY4741 mms2*ΔKAN^r	This study
yDH399	*MATa BY4741 exo1*ΔKAN^r *pGAL-RAD18::HIS3MX6*	This study

[a] The wild-type strain is BY4741 (S288C). All the other strains are derived from BY4741.

For gene disruptions utilizing the *NATMX* or *HIS3MX* cassette, the *xxx*Δ::*KANMX* strain from the deletion array was converted to *xxx*Δ::*NATMX* or *xxx*Δ::*HIS3MX*. The cassette conversion was achieved by amplifying the *NATMX* or *HIS3MX* cassette with primers MX-F (5′-ACATGGAGGCCCAGAATACCCT-3′) and MX-R (5′-CAGTATAGCGACCAGCATTCAC-3′) from plasmids p4339 and pFA6a-His3MX6-pGAL1, respectively (17, 19), and the resulting PCR product was used to transform the *xxx*Δ::*KANMX* strain (the *-MX* cassettes each carry an identical 5′ TEF promoter and 3′ terminator, which facilitates the *KANMX*::*NATMX* or *KANMX*::*HISMX* conversion).

In order to integrate the *pGAL1* promoter into the −1 position of the *RAD18* and *RAD57* genes, a region of plasmid pFA6a-His3MX6-pGAL1 was amplified by PCR using primers that contain 55 bp of *RAD18* or *RAD57* gene sequence (−55 to −1 and +1 to +55), followed by 20 bp homologous to pFA6a-His3MX6-pGAL1 (17). The PCR product was used to transform the indicated target yeast strains and replaced the endogenous *RAD18* or *RAD57* promoter with the *pGAL1* promoter and *HIS3MX* marker. For *pGAL-RAD18*, the primers used were 5′AAACCATCCGCAAGTGAGCATCACAGCTACTAAGAAAAGGCCATTTTTACTACTCGAATTCGAGCTCGTTTAAAC-3′ and 5′-CAGGCTCGGTATTGAAGTAGTCGTGAAGTCGCTTGCAGTGGTTATTTGGTGGTCCATTTGAGATCCGGGTTTT-3′, and for *pGAL-RAD57*, the primers used were 5′-ATGAAAATGATGAACAACCACTGGGAATTCACCATTTTTCAAAGTGTGTAAATTCGAATTCGAGCTCGTTTAAAC-3′ and 5′-TTCATCGTAAAGGTCCATATACGTATTGTCAAATTTTATTGATAAGGCCCTAGGCATTTTGAGATCCGGGTTTT-3′.

Genome-wide low-dose sensitivity screen. The deletion array of ~4,700 viable yeast single-gene knockout strains (Open Biosystems) was replica pinned onto YPD and YPD plus 0.001% MMS plates using a 384-floating-pin replicator (V&P Scientific Inc.). The plates were incubated at

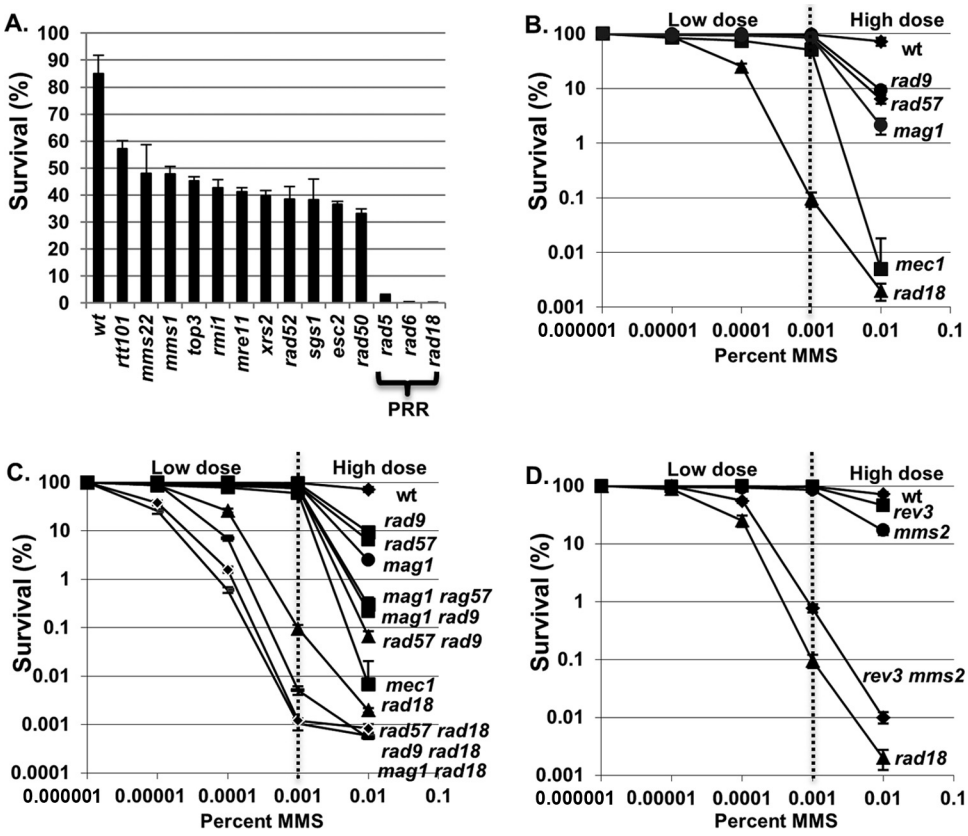

FIG 1 Postreplication repair pathways are required for survival in low-dose MMS. (A) Reconfirmed low-dose sensitivity mutants. Reconstructed yeast deletion mutants were grown to log phase in YPD medium with 0.001% MMS. Cells were taken out after 5 h of incubation at 30°C. Viable cells were determined by the number of CFU on YPD plates after 3 days of incubation at 30°C. Three independent transformants of each strain were tested, and the error bars indicate the standard deviations of viability measurements. wt, wild type. (B) Survival of a *rad18*Δ mutant strain in low-dose MMS compared to other DDR mutants. A panel of yeast mutants was exposed to the indicated concentrations of MMS during log-phase growth. Cells were removed after 5 h of incubation at 30°C and spread onto YPD plates. Viable cells were determined by the number of CFU after 3 days of incubation at 30°C. Each kill curve represents the mean viability from three independent experiments, and the error bars represent the standard deviations of the mean. (C) Survival of *rad18*Δ in low-dose MMS in combination with other DDR mutants. The indicated yeast mutant strains were grown in YPD medium with or without the indicated concentrations of MMS. Cells were taken out after 5 h of incubation at 30°C and spread onto YPD plates. Viable cells were determined by the number of CFU after 3 days of incubation at 30°C. Each kill curve represents the mean of three independent experiments, and the error bars represent the standard deviations of the mean. (D) Either branch of PRR is sufficient for cell survival in low-dose MMS. Wild-type and PRR mutant strains were exposed in log phase to various concentrations of MMS for 5 h. Cells were removed after the exposure and plated on YPD plates for determination of the survival rate as described above. Each kill curve represents the mean viability from three independent experiments, and the error bars represent the standard deviations of the mean.

30°C for 24 h before being scored for growth. The screen was subsequently repeated to control for false positives. Of note, in the initial screen, a *rad18*Δ mutant was not sensitive to 0.001% MMS, while its partner, *rad6*Δ, exhibited strong MMS sensitivity. We independently constructed a *rad18*Δ::*KANMX* gene knockout in a wild-type (BY4741) background, as described above. This newly constructed strain exhibited strong sensitivity to 0.001% MMS (identical to that of *rad6*Δ) (Fig. 1), leading us to believe that our original *rad18*Δ::*KANMX* library strain was of incorrect genotype or harbored a suppressor mutation. For follow-up studies, we used the newly constructed *rad18*Δ.

MMS kill curves. Cells (5×10^7) were harvested from log-phase cultures and resuspended in 10 ml fresh YPD medium with or without MMS (prepared from a master batch of YPD or YPD plus MMS). In order to reduce variability due to the extremely low doses examined in this study, a fresh master mix of 0.1% MMS in YPD medium was prepared, and lower concentrations were achieved by further diluting a proportion of the master mix with YPD. Following the addition of MMS, cultures were incubated at 30°C, and aliquots were taken out after 5 h of incubation (for MMS concentration-dependent kill curves) or at given intervals (for time course experiments). The cells were resuspended in PBS plus 5% sodium thiosulfate (to inactivate the MMS). The cells were sonicated, and cell concentrations were assessed using a Coulter Counter. Viability was determined by plating serial dilutions of cultures onto YPD (or YPG) plates and scoring the number of CFU after 3 to 4 days at 30°C. Viability was calculated as CFU/total cells.

Calculation of MMS-induced mutation frequency. The mutation frequency due to MMS treatment was measured by selection for canavanine resistance (due to forward mutation of the *CAN1* gene) after MMS treatment. Log-phase cells were exposed to MMS in liquid cultures for 5 h at 30°C as described above. Following MMS treatment, the cells were resuspended in PBS plus 5% sodium thiosulfate and subsequently serially diluted and plated onto synthetic defined medium (SD)-Arg-Ser plus 60 mg/liter canavanine (for the measurement of mutation rates) and YPD medium (for viability measurements). The plates were incubated at 30°C for 3 days, and mutations were assessed as the number of CFU on canavanine plates. MMS-induced mutation rates were determined by subtracting the number of mutations observed for cells without MMS treatment. Mutation rates are expressed as the number of canavanine-resistant cells per 10^6 viable cells.

Synchronization and cell cycle analysis. Cells were synchronized in the G_1 phase by the addition of α-factor (Zymo Research; catalog number Y1001) at a final concentration of 5 μM to log-phase cultures or cultures released from G_2 arrest (see below). Cultures were incubated in α-factor for 2 to 3 h at 30°C to achieve G_1 arrest, which was verified microscopically and by fluorescence-activated cell sorter (FACS) analysis. To release cells from G_1 arrest, cells were harvested and washed once with 1 ml of phosphate-buffered saline (PBS) and resuspended in 10 ml fresh YPD medium containing 10 μg/ml pronase (Fisher Scientific; catalog number 50-720-3354). For G_2/M synchronization, 10 μg/ml of nocodazole (Toronto Research Chemicals Inc.; catalog number M330350) was added to log-phase cultures or cultures released from G_1 arrest, and the cells were incubated for 2 h at 30°C. G_2-arrested cells were verified microscopically (as large-budded cells) and by FACS analysis. Cell cycle distributions were determined by flow cytometry (by a method described previously [20]) using a Beckman-Dickson FACSCalibur flow cytometer.

Western blotting. Cell extracts were prepared from log-phase cells, as well as synchronized cells, using a trichloroacetic acid (TCA) lysis method (21). Proteins were analyzed by SDS-PAGE (22). Rad53p was detected with the yC-19 anti-Rad53 antibody (Santa Cruz).

PFGE. To analyze intact yeast chromosomal DNA by pulsed-field gel electrophoresis (PFGE), DNA plugs were prepared using a CHEF (contour-clamped homogeneous electric field) Genomic DNA plug Kit (Bio-Rad; catalog number 170-3591) according to the manufacturer's instructions. Briefly, cells ($\sim 2 \times 10^8$) were harvested at different time points and fixed in 70% ethanol. Following ethanol fixation, the cells were resuspended in 200 μl of suspension buffer (10 mM Tris, pH 7.2, 20 mM NaCl, 50 mM EDTA) and mixed with an equal volume of 2% CleanCut low-melting-point agarose at 50°C. The hot mixture was quickly pipetted into the manufacturer-supplied plug molds and allowed to solidify (each sample produced 3 plugs). In-gel cell lysis was performed by adding lyticase (1 mg/ml) for 2 h at 37°C, followed by 1 mg/ml proteinase K treatment for 24 h at 37°C. In order to test whether the nondenatured DNA sample contained S1-labile ssDNA, a subset of the DNA plugs were digested with 1 U of S1 nuclease (Sigma; catalog number N5661) for 40 min at 30°C in S1 nuclease buffer containing 1 mM phenylmethylsulfonyl fluoride (PMSF) (the undigested set was incubated in the same buffer without S1 nuclease). Both sets of plugs were then loaded on a 1% Megabase agarose gel (Bio-Rad), and genomic DNA was resolved using a Bio-Rad CHEF-DR II system according to the manufacturer's instructions. Following electrophoresis, the gels were stained in 1% ethidium bromide for 2 h and photographed under UV light.

RESULTS

Postreplication repair is required for survival in response to continuous low-dose MMS exposure. While a genome-wide screen for mutants sensitive to high doses of MMS (0.035%) previously identified 103 sensitive mutant strains (23), we hypothesized that a different spectrum of mutants would be sensitive to low-dose MMS (0.001%). To test this hypothesis, we screened ~4,700 unique gene deletion strains representing the yeast haploid deletion collection (24) for mutations conferring sensitivity to 0.001% MMS. As a small percentage of the library strains have been shown to harbor additional mutations (25, 26), we sought to eliminate any false positives by regenerating all 14 deletion mutants that showed low-dose MMS sensitivity in the initial screen (see Materials and Methods). These new deletion mutants were then retested by quantitative colony-forming assay in response to MMS, and all 14 mutants were confirmed to be sensitive to 0.001% MMS (Fig. 1A). Mutations in the PRR genes *rad5*Δ, *rad6*Δ, and *rad18*Δ conferred particularly high (>100-fold) sensitivity, while the remaining mutants exhibited a milder 2- to 3-fold drop in survival. All of the genes identified as being sensitive to low-dose MMS had been previously identified as sensitive to high-dose MMS (23). To reconfirm that PRR mutants are unique among repair genes in their exquisite sensitivity to low-dose MMS, we performed a verification step in which we quantified the sensitivities of a panel of high-dose MMS-sensitive DDR mutants to a range of MMS exposures to confirm that they do not confer substantial sensitivity to low-dose MMS. This panel comprised genes involved in homologous recombination (HR) (*rad57*Δ), base excision repair (BER) (*mag1*Δ), and checkpoint activation (*rad9*Δ and *mec1*Δ) (Fig. 1B). While a *rad18*Δ mutant exhibited a drop in viability in MMS in a dose-dependent manner down to 0.0001% MMS, none of the other mutants exhibited substantial sensitivity to very low-dose MMS, despite significant sensitivity to high-dose (0.01%) treatment. From these results, we conclude that PRR mutants are highly sensitive to low-dose MMS treatment, whereas mutations in other DNA repair pathways (HR, BER, etc.) show minimal effect. Although the other pathways tested (HR, BER, etc.) are far less critical than PRR under low-dose conditions (i.e., ≤0.001% MMS), combining *rad18*Δ with mutations in *rad57*Δ, *rad9*Δ, or *mag1*Δ resulted in an additive increase in sensitivity to low-dose MMS versus *rad18*Δ alone (Fig. 1C), demonstrating that in the absence of *RAD18* these pathways play a compensatory role.

Either PRR subpathway (error free or error prone) is sufficient for survival in response to low-dose MMS. Cells employ two *RAD18*-dependent PRR mechanisms to tolerate DNA lesions (translesion synthesis and error-free HR-directed bypass). To determine whether *RAD18*-dependent survival in low-dose MMS depends on one or both of these mechanisms, we examined the low-dose MMS sensitivities of representative mutants for each PRR subpathway (*REV3*, which is required for translesion synthesis, and *MMS2*, which is required for error-free PRR [8, 27]). As shown in Fig. 1D, a defect in either PRR subpathway alone (*rev3*Δ or *mms2*Δ) does not affect survival in MMS concentrations of ≤0.001%, while both exhibit sensitivity to high-dose (0.01%) MMS (with *mms2*Δ exhibiting slightly higher sensitivity at this dose). In contrast, loss of both branches (*mms2*Δ *rev3*Δ) results in synergistic hypersensitivity to low-dose MMS (Fig. 1D). Thus, we conclude that either PRR subpathway (error free or error prone) is sufficient for survival in response to low-dose MMS. Notably, the *mms2*Δ *rev3*Δ double mutant is slightly more MMS resistant than a *rad18*Δ strain, suggesting that there is some remaining PRR activity in *mms2*Δ *rev3*Δ (possibly through a Rev1-Rad30-dependent translesion synthesis mechanism) (27, 28).

A G_2/M (but not intra-S) checkpoint is activated in PRR-deficient cells in low-dose MMS. As discussed above, wild-type cells exhibit minimal checkpoint activity in low-dose MMS. However, given the extremely low survival rate of PRR-defective *rad18*Δ cells in low-dose MMS, we hypothesized that the absence of PRR would cause a defect in replication fork progression and possibly activate the intra-S-phase checkpoint (29–31). To test this hypothesis, wild-type and *rad18*Δ cells were synchronized into the G_1 phase with α-factor and released into growth medium containing 0.001% MMS. Wild-type cells completed S phase within 30 to 40 min in the presence or absence of low-dose MMS and progressed through G_2/M, as seen by both flow cytometry and the budding index (Fig. 2A). Unexpectedly, MMS-treated *rad18*Δ cells progressed through S phase with kinetics similar to those of wild-type cells and subsequently arrested with 2C DNA content (Fig. 2A), with more than 80% exhibiting a large-budded morphology, which persisted for the duration of the experiment (180

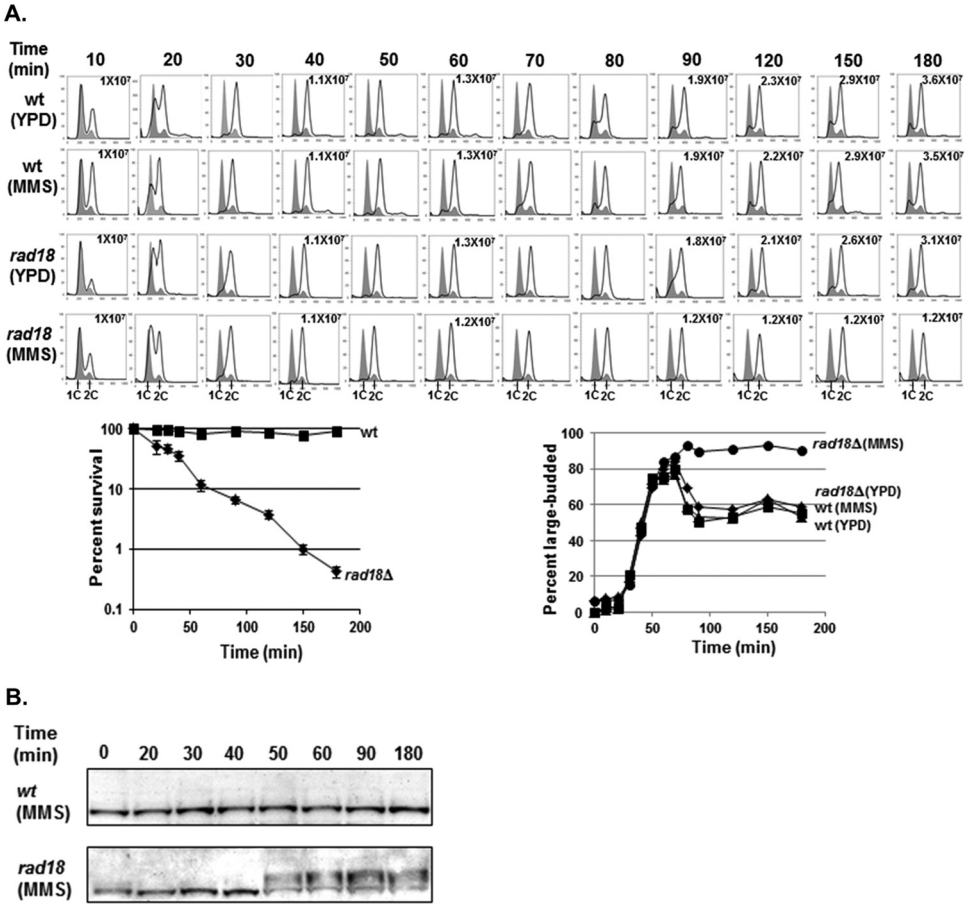

FIG 2 Low-dose MMS activates the G_2/M checkpoint in *rad18*Δ cells. (A) Low-dose MMS triggers G_2/M arrest in *rad18*Δ cells. Wild-type and *rad18*Δ cells were synchronized with α-factor and released into YPD medium ± 0.001% MMS. Cells were removed at the indicated times and analyzed for cell cycle distribution by FACS, for cell morphology by microscopy, and for viability by colony survival assay. Each flow cytometry graph contains two histograms. The shaded histograms represent the cell cycle distribution of α-factor-blocked cultures at time zero. The overlaid histograms represent the cell cycle distributions at various times following release from the G_1 block. The cell number per milliliter is listed for selected time points. Survival curves for wild-type and *rad18*Δ cells at each time point are shown below the cell cycle distribution graphs. Each strain was tested in triplicate, and the error bars represent the standard deviations of mean cell viability. (B) Rad53 phosphorylation in response to 0.001% MMS. Wild-type and *rad18*Δ cells were treated with α-factor and released into YPD medium with 0.001% MMS. Samples were taken out at the indicated times for Western blot analysis with an anti-Rad53 antibody.

min). Thus, *rad18*Δ cells arrest in G_2 phase after exposure to low-dose MMS but do not experience the significant S-phase delay indicative of intra-S-phase checkpoint activation (20, 31).

To confirm that the G_2 arrest of *rad18*Δ cells in low-dose MMS was due to the activation of the G_2/M DNA damage checkpoint, we tested for MMS-induced Rad53 phosphorylation (a G_2/M checkpoint indicator) by Western blotting (21). Indeed, while wild-type cells exhibited no Rad53 phosphorylation in low-dose MMS (consistent with no MMS-dependent changes in cell cycle distribution by FACS), *rad18*Δ cells exhibited Rad53 phosphorylation beginning at ~50 min after the addition of low-dose MMS (Fig. 2B). Of note, Rad53 phosphorylation in *rad18*Δ cells was somewhat delayed after the transition to 2C DNA content by FACS (Fig. 2A and B), suggesting that generating the checkpoint activation signal may require events that occur after the bulk of replication is completed.

Low-dose MMS-induced viability loss in *rad18*Δ cells requires passage through S phase in the presence of MMS. Given that the DDR checkpoint is not activated until after the bulk of replication has been completed, we hypothesized that the G_2/M arrest and the viability loss in *rad18*Δ cells exposed to low-dose MMS are not induced by alkylation lesions directly, but rather, by secondary lesions (such as ssDNA gaps) resulting from incomplete postreplication repair (32, 33). One prediction of this hypothesis is that *rad18*Δ cells exposed to low-dose MMS outside the S phase (i.e., in the G_1 or G_2 phase) should remain viable, since this would preclude the generation of irreparable PRR intermediates. To test this prediction, we induced a mitotic checkpoint arrest in wild-type and *rad18*Δ cells with nocodazole treatment and then released the cells into medium containing both 0.001% MMS and α-factor (to restrict MMS exposure to the G_1 phase). As expected, when the MMS treatment was confined to the G_1 phase (via α-factor treatment), *rad18*Δ cells exhibited significantly higher viability than cells allowed to replicate their genomes in the presence of MMS (no α-factor) (49% viable versus 3.5%) (Fig. 3A). (The ~50% drop in viability with α-factor likely reflects a subset of unrepaired lesions that persist after α-factor is removed; the cells are plated on YPD afterward, at which point they can cycle normally and must cope with any remaining MMS lesions). In conclusion, the MMS sensitivity exhibited by a *rad18*Δ mutant is due

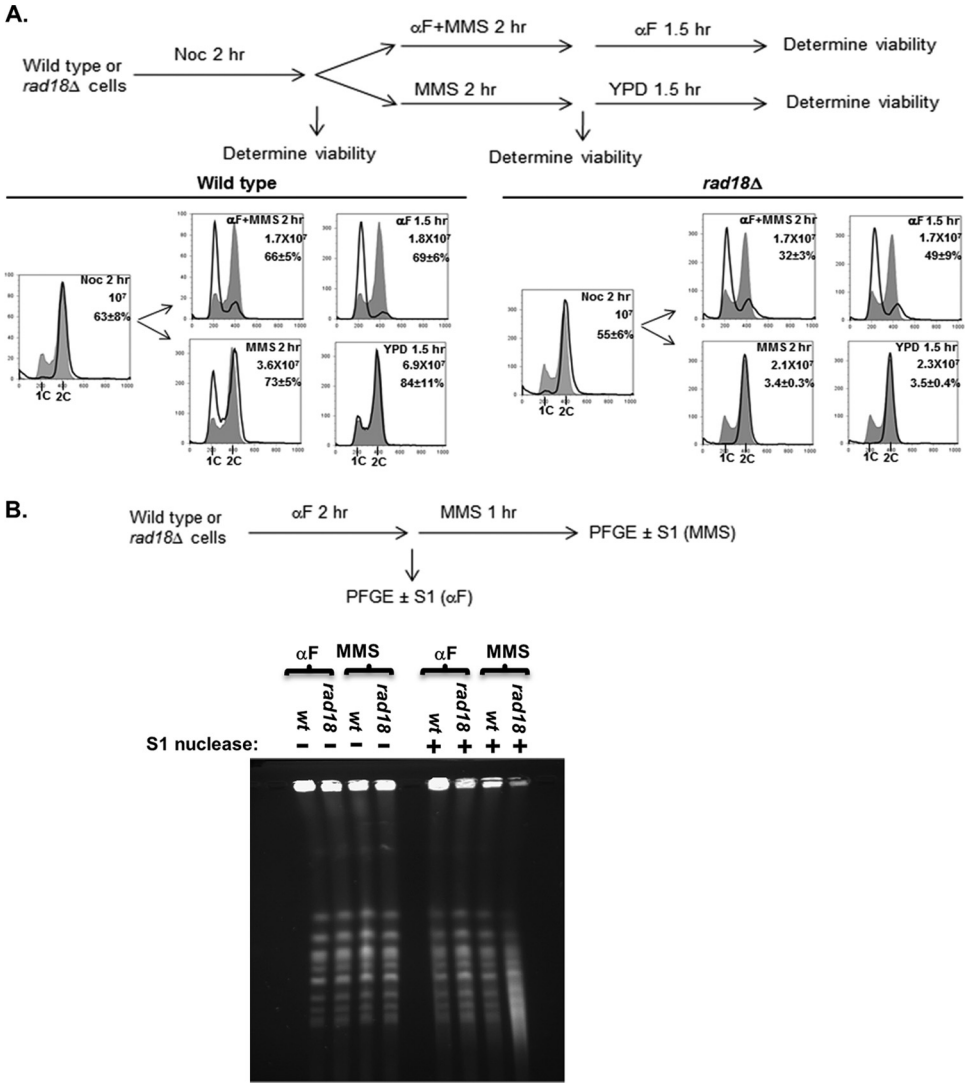

FIG 3 Loss of viability and G_2 arrest in *rad18*Δ cells in low-dose MMS is associated with S phase. (A) Passage through S phase is required for MMS sensitivity. Wild-type and *rad18*Δ cells were synchronized at mitotic checkpoint arrest with nocodazole (Noc) for 2 h and then exposed to 0.001% MMS in the presence or absence of α-factor for a second 2-h period. MMS was then removed, and the cells were incubated for another 1.5 h, with or without α-factor. Cells were withdrawn at the indicated time points for the assessment of cell cycle distributions and survival rates. All incubations occurred at 30°C. In the upper right corner of each graph are shown the duration of treatment, cell number per milliliter, and cell survival percentage at the end of each treatment (each strain was tested in triplicate repeats for survival rates; the mean and standard deviation of the mean survival rate are indicated). The shaded histograms represent the cell cycle distribution of the asynchronous culture before the nocodazole block. The overlaid histograms represent the cell cycle distributions at various times after release. (B) Chromosomes of MMS-treated *rad18*Δ cells show S1 nuclease-sensitive components (ssDNA gaps). α-Factor-blocked wild-type and *rad18*Δ cells were released into YPD medium with 0.001% MMS and 10 μg/ml nocodazole for 60 min. Cells were harvested after α-factor synchronization (αF) and after MMS treatment (MMS). Chromosomal DNA (either S1 treated or mock treated) was analyzed by PFGE.

to DNA damage produced during the S phase, likely caused by a defect in DNA damage tolerance during replication.

Previous reports have demonstrated that cells that enter S phase with irreparable UV lesions generate long stretches of ssDNA, and these ssDNA lesions are later resolved by postreplication repair (32, 33). We hypothesized that low-dose MMS treatment during S phase is also associated with the production of ssDNA gaps that are irreparable in a PRR mutant background (and cause the G_2 arrest). To test this hypothesis, we employed the single-strand-specific S1 endonuclease, which cuts DNA regions containing nicks and ssDNA gaps (34, 35), converting them into double-strand breaks (DSBs) that can be visualized as fragmentation by PFGE (36). Wild-type and *rad18*Δ cells were synchronized in the G_1 phase with α-factor and released into medium containing low-dose MMS (0.001%) plus nocodazole. (The nocodazole treatment was used to arrest wild-type cells at the mitotic checkpoint to minimize the ssDNA component associated with DNA replication and to make the results comparable to those for the G_2-arrested *rad18*Δ cells.) After a 60-min low-dose MMS treatment, chromosomal DNA was isolated in agarose plugs and subjected to S1 nuclease treatment and PFGE (Fig. 3B). For wild-type cells, treatment with low-dose MMS was not associated with detectable S1-dependent chromosomal fragmentation (and thus no ssDNA gaps). In contrast, *rad18*Δ cells exhibited significant

MMS- and S1-dependent chromosomal fragmentation that is indicative of the presence of ssDNA gaps associated with low-dose MMS exposure. From these data, we conclude that the loss of PRR is associated with the production of ssDNA gaps in low-dose MMS, and these lesions are the likely trigger for the prolonged checkpoint activation exhibited by these cells.

Both viability and chromosome integrity in low-dose MMS-treated *rad18*-deficient cells can be rescued in a time-limited fashion by reactivation of *RAD18* in G_2 phase. Recent work has shown that for acute high doses of UV and MMS, PRR can be delayed for a prolonged period past the completion of bulk DNA synthesis and then reactivated to restore a major proportion of cell viability (28, 37). As sensitivity to low-dose MMS for PRR mutants is associated with a prolonged G_2 checkpoint and ssDNA gaps, we hypothesized that reactivation of PRR in these cells would have a 3-fold effect: ssDNA gaps would be eliminated, cells would escape G_2 arrest, and viability would be restored. To test this hypothesis, we constructed a yeast strain harboring a *RAD18* gene under the control of a conditional *GAL* promoter (*GAL-RAD18*) to control the activity of PRR (28). Cells were exposed to low-dose MMS under *RAD18*-repressing conditions (i.e., glucose), and cells were withdrawn at multiple time points for assessment of viability on glucose plates (maintaining *RAD18* repression) and galactose plates (reactivating *RAD18*) (Fig. 4A). As expected, in glucose, cells harboring the *GAL-RAD18* construct exhibited prolonged low-dose MMS-dependent G_2 arrest (data not shown) and loss of viability, mimicking a *rad18*Δ deletion. However, when cells were removed and plated on galactose medium (reactivating *RAD18*) following MMS treatment, there was a marked increase in viability (nearly 100% rescue after up to 4 h in MMS). From these data, we conclude that the loss of viability in PRR-deficient cells in response to low-dose MMS treatment can be rescued by the reactivation of *RAD18*.

Notably, this rescue was evident even after prolonged MMS treatment but began to steadily decrease after the 4-h time point, and no rescue was observed after 8 h in low-dose MMS. We initially hypothesized that the failure to rescue at later time points was a result of new MMS lesions incurred during the prolonged exposure in G_2; however, even after removing the MMS after 3 h, *GAL-RAD18* cells remained arrested, and the galactose-dependent rescue was similarly time limited (data not shown). These data suggest that the loss of *RAD18*-dependent rescue after 8 h was not due to additional MMS lesions but to a secondary mechanism, possibly through further processing of ssDNA to a different lesion irreparable by PRR (32).

To confirm that the *RAD18*-dependent rescue in low-dose MMS correlates with a decrease in ssDNA gaps (indicative of repair by PRR), *GAL-RAD18* cells were exposed to low-dose MMS in glucose medium (*RAD18*-OFF) and then switched to either galactose medium (*RAD18*-ON) or fresh glucose medium in the presence of nocodazole. DNA samples were prepared in agarose plugs and subjected to S1 nuclease digestion and PFGE. As previously observed for *rad18*Δ (Fig. 3B), low-dose MMS-treated *GAL-RAD18* cells in glucose medium exhibited significant S1-dependent chromosomal fragmentation (Fig. 4B). However, when cells were switched to galactose medium (reactivating *RAD18*), a significant reduction in S1 nuclease sensitivity was observed, indicative of the restoration of ssDNA gaps to dsDNA by PRR. From these data, we conclude that the reactivation of *RAD18* after exposure to low-dose MMS is associated with the repair of ssDNA gaps and restoration of cell viability.

The time limit for *RAD18*-dependent rescue in low-dose MMS is *EXO1* dependent. While the reactivation of *GAL-RAD18* restores cell viability in low-dose MMS even after an extended delay (Fig. 4A), we were surprised that the ability to rescue was time limited. It has been previously reported that Exo1 possesses 5′-3′ exonuclease activity, and its processing of NER intermediates generates extended ssDNA gaps (38). We hypothesized that Exo1 enlarges ssDNA gaps in low-dose MMS during the prolonged G_2 arrest (either by a direct resection of the S-phase-dependent ssDNA or by extending new NER ssDNA intermediates that merge with the S-phase-dependent gaps) and that these extended gaps may be irreparable by PRR. This extension of ssDNA gaps into larger PRR-irreparable ssDNA regions could explain the inability to rescue low-dose MMS-treated *GAL-RAD18* cells past 8 h (Fig. 4A). To test this hypothesis, we deleted *EXO1* in a *GAL-RAD18* background and examined cell survival after prolonged incubation in low-dose MMS (Fig. 4C). Indeed, while the galactose-dependent *RAD18* rescue efficiency in an *exo1*Δ background was similar to that of *EXO1* at earlier time points, the ability to rescue cells by reactivation of *RAD18* in *exo1*Δ cells persisted well beyond 8 h. From this, we conclude that the time limit for *RAD18*-dependent rescue in low-dose MMS is due to *EXO1*-dependent resection. Interestingly, we observed a slight drop in rescue in an *exo1*Δ background (Fig. 4C), which may reflect the activities of other nucleases on ssDNA gaps.

Removal of the *SRS2*-dependent block to HR results in an efficient postreplicative rescue independent of *RAD18*. We were surprised that the extreme loss of viability in a *rad18*Δ mutant in low-dose MMS was due to the presence of ssDNA gaps, as it is unclear why these structures could not be repaired by sister chromatid recombination in the G_2 phase in a PRR-independent manner. We hypothesized that while it may be possible for these structures to be physically repaired by recombination, the repression of recombination by some unknown factor suppresses the repair. One candidate for this repression is the Srs2 helicase, which has been shown to suppress HR during DNA replication (39). Deletion of *SRS2* has been shown to rescue a *rad18*Δ mutant after low-dose UV treatment (40). We asked whether a similar effect may occur in low-dose MMS, and especially, whether delayed induction of HR at various time points during the low-dose MMS treatment may be sufficient to rescue *rad18*Δ cells in the absence of *SRS2*. In order to test this, we put *RAD57* under the control of a conditional *GAL* promoter and tested the effects of induction of *RAD57* on cell viability in a *rad18*Δ background. When *rad18*Δ *GAL-RAD57* and *srs2*Δ *rad18*Δ *GAL-RAD57* cells were exposed to low-dose MMS in glucose medium (*RAD57*-OFF), both strains exhibited viability loss and synchronization at G_2/M (Fig. 5A and data not shown). However, when MMS-treated *srs2*Δ *rad18*Δ *GAL-RAD57* cells were plated on galactose medium (reactivating *RAD57*), we observed a complete rescue of viability, indicating that in an *srs2*Δ background, HR can compensate for the loss of *RAD18*.

We note that even when *SRS2* is present, we observed a slight rescue upon reactivation of *GAL-RAD57* (Fig. 5A); this is likely due to *RAD57* overexpression, which may partially overcome *SRS2*-dependent inhibition (Rad57 can physically block Srs2's ability to disrupt Rad51 nucleoprotein filaments) (41). Interestingly, unlike the rescue by *GAL-RAD18*, the reactivation of *GAL-*

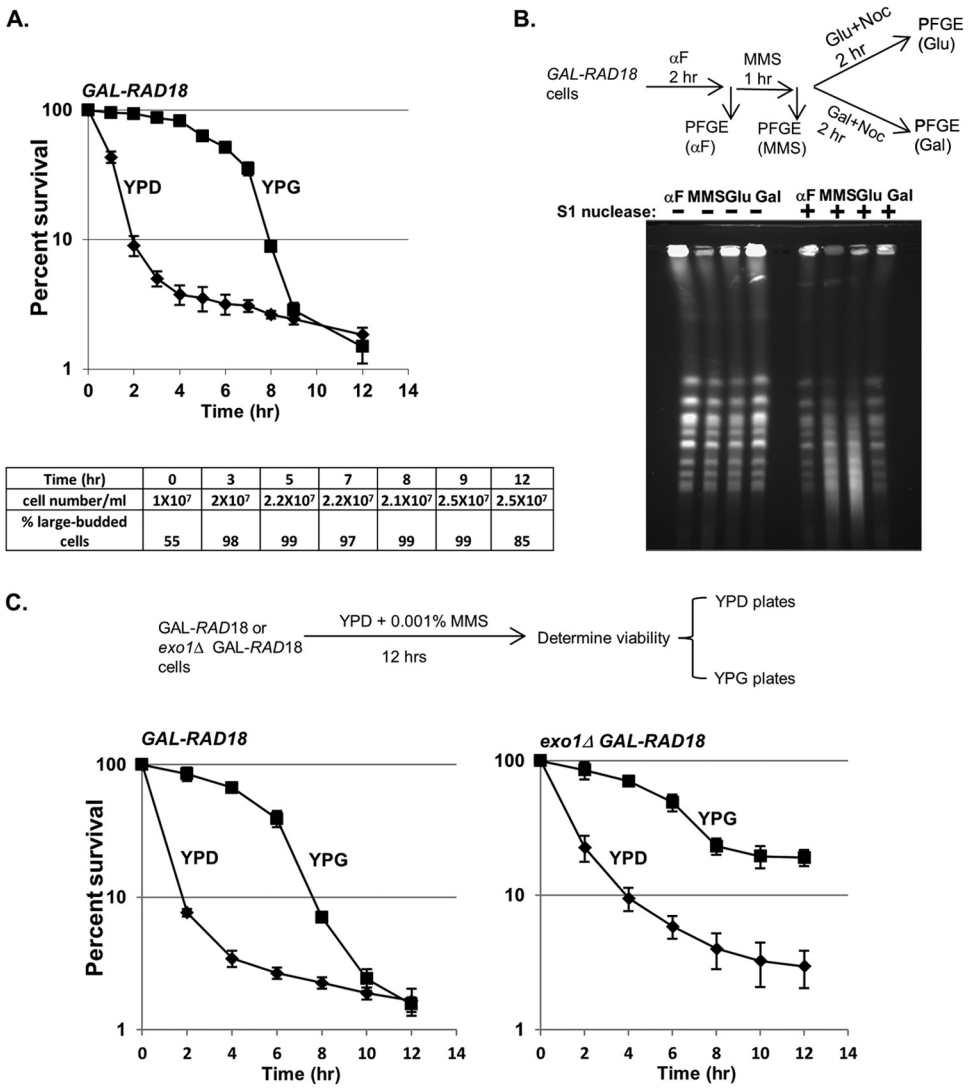

Time (hr)	0	3	5	7	8	9	12
cell number/ml	$1X10^7$	$2X10^7$	$2.2X10^7$	$2.2X10^7$	$2.1X10^7$	$2.5X10^7$	$2.5X10^7$
% large-budded cells	55	98	99	97	99	99	85

FIG 4 Reactivation of Rad18 in G_2 restores viability and chromosome integrity of low-dose MMS-treated *rad18* cells. (A) The viability of PRR-deficient cells can be restored when *RAD18* expression is induced after MMS treatment. Cells harboring a chromosomal *RAD18* gene under the control of a GAL promoter (GAL-*RAD18*) were grown in YPD medium with 0.001% MMS. At the indicated times of exposure, cells were withdrawn and analyzed for plating efficiency on either glucose or galactose plates. Each kill curve represents the mean viability of three independent experiments, and the error bars represent the standard deviations of the mean. At all time points after 2 h of exposure to MMS, the cell density remained essentially unchanged, and *rad18*Δ cells accumulated with a uniform large-budded morphology (bottom). (B) Induction of *RAD18* reduces S1 sensitivity in MMS-treated *GAL-RAD18* cells. *GAL-RAD18* cells were blocked with α-factor, released into YPD medium with 0.001% MMS for 60 min, and then incubated in MMS-free medium containing glucose or galactose for another 2 h in the presence of nocodazole (10 μg/ml). Cells were withdrawn after α-factor synchronization (αF) and MMS exposure and after the subsequent *RAD18* induction (Glu and Gal). Chromosomal DNA was treated with S1 nuclease or mock treated and subjected to PFGE as described for Fig. 3B. (C) The ability for *RAD18*-dependent rescue is prolonged in the absence of *EXO1*. *GAL-RAD18* and *exo1*Δ *GAL-RAD18* cells were grown in YPD with 0.001% MMS for a period of 12 h. The survival rates on glucose or galactose plates were determined as for panel A.

RAD57 allows rescue even after 8 h of MMS exposure (Fig. 5B), suggesting that the *EXO1*-dependent extension of ssDNA can be resolved by HR, but not PRR. From these data, we conclude that *SRS2* represses the HR-dependent repair of ssDNA gaps in PRR-deficient cells.

The preference for error-free and error-prone lesion tolerance is cell cycle dependent. Since *RAD18* is required for the function of either error-free or error-prone PRR, we next asked whether one pathway is more important for survival in low-dose MMS following the reactivation of *GAL-RAD18*. To determine this, we combined the conditional *GAL-RAD18* allele with deletions of either *rev3*Δ (TLS deficient) or *mms2*Δ (error-free-PRR deficient) and tested the abilities of these mutants to be rescued by induction of *GAL-RAD18* at various times during low-dose MMS treatment. While *GAL-RAD18* induction rescued the *mms2*Δ mutant, the efficiency of rescue by activation of *GAL-RAD18* in a *rev3*Δ background was markedly reduced (Fig. 6A), indicating that the postreplicative rescue in low-dose MMS depends on functional translesion synthesis. This is consistent with previous observations for UV lesion bypass (28).

Based on the importance of *REV3*-dependent, error-prone TLS for the rescue of GAL-*RAD18* cells, we predicted that the

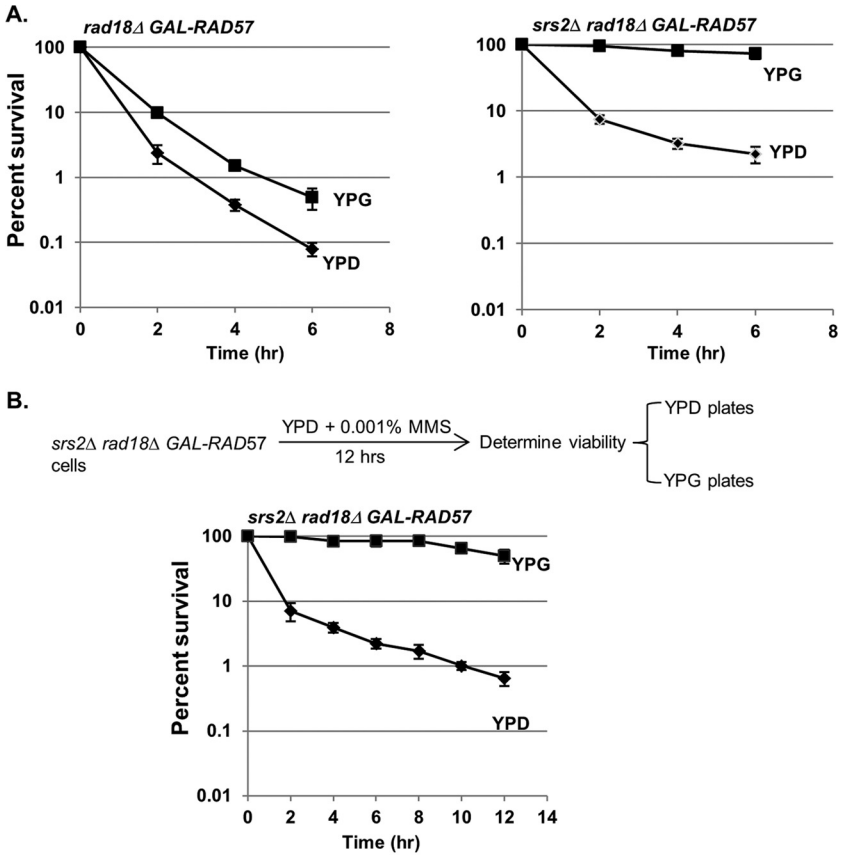

Time (hr)	0	2	4	6	8	10	12
cell number/ml	$7.8X10^6$	$1.4X10^7$	$1.6X10^7$	$1.8X10^7$	$1.9X10^7$	$2.2X10^7$	$2.3X10^7$
% large-budded cells	53	84	87	90	87	85	87

FIG 5 Rescue of *rad18*Δ cells by HR. (A) Induction of *RAD57* results in the rescue of viability in *rad18*Δ cells in the absence of *SRS2*. *rad18*Δ *GAL-RAD57* or *srs2*Δ *rad18*Δ *GAL-RAD57* cells were grown in YPD medium with 0.001% MMS. Kill curves were determined on glucose and galactose plates as described in the legend to Fig. 4A. Each strain was tested in triplicate repeats, and the error bars represent the standard deviations of mean viability. (B) *RAD57* induction rescues viability of *rad18*Δ cells in the absence of *SRS2* after prolonged incubation. *srs2*Δ *rad18*Δ *GAL-RAD18* cells were grown in YPD with 0.001% MMS over a prolonged period (12 h). Cells were withdrawn at the indicated exposure times and analyzed for cell density, cell morphology, and plating efficiency on either YPD or YPG (galactose) plates as described in the legend to Fig. 4A.

reactivation of *RAD18* in G_2 should cause hypermutability in low-dose MMS. To test this prediction, we determined mutation rates in *GAL-RAD18* cells after the induction of *RAD18* following exposure to low-dose MMS for 5 h. As predicted, *GAL-RAD18* cells show significantly elevated MMS-induced mutation rates in low-dose MMS after the induction of *RAD18* compared to wild-type cells (Fig. 6B); this hypermutability is dependent on *REV3* (Fig. 6B), further confirming that inducing PRR in G_2 favors error-prone translesion synthesis. Of note, the *GAL-RAD18* cells exhibited slightly increased mutagenesis relative to the wild type even in the absence of galactose; this likely reflects some low-level *RAD18* expression due to the leakiness associated with the GAL promoter. As a control, we also determined MMS-induced mutation rates in *srs2*Δ *rad18*Δ *GAL-RAD57* cells after *RAD57* induction. While induction of GAL-*RAD57* in G_2 rescues viability in an *srs2*Δ *rad18*Δ mutant (Fig. 5A), this rescue should involve an error-free mechanism and thus should not be associated with hypermutability. As predicted, in contrast to induction of *GAL-RAD18*, hyperactivation of HR after low-dose MMS exposure does not significantly increase the mutation rate (Fig. 6B), indicating that while HR promotes the survival of *rad18*Δ cells in low-dose MMS, this repair involves an error-free mechanism. From these data, we conclude that reactivation of *RAD18*-dependent PRR in G_2 favors the mutagenic translesion synthesis pathway.

Our finding that the error-prone translesion synthesis pathway clearly predominates when *RAD18* is reactivated in G_2 is surprising given previous results showing that the error-free pathway is normally the dominant form of PRR (4, 42). To explain this discrepancy, we hypothesized that the predominance of translesion synthesis may be specific to the G_2 phase, whereas the error-free pathway normally predominates in S phase. Based on this prediction, an error-free-defective *mms2*Δ strain should produce more ssDNA gaps than an error-prone-defective *rev3*Δ strain in low-dose MMS. To test this prediction, we synchronized wild-type, *rev3*Δ, and *mms2*Δ cells in G_1 and released them into growth medium containing 0.001% MMS. While *rev3*Δ cells showed cell cycle progression kinetics similar to those of wild-type cells in low-dose MMS, *mms2*Δ cells exhibited a significant delay in G_2 (30 min) (Fig. 6C). Although MMS-treated *mms2*Δ cells did not ex-

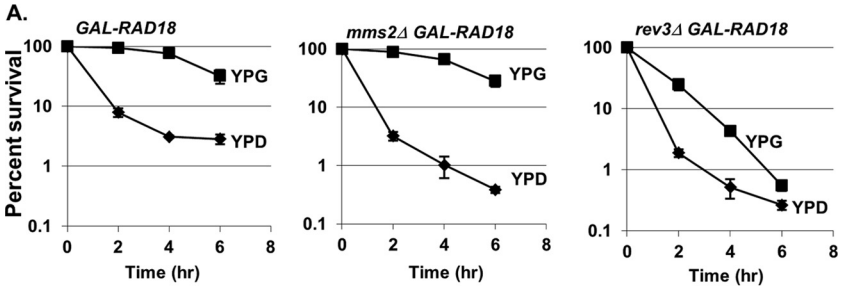

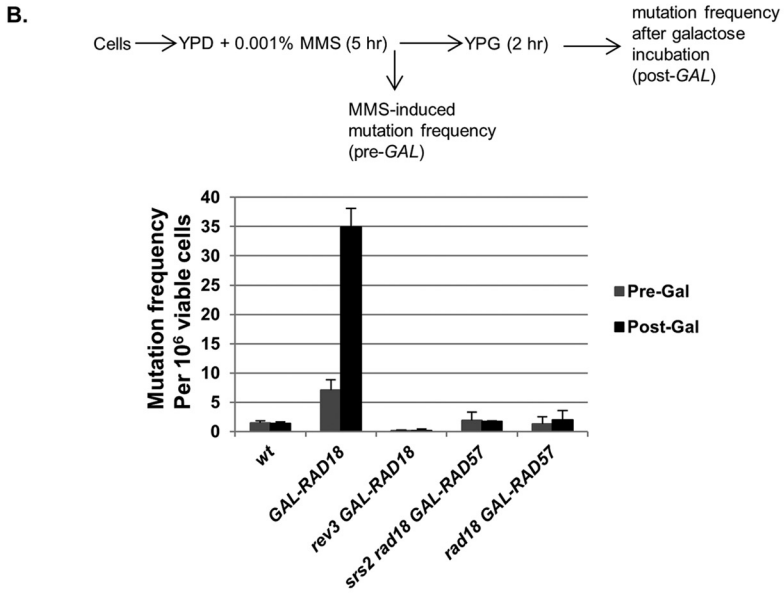

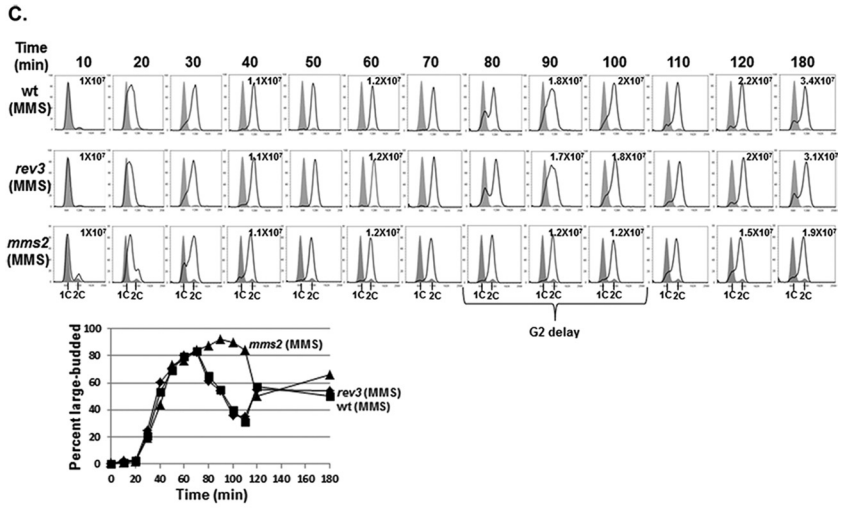

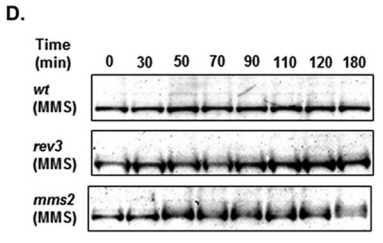

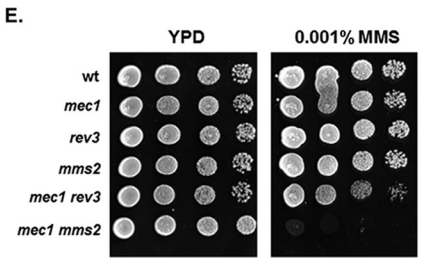

hibit substantially increased levels of Rad53 phosphorylation (Fig. 6D), we found that when *mms2*Δ is combined with deletion of the checkpoint factor *MEC1*, cells fail to grow in low-dose MMS (in contrast, a *rev3*Δ *mec1*Δ strain displays robust growth) (Fig. 6E). From these data, we conclude that loss of the *MMS2*-dependent error-free pathway is associated with a significant G_2 delay and a requirement for *MEC1* for survival in low-dose MMS, while loss of the *REV3*-dependent pathway does not exhibit these phenotypes.

DISCUSSION

Definition of "low-dose" treatment. Our motivation for providing a formal definition for what constitutes a "low dose" of a DNA-damaging agent stemmed from difficulties we experienced in comparing our data with other studies of low-level exposure that span a variety of dose rates, genotoxic agents, and cells/tissues. For example, in previous studies evaluating the role of PRR in response to low-dose UV treatment, Hishida et al. based their choice of UV irradiation dose (0.1 J/m^2/min) on the natural phenomenon (sunlight exposure) that they were attempting to mimic (4, 40); a clear analog for this dose using a chemical carcinogen such as MMS was not immediately apparent. By providing a physiological and agent-agnostic definition of "low-dose" DNA damage based upon the sensitivity of wild-type and mutant cells, we were able to reconcile our MMS results with these previous studies; both 0.1 J/m^2/min UV exposure and 0.001% MMS treatment fail to induce any discernible cellular sensitivity in a wild-type cell population; however, mutant studies reveal an exquisite and profound dependence on PRR for survival in response to low-dose damage (Fig. 1) (4).

PRR mutants are unique in their exquisite sensitivity to low-dose MMS. As the prior Hishida et al. study (4) was UV specific and screened only a small panel of known DDR targets, it remained formally possible that PRR reliance was UV specific or that other, unscreened genes would also be required for survival under low-dose conditions. To answer these questions, we performed a genome-wide screen in response to low-dose treatment with a DNA-alkylating agent (0.001% MMS). Strikingly, we show that while 0.001% MMS treatment of wild-type yeast cells produces no discernible response (for any assay by which we evaluate these cells, including survival [Fig. 1], checkpoint activity [Fig. 2], cell growth and division [Fig. 2], and chromosomal integrity/mutagenesis [Fig. 3B and 6B]), PRR mutants are exquisitely sensitive, and hence DNA damage tolerance is actively employed and critical for viability at this dose. The lethal lesions that render PRR mutants extremely MMS sensitive are unreplicated ssDNA gaps (which can be detected as S1-dependent fragmentation in *rad18* cells by PFGE [Fig. 3B]), and restoration of PRR activity (even after significant delay) eliminates these gaps and rescues cell viability in low-dose MMS (Fig. 4A to C). Due to the exceptional requirement for PRR under low-dose conditions, we were able to glean vital information regarding how PRR functions in the presence (or absence) of cell cycle checkpoints and how timing and context play vital roles in determining which PRR pathway (error free or error prone) is utilized.

The preference for error-free or error-prone PRR is cell cycle dependent. While previous studies have shown a cellular preference for the error-free pathway (4, 42), recent studies using an inducible PRR system show a clear preference for error-prone translesion synthesis (28). In this study, we show that these are not contradictory conclusions, since our data demonstrate that PRR pathway usage depends on timing and context. Specifically, while our data show a preference for the error-free pathway when cells are replicating in low-dose MMS, the error-prone pathway is specifically required for viability when PRR is delayed until the G_2 phase (Fig. 6A). These results provide some clarity with regard to how cells choose error-free versus error-prone repair (in low-dose MMS). During S phase, cells prevent ssDNA gap formation via the *MMS2*-dependent template switch mechanism (without requiring G_2 arrest) but, alternatively, can generate and repair an ssDNA gap using a *REV3*-dependent TLS mechanism (which can be delayed postreplication but requires checkpoint activation). The cell cycle dependence of error-free versus error-prone repair may reflect a necessity for template switching to happen within a brief window of lesion encounter by replicative polymerases, while TLS may be less temporally restricted. Alternatively, cells may directly regulate TLS or error-free factors in a cell cycle-dependent manner in order to carry out this programmed response. Consistent with this hypothesis, *REV1* expression peaks during the G_2 phase of the cell cycle; this transcriptional regulation may be one way in which cells suppress TLS in the S phase but promote it in G_2 (43).

Rescue by reactivation of PRR in MMS has a time limit. The inducible *GAL-RAD18* system also provides information on the stability of ssDNA lesions over a prolonged period. We show that there is a time limit for the delayed repair of ssDNA gaps in G_2/M; the reactivation of PRR is most effective within ~4 h after the initial G_2/M checkpoint activation (Fig. 4A); however, this time limit can be extended by deletion of the Exo1 exonuclease

FIG 6 TLS is required for the rescue of viability upon *RAD18* induction. (A) Reactivation of *RAD18* at G_2 fails to effectively rescue viability in the absence of *REV3*. *GAL-RAD18*, *rev3*Δ *GAL-RAD18*, and *mms2*Δ *GAL-RAD18* cells were exposed to 0.001% MMS over a 6-hour period. Cells were withdrawn at the indicated times during the exposure and analyzed for viability by plating efficiency on either glucose or galactose plates as described for Fig. 4A. Each strain was tested in triplicate repeats, and the error bars represent the standard deviations of the mean. (B) Reactivation of *RAD18* causes hypermutability. Log-phase wild-type, *GAL-RAD18*, or *GAL-RAD57* cells were grown in YPD with 0.001% MMS for 5 h and then incubated in fresh YPG medium for another 2 h. Cells were withdrawn before and after low-dose MMS treatment and before and after galactose incubation (Pre-Gal and Post-Gal) and assayed for viability and the induction of mutation to Can^r. Each strain was tested in triplicate repeats, and the error bars represent the standard deviations of mean viability. (C) *mms2*Δ cells show a G_2 delay in low-dose MMS. Wild-type, *rev3*Δ, and *mms2*Δ cells were synchronized in G_1 with α-factor and released into YPD medium with 0.001% MMS. Cells were removed at the indicated times and analyzed for cell cycle distribution by FACS and for cell morphology by microscopy. Each graph contains two histograms. The shaded histograms represent the cell cycle distribution of α-factor-blocked cultures at time zero. The overlaid histograms represent the cell cycle distribution at the indicated times following release. The cell density in cells per milliliter is listed for selected time points. (D) Detection of Rad53 phosphorylation in wild-type, *mms2*Δ, and *rev3*Δ cells in response to 0.001% MMS. Wild-type, *rev3*Δ, and *mms2*Δ cells were treated with α-factor and released into YPD medium with 0.001% MMS. Samples were taken out at the indicated times for Western blot analysis with an anti-Rad53 antibody. (E) Interactions between *mec1* and PRR mutants in low-dose MMS. The wild type and the indicated mutant strains were grown in YPD to saturation overnight at 30°C. Serial 10-fold dilutions were spotted onto YPD and YPD plus 0.001% MMS plates. (The *mec1*Δ strain is *sml1*Δ *mec1*Δ. The *sml1*Δ single mutation does not affect growth or survival at the tested MMS concentrations [data not shown]).

(Fig. 4C). From these data, we hypothesize that *EXO1*-associated extension of ssDNA gaps leads to large regions of ssDNA that are irreparable by *REV3*-dependent translesion synthesis. There are multiple possible mechanisms. For example, Exo1 could perform end resection directly on the ssDNA-dsDNA junctions at the end of each gap, similar to its role in resection of NER intermediates (38). Alternatively, this gap extension may be due to Exo1's known role in the extension of NER intermediates, and the resection of NER intermediates may encroach upon and merge with nearby ssDNA gaps. While Rev3 is known to be a low-processivity polymerase (44), it is not yet known on how large an ssDNA region Rev3 can act. One possible scenario is that following reactivation of PRR by *GAL-RAD18*, translesion synthesis must act to fill in ssDNA gaps prior to checkpoint adaptation (45), and further *EXO1*-dependent resection at later time points coupled with a low-processivity Rev3 polymerase may cause adaptation to outpace translesion synthesis (resulting in the segregation of incompletely replicated chromosomes). Thus, the multiple-hour delay before *rad18*-dependent ssDNA gaps become irreparable may be due to a low processivity rate for Exo1 at ssDNA gaps or may reflect an inability to maintain repression of Exo1 over prolonged periods (45, 46).

An additional question to be considered is why the Exo1-mediated ssDNA gaps are lethal to *rad18* cells (which presumably have an active HR pathway). In their low-dose UV studies, Hishida et al. discovered that the UV sensitivity of *rad18* cells can be suppressed by deleting the HR inhibitor *SRS2* (40). We extend this to show that the inability to repair ssDNA gaps by HR in *rad18* cells is due to an *SRS2*-dependent block; deletion of *SRS2* rescues viability in *rad18* cells only when HR is active (via *GAL-RAD57*) (Fig. 5). Intriguingly, the *srs2*-dependent repair is not time limited, unlike *EXO1*-dependent TLS repair of ssDNA gaps (Fig. 4). Thus, the question remains why the Srs2 HR block persists, as ssDNA gaps are repairable in its absence. We propose that the repression of HR by Srs2 at ssDNA may be initiated in an irreversible manner at a specific point in the cell cycle (possibly coincidental with the passage of the replication fork); hence, following ssDNA gap formation (a precursor to TLS repair), the option to utilize homologous recombination may no longer be available.

The low-dose hypermutability challenges our assumptions of what is a "safe dose." In this study, we describe the treatment of yeast cells with extremely low doses of MMS (from 0.001% to 0.0001%), which for normal cells do not induce any discernible phenotypes and yet are catastrophic for PRR mutants. Despite this, in the absence of any exogenous damage, a *rad18*Δ mutant exhibits growth characteristics that are similar to those of a wild-type cell. Applying this concept to the human condition raises important issues with regard to how we evaluate "safe" levels of carcinogenic substances. What might represent a negligible level for one person may result in significant unrepaired DNA damage for a second individual (such as someone who carries one or more mutations in PRR genes). While low-dose X rays have been a mainstay of diagnostic medical and dental procedures for decades and have recently become ubiquitous in airport security measures (47–49), estimations of the cancer risk associated with these sources are extrapolated from studies involving subjects who have encountered significantly higher doses (i.e., nuclear accident victims and atomic bomb survivors), largely ignoring individual genetic risk (49–54). Underestimating the carcinogenic potential of low-dose DNA damage is of critical importance, as evidenced by recent studies showing increased risks for malignancy related to radiation exposure from medical procedures (47, 48, 55, 56). An interesting question is whether we could identify at-risk individuals based upon their cellular proficiency in the low-dose (i.e., PRR-dependent) DNA damage response.

ACKNOWLEDGMENTS

We thank Brenda Andrews and Charles Boone for strains and plasmids used in this study and anonymous reviewers for helpful suggestions.

B.D.P. was supported by a U.S. Department of Defense Breast Cancer Research Program predoctoral fellowship. This work was supported by NIH grant R01 CA 129604.

REFERENCES

1. **Lazzaro F, Giannattasio M, Puddu F, Granata M, Pellicioli A, Plevani P, Muzi-Falconi M.** 2009. Checkpoint mechanisms at the intersection between DNA damage and repair. DNA Repair **8**:1055–1067.
2. **Drabløs F, Feyzi E, Aas PA, Vaagbø CB, Kavli B, Bratlie MS, Peña-Diaz J, Otterlei M, Slupphaug G, Krokan HE.** 2004. Alkylation damage in DNA and RNA-repair mechanisms and medical significance. DNA Repair **3**:1389–1407.
3. **Lindahl T.** 1993. Instability and decay of the primary structure of DNA. Nature **362**:709–715.
4. **Hishida T, Kubota Y, Carr AM, Iwasaki H.** 2009. *RAD6-RAD18-RAD5*-pathway-dependent tolerance to chronic low-dose ultraviolet light. Nature **457**:612–615.
5. **Tercero JA, Longhese MP, Diffley JF.** 2003. A central role for DNA replication forks in checkpoint activation and response. Mol. Cell **11**:1323–1336.
6. **Murakami-Sekimata A, Huang D, Piening BD, Bangur C, Paulovich AG.** 2010. The *Saccharomyces cerevisiae RAD9*, *RAD17* and *RAD24* genes are required for suppression of mutagenic post-replicative repair during chronic DNA damage. DNA Repair **9**:824–834.
7. **Shulman LN.** 1993. The biology of alkylating-agent cellular injury. Hematol. Oncol. Clin. North Am. **7**:325–335.
8. **Broomfield S, Chow BL, Xiao W.** 1998. MMS2, encoding an ubiquitin-conjugating-enzyme-like protein, is a member of the yeast error-free postreplication repair pathway. Proc. Natl. Acad. Sci. U. S. A. **95**:5678–5683.
9. **Prakash L, Prakash S.** 1977. Isolation and characterization of MMS-sensitive mutants of Saccharomyces cerevisiae. Genetics **86**:33–55.
10. **Prakash S, Prakash L.** 1977. Increased spontaneous mitotic segregation in MMS-sensitive mutants of Saccharomyces cerevisiae. Genetics **87**:229–236.
11. **Tercero JA, Diffley JF.** 2001. Regulation of DNA replication fork progression through damaged DNA by the Mec1/Rad53 checkpoint. Nature **412**:553–557.
12. **Andersen PL, Xu F, Xiao W.** 2008. Eukaryotic DNA damage tolerance and translesion synthesis through covalent modifications of PCNA. Cell Res. **18**:162–173.
13. **Ulrich HD, Walden H.** 2010. Ubiquitin signaling in DNA replication and repair. Nat. Rev. Mol. Cell Biol. **11**:479–489.
14. **Ulrich HD.** 2011. Timing and spacing of ubiquitin-dependent DNA damage bypass. FEBS Lett. **585**:2861–2867.
15. **Nelson JR, Lawrence CW, Hinkle DC.** 1996. Thymine-thymine dimer bypass by yeast DNA polymerase zeta. Science **272**:1646–1649.
16. **Blastyák A, Pintér L, Unk I, Prakash L, Prakash S, Haracska L.** 2007. Yeast Rad5 protein required for postreplication repair has a DNA helicase activity specific for replication fork regression. Mol. Cell **28**:167–175.
17. **Longtine MS, McKenzie A, III, Demarini DJ, Shah NG, Wach A, Brachat A, Philippsen P, Pringle JR.** 1998. Additional modules for versatile and economical PCR-based gene deletion and modification in Saccharomyces cerevisiae. Yeast **14**:953–961.
18. **Reid RJD, Sunjevaric I, Keddache M, Rothstein R.** 2002. Efficient PCR-based gene disruption in *Saccharomyces* strains using intergenic primers. Yeast **19**:319–328.
19. **Tong AH, Boone C.** 2006. Synthetic genetic array analysis in Saccharomyces cerevisiae. Methods Mol. Biol. **313**:171–192.
20. **Paulovich AG, Margulies RU, Garvik BM, Hartwell LH.** 1997. RAD9, RAD17, and RAD24 are required for S phase regulation in Saccharomyces cerevisiae in response to DNA damage. Genetics **145**:45–62.

21. **Pellicioli A, Lucca C, Liberi G, Marini F, Lopes M, Plevani P, Romano A, Di Fiore PP, Foiani M.** 1999. Activation of Rad53 kinase in response to DNA damage and its effect in modulating phosphorylation of the lagging strand DNA polymerase. EMBO J. **18**:6561–6572.
22. **Laemmli UK.** 1970. Cleavage of structural proteins during the assembly of the head of bacteriophage T4. Nature **227**:680–685.
23. **Chang M, Bellaoui M, Boone C, Brown GW.** 2002. A genome-wide screen for methyl methanesulfonate-sensitive mutants reveals genes required for S phase progression in the presence of DNA damage. Proc. Natl. Acad. Sci. U. S. A. **99**:16934–16939.
24. **Winzeler EA, Shoemaker DD, Astromoff A, Liang H, Anderson K, Andre B, Bangham R, Benito R, Boeke JD, Bussey H, Chu AM, Connelly C, Davis K, Dietrich F, Dow SW, El Bakkoury M, Foury F, Friend SH, Gentalen E, Giaever G, Hegemann JH, Jones T, Laub M, Liao H, Liebundguth N, Lockhart DJ, Lucau-Danila A, Lussier M, M'Rabet N, Menard P, Mittmann M, Pai C, Rebischung C, Revuelta JL, Riles L, Roberts CJ, Ross-MacDonald P, Scherens B, Snyder M, Sookhai-Mahadeo S, Storms RK, Véronneau S, Voet M, Volckaert G, Ward TR, Wysocki R, Yen GS, Yu K, Zimmermann K, Philippsen P, Johnston M, Davis RW.** 1999. Functional characterization of the *Saccharomyces cerevisiae* genome by gene deletion and parallel analysis. Science **285**:901–906.
25. **Grunenfelder B, Winzeler EA.** 2002. Treasures and traps in genome-wide data sets: case examples from yeast. Nat. Rev. Genet. **3**:653–661.
26. **Hughes TR, Roberts CJ, Dai H, Jones AR, Meyer MR, Slade D, Burchard J, Dow S, Ward TR, Kidd MJ, Friend SH, Marton MJ.** 2000. Widespread aneuploidy revealed by DNA microarray expression profiling. Nat. Genet. **25**:333–337.
27. **Barbour L, Ball LG, Zhang K, Xiao W.** 2006. DNA damage checkpoints are involved in postreplication repair. Genetics **174**:1789–1800.
28. **Daigaku Y, Davies AA, Ulrich HD.** 2010. Ubiquitin-dependent DNA damage bypass is separable from genome replication. Nature **465**:951–955.
29. **Barbour L, Xiao W.** 2003. Regulation of alternative replication bypass pathways at stalled replication forks and its effects on genome stability: a yeast model. Mutat. Res. **532**:137–155.
30. **Gangavarapu V, Prakash S, Prakash L.** 2007. Requirement of RAD52 group genes for postreplication repair of UV-damaged DNA in Saccharomyces cerevisiae. Mol. Cell. Biol. **27**:7758–7764.
31. **Paulovich AG, Hartwell LH.** 1995. A checkpoint regulates the rate of progression through S phase in *S. cerevisiae* in response to DNA damage. Cell **82**:841–847.
32. **Lopes M, Foiani M, Sogo JM.** 2006. Multiple mechanisms control chromosome integrity after replication fork uncoupling and restart at irreparable UV lesions. Mol. Cell **21**:15–27.
33. **Prakash L.** 1981. Characterization of postreplication repair in Saccharomyces cerevisiae and effects of rad6, rad18, rev3 and rad52 mutations. Mol. Gen. Genet. **184**:471–478.
34. **Geigl EM, Eckardt-Schupp F.** 1991. The repair of double-strand breaks and S1 nuclease-sensitive sites can be monitored chromosome-specifically in Saccharomyces cerevisiae using pulse-field gel electrophoresis. Mol. Microbiol. **5**:1615–1620.
35. **Ma W, Panduri V, Sterling JF, Van Houten B, Gordenin DA, Resnick MA.** 2009. The transition of closely opposed lesions to double-strand breaks during long-patch base excision repair is prevented by the coordinated action of DNA polymerase δ and Rad27/Fen1. Mol. Cell. Biol. **29**:1212–1221.
36. **Chu G, Vollrath D, Davis RW.** 1986. Separation of large DNA molecules by contour-clamped homogeneous electric fields. Science **234**:1582–1585.
37. **Karras GI, Jentsch S.** 2010. The *RAD6* DNA damage tolerance pathway operates uncoupled from the replication fork and is functional beyond S phase. Cell **141**:255–267.
38. **Giannattasio M, Follonier C, Tourrière H, Puddu F, Lazzaro F, Pasero P, Lopes M, Plevani P, Muzi-Falconi M.** 2010. Exo1 competes with repair synthesis, converts NER intermediates to long ssDNA gaps, and promotes checkpoint activation. Mol. Cell **40**:50–62.
39. **Pfander B, Moldovan GL, Sacher M, Hoege C, Jentsch S.** 2005. SUMO-modified PCNA recruits Srs2 to prevent recombination during S phase. Nature **436**:428–433.
40. **Hishida T, Hirade Y, Haruta N, Kubota Y, Iwasaki H.** 2010. Srs2 plays a critical role in reversible G_2 arrest upon chronic and low doses of UV irradiation via two distinct homologous recombination-dependent mechanisms in postreplication repair-deficient cells. Mol. Cell. Biol. **30**:4840–4850.
41. **Liu J, Renault L, Veaute X, Fabre F, Stahlberg H, Heyer WD.** 2011. Rad51 paralogues Rad55-Rad57 balance the antirecombinase Srs2 in Rad51 filament formation. Nature **479**:245–248.
42. **Zhang H, Lawrence CW.** 2005. The error-free component of the *RAD6/RAD18* DNA damage tolerance pathway of budding yeast employs sister-strand recombination. Proc. Natl. Acad. Sci. U. S. A. **102**:15954–15959.
43. **Waters LS, Walker GC.** 2006. The critical mutagenic translesion DNA polymerase Rev1 is highly expressed during G(2)/M phase rather than S phase. Proc. Natl. Acad. Sci. U. S. A. **103**:8971–8976.
44. **Broomfield S, Hryciw T, Xiao W.** 2001. DNA postreplication repair and mutagenesis in *Saccharomyces cerevisiae*. Mutat. Res. **486**:167–184.
45. **Toczyski DP, Galgoczy DJ, Hartwell LH.** 1997. *CDC5* and CKII control adaptation to the yeast DNA damage checkpoint. Cell **90**:1097–1106.
46. **Segurado M, Diffley JF.** 2008. Separate roles for the DNA damage checkpoint protein kinases in stabilizing DNA replication forks. Genes Dev. **22**:1816–1827.
47. **Claus EB, Calvocoressi L, Bondy ML, Schildkraut JM, Wiemels JL, Wrensch M.** 2012. Dental X-rays and risk of meningioma. Cancer **118**:4530–4537.
48. **Longstreth WT, Jr, Phillips LE, Drangsholt M, Koepsell TD, Custer BS, Gehrels JA, van Belle G.** 2004. Dental X-rays and the risk of intracranial meningioma: a population-based case-control study. Cancer **100**:1026–1034.
49. **Nguyen PK, Wu JC.** 2011. Radiation exposure from imaging tests: is there an increased cancer risk? Expert Rev. Cardiovasc. Ther. **9**:177–183.
50. **Brenner DJ.** 2009. Extrapolating radiation-induced cancer risks from low doses to very low doses. Health Phys. **97**:505–509.
51. **Goodhead DT.** 2010. New radiobiological, radiation risk and radiation protection paradigms. Mutat. Res. **687**:13–16.
52. **Mullenders L, Atkinson M, Paretzke H, Sabatier L, Bouffler S.** 2009. Assessing cancer risks of low-dose radiation. Nat. Rev. Cancer **9**:596–604.
53. **Preston DL, Pierce DA, Shimizu Y, Cullings HM, Fujita S, Funamoto S, Kodama K.** 2004. Effect of recent changes in atomic bomb survivor dosimetry on cancer mortality risk estimates. Radiat. Res. **162**:377–389.
54. **Preston DL, Ron E, Tokuoka S, Funamoto S, Nishi N, Soda M, Mabuchi K, Kodama K.** 2007. Solid cancer incidence in atomic bomb survivors: 1958–1998. Radiat. Res. **168**:1–64.
55. **Baerlocher MO, Detsky AS.** 2010. Discussing radiation risks associated with CT scans with patients. JAMA **304**:2170–2171.
56. **Brenner DJ, Hall EJ.** 2007. Computed tomography—an increasing source of radiation exposure. N. Engl. J. Med. **357**:2277–2284.

DNA Repair 9 (2010) 824–834

Contents lists available at ScienceDirect

DNA Repair

journal homepage: www.elsevier.com/locate/dnarepair

The *Saccharomyces cerevisiae RAD9*, *RAD17* and *RAD24* genes are required for suppression of mutagenic post-replicative repair during chronic DNA damage

Akiko Murakami-Sekimata[1,2], Dongqing Huang[2], Brian D. Piening, Chaitanya Bangur, Amanda G. Paulovich*

Fred Hutchinson Cancer Research Center, 1100 Fairview Avenue N., P.O. Box 19024, Seattle, WA 98109-1024, USA

ARTICLE INFO

Article history:
Received 1 December 2009
Received in revised form 25 March 2010
Accepted 16 April 2010
Available online 15 May 2010

Keywords:
DNA repair
Cell cycle
RAD9
Post-replication repair

ABSTRACT

In *Saccharomyces cerevisiae*, a DNA damage checkpoint in the S-phase is responsible for delaying DNA replication in response to genotoxic stress. This pathway is partially regulated by the checkpoint proteins Rad9, Rad17 and Rad24. Here, we describe a novel hypermutable phenotype for *rad9Δ*, *rad17Δ* and *rad24Δ* cells in response to a chronic 0.01% dose of the DNA alkylating agent MMS. We report that this hypermutability results from DNA damage introduction during the S-phase and is dependent on a functional translesion synthesis pathway. In addition, we performed a genetic screen for interactions with *rad9Δ* that confer sensitivity to 0.01% MMS. We report and quantify 25 genetic interactions with *rad9Δ*, many of which involve the post-replication repair machinery. From these data, we conclude that defects in S-phase checkpoint regulation lead to increased reliance on mutagenic translesion synthesis, and we describe a novel role for members of the S-phase DNA damage checkpoint in suppressing mutagenic post-replicative repair in response to sublethal MMS treatment.

1. Introduction

The DNA damage response (DDR) consists of a highly coordinated network of cellular processes tasked with maintaining genomic integrity despite continual damage from a wide variety of endogenous and exogenous agents. A critical step in this response is cell cycle arrest, in which a damage-induced signal triggers a checkpoint at G1, intra-S, or G2/M [1–3]. Notably, mutations in genes involved in DDR checkpoints are associated with predisposition to cancer in mammals (e.g. ATM, BRCA1, p53) [4].

Methylmethanesulfonate (MMS) is a monofunctional alkylating agent which generates methylated DNA lesions and triggers checkpoint activation; it is commonly referred to as "radiomimetic" [5]. Multiple pathways coordinate to repair MMS lesions, which include direct reversal (dependent on the *MGT1* alkyltransferase), base and nucleotide excision repair, post-replication repair, and homologous recombinational repair [6]. In response to sublethal doses of DNA alkylating agents, budding yeast synchronize into a lengthened S-phase due to an intra-S-phase checkpoint that is dependent on *RAD53* and *MEC1* [3]. While the budding yeast checkpoint adapter Rad9 is required for DNA damage-induced arrest in the G1 and G2/M phases, its role in intra-S is not absolute, since deletion of *RAD9* is associated with partial loss of S-phase slowing in response to MMS [7]. Members of the *RAD24* epistasis group (RAD24, RAD17, DDC1 and MEC3) exhibit a similar partial defect in S-phase slowing [7–9]; however members of this group can enhance the MMS sensitivity of *rad9Δ* [7].

RAD9 has homology to the mammalian BRCA1 gene. Like BRCA1, Rad9 has BRCT and Tudor domains, which are important for protein–protein interactions mostly involved in DNA repair or cell cycle regulation [10]. Rad9 serves as an adapter in the Mec1/Tel1-dependent checkpoint response to DNA damage. An early step in the cellular response to DNA damage is modification of histone tails near the site of damage (e.g. methylation, *MEC1*- or *TEL1*-dependent phosphorylation). Rad9p is subsequently recruited to the damaged site (through the association of its Tudor domains with phosphorylated histone H2A and methylated histone H3) and oligomerizes via its BRCT domains [11]. Once recruited to the damaged site, Rad9p is also phosphorylated in a Mec1/Tel1-dependent manner, and its phosphorylated S/T-Q residues create a binding site for the FHA domain of the checkpoint effecter kinase Rad53 [12–17]. Thus, oligomeric assembly of phosphorylated Rad9p is likely to serve as a platform for the enrichment of Rad53p and stimulation of its trans-autophosphorylation and phosphorylation by Mec1p and Tel1p. These phosphorylation events activate Rad53p and allow it to trigger downstream events in the DDR [18,19].

* Corresponding author at: Fred Hutchinson Cancer Research Center, 1100 Fairview Avenue N., LE-360, P.O. Box 19024, Seattle, WA 98109-1024, USA. Tel.: +1 206 667 1912; fax: +1 206 667 2277.
E-mail address: apaulovi@fhcrc.org (A.G. Paulovich).
[1] Present address: Department of Health Sciences, Graduate School of Medicine, Tohoku University, 2-1 Seiryo, Aoba-ku, Sendai 980-8575, Japan.
[2] These authors contributed equally to this work.

1568-7864/$ – see front matter © 2010 Elsevier B.V. All rights reserved.
doi:10.1016/j.dnarep.2010.04.007

Members of the *RAD24* epistasis group comprise a damage-specific DNA clamp known as the 9-1-1 complex, which is involved in DNA damage checkpoint regulation. The 9-1-1 clamp is composed of three subunits, Rad17, Ddc1 and Mec3. It is loaded on to the damage site by the alternative heteropentameric replication factor C (RFC) complex, in which one subunit, Rfc1, is replaced by the checkpoint-specific subunit Rad24 [20]. Mec1-dependent phoshorylation and activation of Rad9 and Rad53 is severely reduced in *rad17*, *mec3*, *ddc1* and *rad24* mutants [21]. Putative functions of the 9-1-1 complex involve activation of Mec1 kinase activity and recruitment of other factors that could propagate the checkpoint response pathway or facilitate the processivity of the replication fork [21,22].

Both *RAD9* and the *RAD24* group encode for proteins that are required for efficient S-phase checkpoint regulation in response to alkylation damage, and the role of this checkpoint is believed to be to allow a damaged cell time to repair DNA lesions prior to the arrival of the replication fork [23]. If lesions are left unrepaired, cells utilize one of three independent post-replication repair (PRR) mechanisms to bypass the lesion [24]. In the first PRR mechanism, a switch to an error-prone translesion synthesis (TLS) polymerase occurs, which is triggered by a Rad6–Rad18 mediated mono-ubiquitination of PCNA. One of the TLS polymerases is the Polζ complex, composed of Rev3, Rev7, Rev1, and likely additional proteins. Polζ is able to replicate over a damaged template much more efficiently than major replicases, inserting a noncognate nucleotide [25]. A second mechanism employs polyubiquitination of PCNA by the Mms2–Ubc13–Rad5 complex, which promotes error-free lesion bypass through a mechanism involving regression of the replication fork [26]. A third mechanism depends on Rad52, which promotes homologous recombination (HR) between sister chromatids [27]. Genetic interactions between *RAD9* and PRR genes (e.g. *MMS2*, *REV3*) have been reported [28].

In this study, we describe a novel hypermutable phenotype for mutants lacking *RAD9* or members of the *RAD24* epistasis group. We show that the phenotype occurs exclusively when cells are treated with a chronic low-dose treatment of MMS, and not when a higher dose is applied. Importantly, we demonstrate that different doses of MMS yield different effects on the cell cycle distribution, a phenomenon which is responsible for the dose-dependent hypermutability of S-phase checkpoint mutants. We show that the hypermutable phenotype of *rad9Δ* cells is dependent on *rev3Δ*, indicating that the mutability of such cells is due to hyperactivation of the error-prone post-replication repair pathway. Consistent with (and extending) previous work linking *RAD9* to the PRR pathway, we show that *RAD9* interacts with a large number of PRR genes that function in both error-prone (*REV1*, *REV3*, *REV7*) and error-free (*RAD5*, *MMS2*, *UBC13*) pathways, and present a model in which *RAD9* plays a role in channeling lesions at the replication fork.

2. Materials and methods

2.1. Media and growth conditions

YEPD and dropout media have been previously described [29]. MMS was purchased from Sigma (Cat# M4016). YEPD and synthetic plates containing MMS were freshly prepared the evening prior to use. Magic medium (SC-Leu-His-Arg; 200 mg/L G418, 60 mg/L L-canavanine) used in the synthetic interaction screen was prepared according to Pan et al. [30].

2.2. Yeast strains

Saccharomyces cerevisiae strains used in this study are listed in Table 1. Strain BY4741 was purchased from Open Biosystems. Yeast strains with the designation yMP have been previously described [7]. All gene disruptions were achieved by homologous recombination at their chromosomal loci by standard PCR-based methods [31]. Briefly, a deletion cassette with a 0.5 kb region flanking the target ORF was amplified by PCR from the corresponding *xxxΔKAN*^{r} strain of the deletion array (Open Biosystems) and transformed into the target strain for gene knockout. The primers used in the gene disruptions are designed using 20 bp sequences which are 0.5 kb upstream and downstream of the target gene.

2.3. rad9Δ double deletion library construction and screening

The *rad9Δ* double deletion library was constructed using the dSLAM methodology [32]. The pooled heterozygous diploid deletion library was a gift from Jef Boeke (Johns Hopkins). A *rad9Δ* deletion cassette with a 1.5 kb region flanking the *RAD9* ORF was amplified by PCR (forward primer: 5′-AGCTCTTGAACAACATACTCTCAG-3′; reverse primer: 5′-GAGATTCATCAAACAGATTGATCGC-3′) and transformed into the library. Selection of the *rad9Δ::URA3* diploids was performed on synthetic defined medium plates without uracil (SD-URA). Diploids were subsequently sporulated via replication onto SPO plates and incubation at room temperature for 5 days. Spores were replicated onto magic medium (MM)–URA plates to select *MAT***a** *rad9Δ::URA3* double mutant haploid cells. Haploid double-deletion cells were replicated onto complete synthetic medium with or without 0.01% MMS. Clones exhibiting sensitivity to MMS were streaked for single colonies on complete SD-medium. Eight colonies per candidate were subsequently grown overnight in synthetic liquid medium to saturation, and 2 μl of saturated culture were spotted on complete SD-medium ±0.01% MMS and scored after 2–3 days. For each candidate, UPTAG and DOWNTAG barcodes were sequenced to identify the corresponding gene deletion using primers and methods previously described [33,34].

2.4. MMS kill curves and cell cycle analysis

MMS kill curves were performed as previously described [3,7]. Briefly, log-phase cells (5×10^7 cells) were harvested from YPD medium and resuspended in 10 ml YPD with a specified concentration of pre-diluted liquid MMS solution. One MMS solution was used for all cultures in a single experiment to ensure identical MMS concentration across all cultures, and control strains (wild type, *xxxΔ*, and *rad9Δ*) were always run on the same day as the double mutants to control for day-to-day variation in MMS preparations. Cultures were incubated at 30 °C, and aliquots were taken out at given intervals. The cells were resuspended in PBS + 5% sodium thiosulfate (to inactivate the MMS). Cells were sonicated, and cell concentrations were assessed using a Coulter Counter. Viability was determined by plating serial dilutions of cultures onto YPD and scoring the number of colony-forming units (CFUs) after 3–4 days at 30 °C. Viability was calculated as CFU/total cells. Cell cycle distributions were determined by flow cytometry of propidium iodide (PI)-stained cells using a method described previously [7]. Distributions of PI-stained cells were assessed using a Beckman Dickson Calibur flow cytometer.

2.5. Ionizing radiation (IR) kill curves

Log-phase cells grown at 30 °C in YEPD were harvested, sonicated, and counted using a Coulter Counter. 1×10^8 cells were resuspended in 2 ml PBS, sonicated, and serially diluted. Dilutions were spread onto fresh YEPD plates and exposed to gamma irradiation using a Mark II cesium-137 irradiator (JL Shepherd & Associates) operated at a dose rate of 800 cGy/min. Following IR, plates were immediately transferred to an incubator, and allowed to grow for 3 days at 30 °C. Viability was calculated as CFU/total

Table 1
Saccharomyces cerevisiae strains.

Strain	Genotype	Source
BY4741	*MAT***a** *his3Δ1 leu2Δ0 met15Δ0 ura3Δ0*	Open Biosystems
CB1021	*MAT***a** *ura3Δ0 leu2Δ0 his3Δ1 lys2Δ0 MET15 can1Δ::LEU2 + -MFA1pr-HIS3 rad9::URA3*	This study
yAM1184–86	*MAT***a** *ura3Δ0 leu2Δ0 his3Δ1 lys2Δ0 MET15 can1Δ::LEU2+-MFA1pr-HIS3 sgs1::KAN^R*	This study
yAM1187–89	*MAT***a** *ura3Δ0 leu2Δ0 his3Δ1 lys2Δ0 MET15 can1Δ::LEU2+-MFA1pr-HIS3 sgs1::KAN^R rad9::URA3*	This study
yAM1202–4	*MAT***a** *ura3Δ0 leu2Δ0 his3Δ1 lys2Δ0 MET15 can1Δ::LEU2+-MFA1pr-HIS3 rev1::KAN^R*	This study
yAM1205–7	*MAT***a** *ura3Δ0 leu2Δ0 his3Δ1 lys2Δ0 MET15 can1Δ::LEU2+-MFA1pr-HIS3 rev1::KAN^R rad9::URA3*	This study
yAM1208–10	*MAT***a** *ura3Δ0 leu2Δ0 his3Δ1 lys2Δ0 MET15 can1Δ::LEU2+-MFA1pr-HIS3 rad17::KAN^R*	This study
yAM1211–13	*MAT***a** *ura3Δ0 leu2Δ0 his3Δ1 lys2Δ0 MET15 can1Δ::LEU2+-MFA1pr-HIS3 rad17::KAN^R rad9::URA3*	This study
yAM1214–16	*MAT***a** *ura3Δ0 leu2Δ0 his3Δ1 lys2Δ0 MET15 can1Δ::LEU2+-MFA1pr-HIS3 rad55::KAN^R*	This study
yAM1217–19	*MAT***a** *ura3Δ0 leu2Δ0 his3Δ1 lys2Δ0 MET15 can1Δ::LEU2+-MFA1pr-HIS3 rad55::KAN^R rad9::URA3*	This study
yAM1220–22	*MAT***a** *ura3Δ0 leu2Δ0 his3Δ1 lys2Δ0 MET15 can1Δ::LEU2+-MFA1pr-HIS3 isw1::KAN^R*	This study
yAM1223–25	*MAT***a** *ura3Δ0 leu2Δ0 his3Δ1 lys2Δ0 MET15 can1Δ::LEU2+-MFA1pr-HIS3 isw1::KAN^R rad9::URA3*	This study
yAM1226–28	*MAT***a** *ura3Δ0 leu2Δ0 his3Δ1 lys2Δ0 MET15 can1Δ::LEU2+-MFA1pr-HIS3 rev3::KAN^R*	This study
yAM1229–31	*MAT***a** *ura3Δ0 leu2Δ0 his3Δ1 lys2Δ0 MET15 can1Δ::LEU2+-MFA1pr-HIS3 rev3::KAN^R rad9::URA3*	This study
yAM1238–40	*MAT***a** *ura3Δ0 leu2Δ0 his3Δ1 lys2Δ0 MET15 can1Δ::LEU2+-MFA1pr-HIS3 ddc1::KAN^R*	This study
yAM1241–43	*MAT***a** *ura3Δ0 leu2Δ0 his3Δ1 lys2Δ0 MET15 can1Δ::LEU2+-MFA1pr-HIS3 ddc1::KAN^R rad9::URA3*	This study
yAM1244–46	*MAT***a** *ura3Δ0 leu2Δ0 his3Δ1 lys2Δ0 MET15 can1Δ::LEU2+-MFA1pr-HIS3 ubc13::KAN^R*	This study
yAM1247–49	*MAT***a** *ura3Δ0 leu2Δ0 his3Δ1 lys2Δ0 MET15 can1Δ::LEU2+-MFA1pr-HIS3 ubc13::KAN^R rad9::URA3*	This study
yAM1250–52	*MAT***a** *ura3Δ0 leu2Δ0 his3Δ1 lys2Δ0 MET15 can1Δ::LEU2+-MFA1pr-HIS3 esc2::KAN^R*	This study
yAM1253–55	*MAT***a** *ura3Δ0 leu2Δ0 his3Δ1 lys2Δ0 MET15 can1Δ::LEU2+-MFA1pr-HIS3 esc2::KAN^R rad9::URA3*	This study
yAM1280–82	*MAT***a** *ura3Δ0 leu2Δ0 his3Δ1 lys2Δ0 MET15 can1Δ::LEU2+-MFA1pr-HIS3 mus81::KAN^R*	This study
yAM1283–85	*MAT***a** *ura3Δ0 leu2Δ0 his3Δ1 lys2Δ0 MET15 can1Δ::LEU2+-MFA1pr-HIS3 mus81::KAN^R rad9::URA3*	This study
yAM1286–88	*MAT***a** *ura3Δ0 leu2Δ0 his3Δ1 lys2Δ0 MET15 can1Δ::LEU2+-MFA1pr-HIS3 rad5::KAN^R*	This study
yAM1289–91	*MAT***a** *ura3Δ0 leu2Δ0 his3Δ1 lys2Δ0 MET15 can1Δ::LEU2+-MFA1pr-HIS3 rad5::KAN^R rad9::URA3*	This study
yAM1292–94	*MAT***a** *ura3Δ0 leu2Δ0 his3Δ1 lys2Δ0 MET15 can1Δ::LEU2+-MFA1pr-HIS3 msn1::KAN^R*	This study
yAM1295–97	*MAT***a** *ura3Δ0 leu2Δ0 his3Δ1 lys2Δ0 MET15 can1Δ::LEU2+-MFA1pr-HIS3 msn1::KAN^R rad9::URA3*	This study
yAM1304–6	*MAT***a** *ura3Δ0 leu2Δ0 his3Δ1 lys2Δ0 MET15 can1Δ::LEU2+-MFA1pr-HIS3 uip5::KAN^R*	This study
yAM1307–9	*MAT***a** *ura3Δ0 leu2Δ0 his3Δ1 lys2Δ0 MET15 can1Δ::LEU2+-MFA1pr-HIS3 uip5::KAN^R rad9::URA3*	This study
yAM1328–30	*MAT***a** *ura3Δ0 leu2Δ0 his3Δ1 lys2Δ0 MET15 can1Δ::LEU2+-MFA1pr-HIS3 mgt1::KAN^R*	This study
yAM1331–33	*MAT***a** *ura3Δ0 leu2Δ0 his3Δ1 lys2Δ0 MET15 can1Δ::LEU2+-MFA1pr-HIS3 mgt1::KAN^R rad9::URA3*	This study
yAM1340–42	*MAT***a** *ura3Δ0 leu2Δ0 his3Δ1 lys2Δ0 MET15 can1Δ::LEU2+-MFA1pr-HIS3 bbc1::KAN^R*	This study
yAM1343–45	*MAT***a** *ura3Δ0 leu2Δ0 his3Δ1 lys2Δ0 MET15 can1Δ::LEU2+-MFA1pr-HIS3 bbc1::KAN^R rad9::URA3*	This study
yAM1370–72	*MAT***a** *ura3Δ0 leu2Δ0 his3Δ1 lys2Δ0 MET15 can1Δ::LEU2+-MFA1pr-HIS3 mms2::KAN^R*	This study
yAM1373–75	*MAT***a** *ura3Δ0 leu2Δ0 his3Δ1 lys2Δ0 MET15 can1Δ::LEU2+-MFA1pr-HIS3 mms2::KAN^R rad9::URA3*	This study
yAM1388–90	*MAT***a** *ura3Δ0 leu2Δ0 his3Δ1 lys2Δ0 MET15 can1Δ::LEU2+-MFA1pr-HIS3 mms1::KAN^R*	This study
yAM1391–93	*MAT***a** *ura3Δ0 leu2Δ0 his3Δ1 lys2Δ0 MET15 can1Δ::LEU2+-MFA1pr-HIS3 mms1::KAN^R rad9::URA3*	This study
yAM1394–96	*MAT***a** *ura3Δ0 leu2Δ0 his3Δ1 lys2Δ0 MET15 can1Δ::LEU2+-MFA1pr-HIS3 pot1::KAN^R*	This study
yAM1397–99	*MAT***a** *ura3Δ0 leu2Δ0 his3Δ1 lys2Δ0 MET15 can1Δ::LEU2+-MFA1pr-HIS3 pot1::KAN^R rad9::URA3*	This study
yAM1418–20	*MAT***a** *ura3Δ0 leu2Δ0 his3Δ1 lys2Δ0 MET15 can1Δ::LEU2+-MFA1pr-HIS3 rev7::KAN^R*	This study
yAM1421–23	*MAT***a** *ura3Δ0 leu2Δ0 his3Δ1 lys2Δ0 MET15 can1Δ::LEU2+-MFA1pr-HIS3 rev7::KAN^R rad9::URA3*	This study
yAM1448–50	*MAT***a** *ura3Δ0 leu2Δ0 his3Δ1 lys2Δ0 MET15 can1Δ::LEU2+-MFA1pr-HIS3 mms4::KAN^R*	This study
yAM1451–53	*MAT***a** *ura3Δ0 leu2Δ0 his3Δ1 lys2Δ0 MET15 can1Δ::LEU2+-MFA1pr-HIS3 mms4::KAN^R rad9::URA3*	This study
yAM1454–56	*MAT***a** *ura3Δ0 leu2Δ0 his3Δ1 lys2Δ0 MET15 can1Δ::LEU2+-MFA1pr-HIS3 rad54::KAN^R*	This study
yAM1457–79	*MAT***a** *ura3Δ0 leu2Δ0 his3Δ1 lys2Δ0 MET15 can1Δ::LEU2+-MFA1pr-HIS3 rad54::KAN^R rad9::URA3*	This study
yAM1472–74	*MAT***a** *ura3Δ0 leu2Δ0 his3Δ1 lys2Δ0 MET15 can1Δ::LEU2+-MFA1pr-HIS3 yil158w::KAN^R*	This study
yAM1475–77	*MAT***a** *ura3Δ0 leu2Δ0 his3Δ1 lys2Δ0 MET15 can1Δ::LEU2+-MFA1pr-HIS3 yil158w::KAN^R rad9::URA3*	This study
yAM1490–92	*MAT***a** *ura3Δ0 leu2Δ0 his3Δ1 lys2Δ0 MET15 can1Δ::LEU2+-MFA1pr-HIS3 psy3::KAN^R*	This study
yAM1493–95	*MAT***a** *ura3Δ0 leu2Δ0 his3Δ1 lys2Δ0 MET15 can1Δ::LEU2+-MFA1pr-HIS3 psy3::KAN^R rad9::URA3*	This study
yAM1655–57	*MAT***a** *ura3Δ0 leu2Δ0 his3Δ1 lys2Δ0 MET15 can1Δ::LEU2+-MFA1pr-HIS3 ixr1::KAN^R*	This study
yAM1658–60	*MAT***a** *ura3Δ0 leu2Δ0 his3Δ1 lys2Δ0 MET15 can1Δ::LEU2+-MFA1pr-HIS3 ixr1::KAN^R rad9::URA3*	This study
yMP10381	*MAT***a** *ade2 ade3-130 leu2 trp1 ura3 cyh2 SCR::URA3*	Paulovich Lab
yMP10382	*MAT***a** *ade2 ade3-130 leu2 trp1 ura3 cyh2 rev3Δ::LEU2 SCR::URA3*	Paulovich Lab
yMP11006	*MAT***a** *ade2 ade3-130 leu2 trp1 ura3 cyh2 rad24Δ::TRP1 SCR::URA3*	Paulovich Lab
yMP11030	*MAT***a** *ade2 ade3-130 leu2 trp1 ura3 cyh2 SCR::URA3 rad9Δ::LEU2*	Paulovich Lab
yMP11089	*MAT***a** *ade2 ade3-130 leu2 trp1 ura3 cyh2 rad17Δ::LEU2 SCR::URA3*	Paulovich Lab
yMP11450	*MAT***a** *ade2 ade3-130 leu2 trp1 ura3 cyh2 SCR::URA3 rad52Δ::LEU2*	Paulovich Lab
yDH27–29	*MAT***a** *ade2 ade3-130 leu2 trp1 ura3 cyh2 bbc1Δ::KAN^r SCR::URA3*	This study
yDH30–32	*MAT***a** *ade2 ade3-130 leu2 trp1 ura3 cyh2 rad9Δ::LEU2 bbc1Δ::KAN^r SCR::URA3*	This study
yDH33–35	*MAT***a** *ade2 ade3-130 leu2 trp1 ura3 cyh2 isw1Δ::KAN^r SCR::URA3*	This study
yDH36–38	*MAT***a** *ade2 ade3-130 leu2 trp1 ura3 cyh2 rad9Δ::LEU2 isw1Δ::KAN^r SCR::URA3*	This study
yDH39–41	*MAT***a** *ade2 ade3-130 leu2 trp1 ura3 cyh2 yil158wΔ::KAN^r SCR::URA3*	This study
yDH42–44	*MAT***a** *ade2 ade3-130 leu2 trp1 ura3 cyh2 rad9Δ::LEU2 yil158wΔ::KAN^r SCR::URA3*	This study
yDH45–47	*MAT***a** *ade2 ade3-130 leu2 trp1 ura3 cyh2 pot1Δ::KAN^r SCR::URA3*	This study
yDH48–50	*MAT***a** *ade2 ade3-130 leu2 trp1 ura3 cyh2 rad9Δ::LEU2 pot1Δ::KAN^r SCR::URA3*	This study
yDH51–53	*MAT***a** *ade2 ade3-130 leu2 trp1 ura3 cyh2 rev3Δ::LEU2 rad9Δ::KAN^r SCR::URA3*	This study
yDH54–56	*MAT***a** *ade2 ade3-130 leu2 trp1 ura3 cyh2 rev3Δ::LEU2 bbc1Δ::KAN^r SCR::URA3*	This study
yDH57–59	*MAT***a** *ade2 ade3-130 leu2 trp1 ura3 cyh2 rev3Δ::LEU2 isw1Δ::KAN^r SCR::URA3*	This study
yDH60–62	*MAT***a** *ade2 ade3-130 leu2 trp1 ura3 cyh2 rev3Δ::LEU2 yil158wΔ::KAN^r SCR::URA3*	This study
yDH63–65	*MAT***a** *ade2 ade3-130 leu2 trp1 ura3 cyh2 rev3Δ::LEU2 pot1Δ::KAN^r SCR::URA3*	This study
yDH66–68	*MAT***a** *ade2 ade3-130 leu2 trp1 ura3 cyh2 rad52Δ::LEU2 bbc1Δ::KAN^r SCR::URA3*	This study
yDH69–71	*MAT***a** *ade2 ade3-130 leu2 trp1 ura3 cyh2 rad52Δ::LEU2 isw1Δ::KAN^r SCR::URA3*	This study
yDH72–74	*MAT***a** *ade2 ade3-130 leu2 trp1 ura3 cyh2 rad52Δ::LEU2 yil158wΔ::KAN^r SCR::URA3*	This study
yDH75–77	*MAT***a** *ade2 ade3-130 leu2 trp1 ura3 cyh2 rad52Δ::LEU2 pot1Δ::KAN^r SCR::URA3*	This study

CB1021 is congenic with BY4741 (S288C). The yAM strains are isogenic with CB1021. The remaining strains are all congenic with yMP10381 (A364a).

Table 2
RAD9-interacting genes.

Gene	Class[a]	Viability for single (%) (*xxxΔ*)[b]	Viability for double (%) (*xxxΔ rad9Δ*)[b]	Ratio[c]	*p*-value[d]
RAD5	Error-free bypass	0.016 ± 0.01	0[e]	∞[e]	ND[e]
UBC13	Error-free bypass	12 ± 2	0.023 ± 0.02	357.7	0.0015
REV7	Error-prone bypass	31 ± 3	0.037 ± 0.04	223.1	0.0015
MMS2	Error-free bypass	15 ± 1	0.078 ± 0.012	172.8	0.0011
REV1	Error-prone bypass	60 ± 21	0.12 ± 0.10	64.7	0.0016
RAD54	HR	12 ± 6	0.17 ± 0.11	47.4	0.0016
REV3	Error-prone bypass	76 ± 15	0.20 ± 0.12	40.8	0.0016
MMS1	HR intermediate resolution	54 ± 8	0.25 ± 0.05	33.0	0.0016
ELG1	Clamp loader	28 ± 1	0.37 ± 0.22	22.4	0.0018
DDC1	9-1-1 complex	12 ± 2	0.41 ± 0.10	20.4	0.0017
MGT1	Methyltransferase	39 ± 6	0.42 ± 0.16	19.9	0.0018
MUS81	HR intermediate resolution	2.7 ± 0.4	0.14 ± 0.05	18.9	0.0040
MMS4	HR intermediate resolution	3.6 ± 0.2	0.20 ± 0.09	17.8	0.0011
ISW1	Chromatin	41 ± 12	0.52 ± 0.17	16.1	0.0018
POT1	Fatty acid oxidation	34 ± 14	0.54 ± 0.41	15.4	0.0022
RAD17	9-1-1 complex	6 ± 0.7	0.43 ± 0.09	14.2	0.0028
SGS1	HR intermediate resolution	28 ± 5	0.67 ± 0.23	12.5	0.0020
RAD55	HR	18 ± 8	0.70 ± 0.33	12.0	0.0021
BBC1	Actin patch	84 ± 24	0.73 ± 0.65	11.4	0.0030
IXR1	Chromatin	29 ± 10	0.99 ± 0.29	8.4	0.0022
YIL158W	unknown	60 ± 11	1.3 ± 0.8	6.3	0.0047
ESC2	HR intermediate resolution	18 ± 5	1.3 ± 0.9	6.1	0.0050
UIP5	Unknown	29 ± 4	1.4 ± 0.3	5.8	0.0027
PSY3	Error-free bypass	30 ± 11	1.5 ± 0.5	5.5	0.0035
MSN1	Transcription	24 ± 6	1.6 ± 0.8	5.0	0.0048

[a] Gene functions are classified according to annotations in Saccharomyces Genome Database (www.yeastgenome.org) and the literature referenced in the database (see Supplemental Table S1). *PSY3* was very recently assigned to the error-free bypass branch of PRR pathway by Ball et al. [56].
[b] Cells were exposed to 0.01% MMS in liquid rich medium for 5 h. Wild type is BY4741 (S288C). Error represents the standard deviation calculated for three independent biological experiments performed on 3 subsequent days on three independent segregants for each double mutant. After MMS treatment, the survival rate for wild type and *rad9Δ* strains are 76 ± 13% and 8.3 ± 0.8%.
[c] Ratio is calculated as the viability of the most sensitive single mutant (i.e. either *rad9Δ* or *xxxΔ*) versus the viability of the *rad9Δ xxxΔ* double mutant.
[d] The *p*-values for the reliability of the difference of survival rates between the single and double mutants were calculated using *t*-tests.
[e] There were no viable colonies for the *rad5Δ rad9Δ* double mutant after 5 h exposure to 0.01% MMS; 2×10^4 cells were plated; hence, viability was ≤0.005%. (*p*-value cannot be accurately calculated.)

cells. Control cells were always irradiated on the same day as mutant strains, and three independent isolates were tested for each mutant strain over a 3-day period.

2.6. MMS-induced mutation and SCE rate

MMS-induced mutation and sister chromatid exchange (SCE) rates were measured as previously described [35]. Briefly, mutation rates were measured by selection for canavanine resistance (due to forward mutation of the *CAN1* gene). Mutation rates were determined in both the BY4741 and A364a backgrounds. SCE rates were measured in the A364a background, previously engineered to carry a *SCR::URA3* sister chromatid recombination substrate [36,37]. SCE and mutation rates were measured simultaneously (i.e. side by side on the same days with the same cell cultures) for these studies, and controls were always examined concurrently on the same day alongside mutant strains. MMS treatment of cells was performed exactly the same as described in Section 2.4. Following inactivation of the MMS by resuspension of cells in PBS + 5% sodium thiolsulfate, cells were serially diluted and plated onto SD-Arg-Ser + 60 mg/L canavanine medium (for measurement of mutation rates), SD-His medium (for measurement of SCE rates), and YPD medium (for viability). Plates were incubated at 30 °C for 3 days, and numbers of mutants/recombinants were assessed by the number of CFUs on the respective selection plates. Mutation rates were expressed as canavanine-resistant cells per 10^6 viable cells. SCE rates were expressed as His^+ cells per 10^6 viable cells. For both mutation and SCE, the rates after MMS induction were determined by subtracting the observed numbers of mutants or recombinants in the starting culture (i.e. pre-MMS exposure) from the number observed post-MMS exposure.

3. Results

3.1. A synthetic sensitivity screen reveals 25 interactions with RAD9, many of which involve post-replication repair

Synthetic enhancement genetics can be used to examine how mutations in two genes interact to modulate a phenotype and to uncover useful information about the functions of the interacting genes and their relationship [38]. We performed a genetic screen to identify second site mutations that enhance the DNA damage sensitivity of the *rad9Δ* mutant to chronic sublethal (0.01%) MMS treatment. We utilized a screening protocol derived from the dSLAM procedure [32]. Briefly, a *rad9Δ::URA3* query construct was introduced to a haploid-convertible heterozygous diploid yeast knockout library pool by integrative transformation. Following sporulation, the haploid double mutants carrying both the *rad9Δ* allele and a second gene disruption were selected and subsequently screened for sensitivity on synthetic complete media plates containing 0.01% MMS. A total of 27,000 colonies were screened from the double deletion library. From this, 337 individual double deletion mutants were found to be sensitive to MMS, of which 202 unique double mutants were identified by sequencing of the flanking barcode regions.

Our initial screen was not exclusive for the enhancement phenotype we sought, since all *single* mutants conferring significant sensitivity to MMS also would be recovered (in addition to the desired *rad9Δ*-interacting genes). Thus we performed a quantitative counter screen comparing the sensitivity of each double mutant candidate (*xxxΔ rad9Δ*) to the original single mutants (*xxxΔ*) from the deletion library by assessing viability following a 5-h exposure to 0.01% MMS in liquid rich medium. This counter screen identified a subset of 25 yeast gene disruptions that signif-

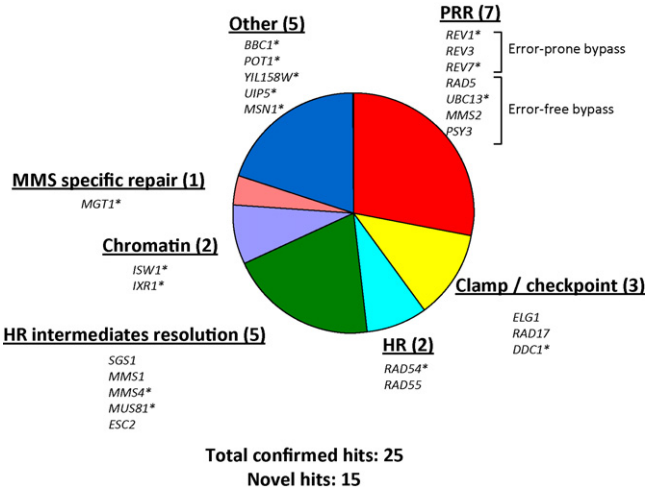

Fig. 1. Pie chart summarizing the results of the *rad9Δ* synthetic genetic screen in the presence of 0.01% methylmethane sulfonate (MMS). Genes were categorized according to their annotations in the Saccharomyces Genome Database (www.yeastgenome.org). The genes showing interactions with *RAD9* include genes functioning to accommodate DNA damage during replication and others that are previously unknown to be involved in the DNA damage response. Genes listed with asterisks represent interactions not previously identified. Fifteen novel *RAD9* genetic interactions were uncovered in this screen. Abbreviations are as follows: PRR, post-replication repair; HR, homologous recombination.

icantly enhance the sensitivity of the *rad9Δ* mutant, such that the *xxxΔ rad9Δ* double mutant was more sensitive to MMS than either the *rad9Δ* or the *xxxΔ* single mutants.

To reconfirm the enhanced sensitivity, we reconstructed individual gene deletions of the 25 genes in a wild type or *rad9Δ* background by mating each single deletion strain to a *rad9Δ* strain. Three independent segregants of each double or single mutant were subjected to a second round of MMS liquid kill curve testing. All 25 of the double mutants (*xxxΔ rad9Δ*) exhibited a 5-fold or greater enhanced sensitivity to MMS than either single mutant (*xxxΔ* or *rad9Δ*) ($p < 0.01$) (Table 2 and Supplemental Fig. S1). These genes comprised a number of different functional categories (Fig. 1), and 15 out of the 25 interactions were previously unobserved (indicated by an asterisk in Fig. 1). The severity of the interaction with *rad9Δ* varied significantly among these categories (Table 2). Notably, genes involved in PRR exhibited the highest degree of interaction with *rad9Δ* (Table 2 and Supplemental Fig. S1). Genes involved in homologous recombination repair (HR) and resolution of HR intermediates as well as direct reversal of alkylation (*MGT1*) and other aspects of DNA repair (*IXR1*) also enhanced the sensitivity of *rad9Δ*.

Interestingly, we also identified a number of genes not previously known to function in the DDR, including *ISW1* (chromatin remodeling), *POT1* (fatty acid metabolism), *BBC1* (localized to actin patches), *MSN1* (transcription), and two uncharacterized genes, *YIL158W* and *UIP5*. In order to determine whether these interactions displayed general DNA damage sensitivity or MMS-specific sensitivity, we tested whether these genes enhanced *rad9Δ* sensitivity to ionizing radiation as well. Four of the candidates (*BBC1*, *ISW1*, *YIL158W* and *POT1*) displayed cross-sensitivity to ionizing radiation, suggesting that these genes are important for surviving DNA damage in *rad9Δ* cells (Supplemental Fig. S2).

3.2. The rad9Δ mutant shows a dose-dependent, REV3-dependent hypermutable phenotype in MMS

Cells have multiple repair options available for handling any single lesion; however the cellular mechanism for choosing which pathway to utilize is poorly understood. In light of results from our screen and recent data linking checkpoint genes to choice of PRR mechanism [39], we sought to explore the role of the *S. cerevisiae* checkpoint gene *RAD9* in such a function. We hypothesized that if *RAD9* contributed to regulation of mutagenic versus error-free PRR in the S-phase, then the *rad9Δ* mutant might exhibit a hypermutable phenotype when treated with the DNA alkylating agent MMS. To test this prediction, we exposed cells to 0.01% MMS in liquid culture for 5 h and assayed induction of mutations by measuring forward mutation to canavanine resistance. As shown in Fig. 2A, the *rad9Δ* mutant shows significant elevation of MMS-induced mutation rate compared to wild type ($p \leq 0.01$).

At first glance, this result contradicts a previous report by Barbour et al. that the *rad9Δ* mutant is *not* hypermutable in the presence of MMS [28]. However, we subsequently noted that the MMS exposures were very different between these two studies; in our study, cells were exposed for 5 h to 0.01% MMS, whereas in the Barbour et al. study, cells were exposed to a higher concentration of MMS (0.05%) for half an hour. We hypothesized that this critical difference in exposure might explain the discordant results in the two studies. To test this, we measured MMS-induced mutation rates in the same strains under the two conditions (5 h at 0.01% MMS versus 0.5 h at 0.05% MMS; see Fig. 2A). Consistent with the report of Barbour et al., we saw no hypermutable phenotype of *rad9Δ* at the 0.05% MMS dose, demonstrating the dose-dependence of the *rad9Δ* hypermutable phenotype (Fig. 2A).

To test whether the *rad9Δ* MMS dose-dependent hypermutable phenotype was specific to the BY4741 strain background, we repeated the mutagenesis studies in the A364a strain background. As shown in Fig. 2B, the MMS dose-dependent hypermutable phenotype is recapitulated in the A364a background; furthermore, the hypermutable phenotype could also be detected at a 10-fold lower MMS exposure (0.001%) (Fig. 2C). We conclude that the hypermutable phenotype of *rad9Δ* in MMS is dose-dependent and is not unique to the BY4741 strain background.

To determine whether the hypermutable phenotype was dependent on the canonical *REV3*-dependent error-prone PRR pathway, we tested whether the recovery of *can1* mutants in the *rad9Δ* background was *REV3*-dependent. We constructed a *rad9Δ rev3Δ* double mutant and repeated the mutagenesis experiment. As shown in Fig. 2C, the hypermutable phenotype of *rad9Δ* cells is dependent on *REV3*, demonstrating that the hypermutable phenotype is due to increased activity of the error-prone *REV3*-dependent branch of the PRR pathway.

In addition to mutagenic damage tolerance mechanisms, PRR can also employ homologous recombination (HR), which can be tested by measuring sister chromatid exchange (SCE) rates. Thus, we asked whether *rad9Δ* has an effect on SCE induction in the presence of MMS. We observed that wild type and *rad9Δ* cells exhibited no significant difference in SCE induction in either the 0.01% (5 h) or the 0.05% (0.5 h) MMS conditions (Fig. 2B). Thus, we conclude that while *rad9Δ* mutation affects MMS-inducible mutation rates, there is no effect on the rate of MMS-inducible SCE in these cells.

3.3. The dose-dependence of the hypermutable phenotype in rad9Δ correlates with differences in cell cycle distribution in response to different doses of MMS

One possible explanation for the dose-dependence of the *rad9Δ* hypermutable phenotype is that in 0.05% MMS, lesion density is high enough to produce multiple lesions in a short track of DNA, which is more likely to degrade or be processed to a DSB than to induce mutagenic translesion synthesis. However, our data do not support this model. For example, if more DSB were being produced in the 0.05% versus 0.01% MMS conditions, we would expect to see higher rates of sister chromatid recombination in the former. In contrast, we see a higher level of sister chromatid exchange

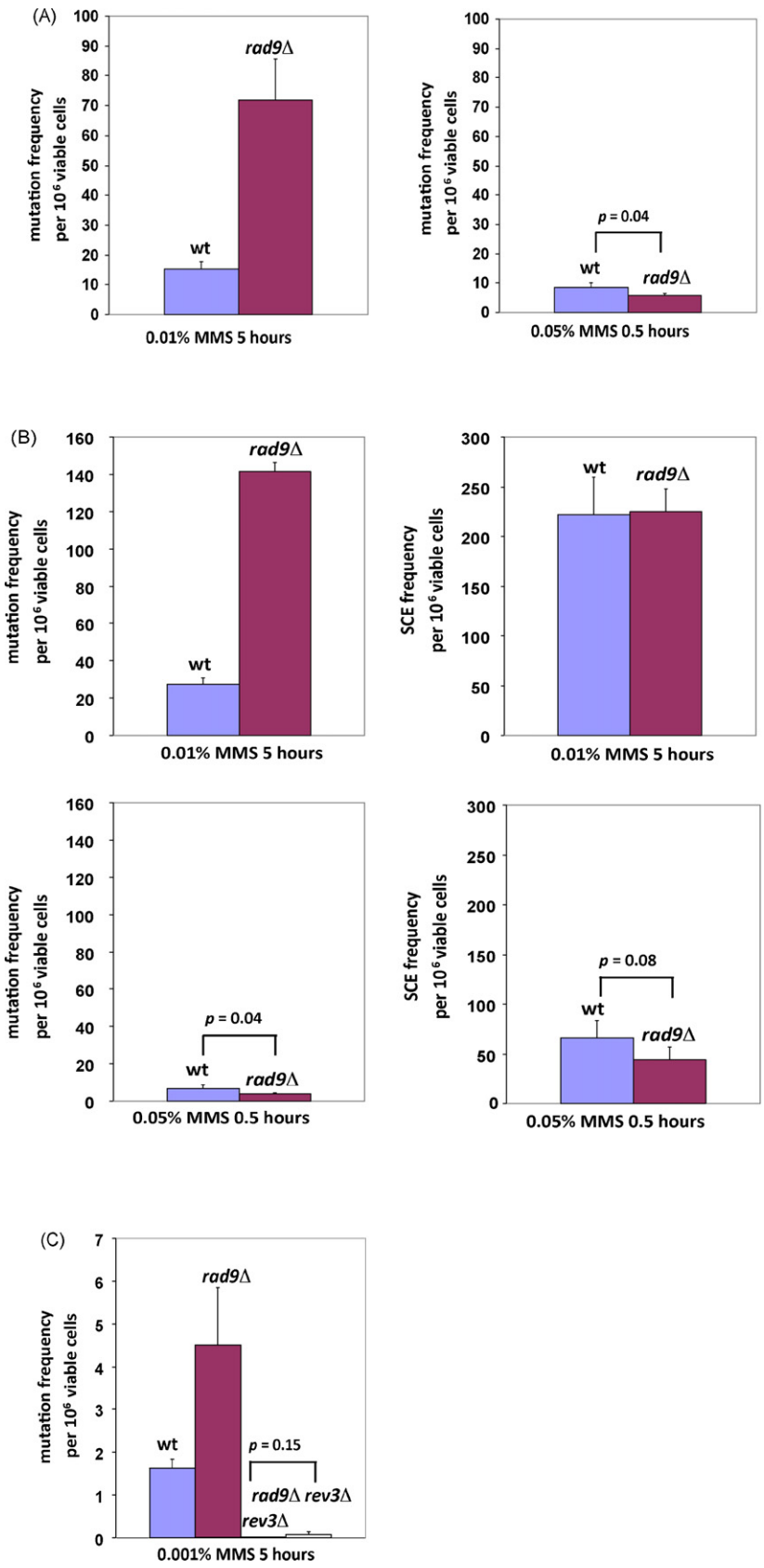

Fig. 2. MMS dose-dependent hypermutation phenotype in the *rad9Δ* mutant. (A) Log-phase wild type (BY4741) and *rad9Δ* (CB1021) cells (BY4741 background) were grown in the presence of 0.01% MMS for 5 h and then harvested for the determination of survival (62 ± 5% and 4.8 ± 0.5% for wild type and *rad9Δ* cells, respectively) and a induction of mutation to Can^R (upper panel). In parallel, the survival and mutation rates were also determined for wild type and *rad9Δ* cells grown for a shorter time (0.5 h) in higher concentration (0.05%) of MMS (lower panel, the survival rate for wild type and *rad9Δ* were 98 ± 3% and 73 ± 4%, respectively). Each strain was tested in triplicate, and the error bars represent the standard deviations. (B) Yeast cells from a different genetic background (A364a) were tested for mutation to Can^R as well as induction of SCE after

induction in the 0.01% MMS conditions (Fig. 2B). Also *not* consistent with there being more DSB in the 0.05% conditions, the 0.01% MMS condition introduces more lethal damage (DSBs are lethal in haploid yeast cells), evidenced by lower survival of *rad9Δ*, indicating that a concentration of 0.01% MMS at 5 h is a higher *effective dose* than 0.05% MMS at ½ h. Thus it is unlikely that the possibility of fewer DSBs at the lower concentration explains the hypermutable phenotype.

Since it has been documented that DNA repair and DNA damage tolerance mechanisms differ throughout the cell cycle [36,40], a second possible explanation for the dose-dependence of the *rad9Δ* hypermutable phenotype is that cell cycle distributions differ significantly between the 0.01% and 0.05% MMS conditions used in these studies. (We previously demonstrated that 0.015–0.03% MMS exposure induces a regulated slowing of S-phase progression, termed the intra-S-phase checkpoint [3,7,40]; the 0.05% dose used in the Barbour et al. study was not previously tested for S-phase effects.) To test this hypothesis, we treated wild type and *rad9Δ* cells with either 0.01% or 0.05% MMS for a period of 5 h, withdrawing cells at multiple time points throughout the treatment for assessment of cell cycle distribution by flow cytometry. As seen in Fig. 3A, wild type cells treated with 0.01% of MMS accumulate in the S-phase over the course of 5 h, as previously described [3,7]. Also as previously described [7], *rad9Δ* cells treated with the same dose show reduced accumulation in the S-phase, proceeding through to the G2 phase faster than wild type. In dramatic contrast, there is no observable accumulation of *rad9Δ* cells in the S-phase during a 30 min pulse of an asynchronous culture with 0.05% MMS (Fig. 3A), the conditions used in the Barbour et al. study. Based on these data, the majority of MMS-induced DNA damage in our experiments (0.01% MMS) is introduced during the S-phase of the cell cycle, whereas the majority of damage was induced outside of the S-phase in the 0.05% MMS condition used in the Barbour et al. study. Moreover, if we treat cells with 0.05% MMS past the 30 min pulse, we see a synchronization represented by a strong G1 peak (Fig. 3A). We confirmed that these cells were accumulating in the G1 phase through the observation that the majority of cells at the higher dose remain unbudded (Fig. 3B). However, a proportion of budded cells remain, suggesting that though replication is suppressed, it may not entirely be due to accumulation in the G1 phase. It is possible that a small proportion of cells progress into the S-phase upon treatment with 0.05% MMS, but the replication forks may only progress for very small distances in response to high doses (producing a "G1-like" S-phase peak). Nonetheless, these results are consistent with the hypothesis that the defect in the intra-S-phase checkpoint in *rad9Δ* cells leads to a higher mutation rate in the 0.01% MMS treatment (where cells are replicating), but not in the 0.05% MMS treatment (where replication is suppressed). Importantly, it has been demonstrated that cells are most susceptible to mutagenesis in the S-phase of the cell cycle [40].

If the dose-dependent *rad9Δ* hypermutable phenotype was due to a defect in the intra-S-phase DNA damage checkpoint, then we predicted that other mutations (e.g. *rad17Δ* and *rad24Δ*) affecting this checkpoint might also exhibit dose-dependent hypermutability in MMS [7]. To test this prediction, we measured mutation and SCE induction in *rad17Δ* and *rad24Δ* mutants in 0.01% MMS. As shown in Fig. 3C, the *rad17Δ* and *rad24Δ* mutants phenocopy *rad9Δ*, displaying hypermutability in response to a 5 h exposure to 0.01% MMS, but no effect on MMS-induced SCE. Like *rad9Δ*, both *rad17Δ* and *rad24Δ* mutants display reduced accumulation in the S-phase after chronic MMS treatment [7], a phenotype that is not evident following a pulse of 0.05% MMS (Supplemental Fig. S3). The observation that additional intra-S-phase checkpoint-defective mutants exhibit similarly enhanced MMS-inducible mutation rates is consistent with a model wherein the hypermutable phenotype is a result of inappropriate S-phase progression in the presence of MMS-induced damage.

4. Discussion

4.1. DNA damage, RAD9 and the S-phase

As described in this study, MMS dose has a profound impact on cell cycle distributions. In the previous study by Barbour et al. [28], a rapid 30 min pulse with 0.05% MMS is not associated with accumulation of cells in S-phase (Fig. 3), and base excision repair is likely to remove alkylation damage, in most cases prior to entry into the S-phase (after the MMS is withdrawn). As a result, there is little consequence to the genetic integrity of the cell. However, if residual damage remains once cells enter the S-phase, or if damage is introduced during the S-phase (as is the case in the 0.01% MMS condition used in our experiments), replication forks encounter the damage and stall, and cells are forced to employ damage tolerance mechanisms, some of which are mutagenic. This hypothesis is consistent with studies of Ostroff et al. and Kadyk et al. that demonstrated that cells are most susceptible to UV-induced mutagenesis and sister chromatid exchange during the S-phase of the cell cycle [37,40].

There are three potential outcomes for a stalled replication fork (Fig. 4). First, DNA repair proteins (e.g. base excision repair) may remove the offending lesion, allowing the fork to resume replication. Second, the lesion can be tolerated (i.e. circumnavigated, rather than being removed) either by template switching (dependent on *MMS2*, *UBC13*, *RAD5*) or by mutagenic translesion synthesis (dependent on *REV1*, *REV3*, *REV7*). Third, the stalled fork may collapse, and occasional fork collapses are repaired by homologous recombination (HR) [41]. *MEC1* is required for stabilizing stalled forks; hence in the *mec1* mutant stalled forks collapse irreversibly at high rates, resulting in rapid death [42].

Our genome-wide screen revealed extensive interactions between *RAD9* and post-replication repair genes required for tolerating unrepaired DNA damage during the S-phase. We can infer from the heightened importance of post-replication repair in *rad9Δ* cells that replication forks are encountering lesions more frequently in the *rad9Δ* mutant than in the wild type. This could be due to: (i) a general decrease in the efficiency of repair or reversal of alkylation damage in the *rad9Δ* mutant, and/or (ii) abnormal coordination between DNA replication and alkylation damage repair or reversal in the *rad9Δ* mutant, resulting in an increase in the number of lesions' being encountered by replication forks. There are data suggesting that either or both of these mechanisms could occur, as discussed below.

RAD9 has been implicated in nucleotide excision repair of UV-damaged DNA [43,44]. Recent studies have suggested that *RAD9* is required for repair of the transcribed strands and the non-transcribed strands of active genes (but not for repair of transcriptionally inactive DNA sequences), possibly through the up-regulation of genes involved in the repair process [45]. There are no studies reported to look for a role, either direct or indirect,

MMS exposure (as above). The survival rates for wild type (yMP10381) and *rad9Δ* (yMP11030) were 79 ± 6% and 3.1 ± 0.2%, respectively in the 0.01%/5 h MMS treatment; the survival rates for wild type and *rad9Δ* were 88 ± 6% and 84 ± 2%, respectively in the 0.05%/0.5 h MMS treatment. Each strain was tested in triplicate, and the error bars represent standard deviations. (C) The MMS-induced hypermutability of *rad9Δ* is *REV3*-dependent. Wild type (yMP10381), *rad9Δ* (yMP11030), *rev3Δ* (yMP10382), and *rad9Δ rev3Δ* (yDH51, yDH52, yDH53) cells were tested for survival and mutation to Can^R after treatment with a very low concentration of MMS (0.001%) for 5 h (low concentration MMS was required due to the high sensitivity of the *rad9Δ rev3Δ* double mutant, Table 2). The survival rates for wild type, *rad9Δ*, *rev3Δ* and *rad9Δ rev3Δ* cells were 93 ± 3%, 63 ± 4%, 90 ± 12% and 12 ± 1%, respectively. Each strain was tested in triplicate, and the error bars represent standard deviations.

of *RAD9* in promoting base excision repair or direct reversal of alkylation damage, and this would be an interesting area of follow-up investigation.

We previously showed that in the continuous presence of MMS, the rate of S-phase progression is dramatically slowed by an intra-S-phase checkpoint in wild type cells [3], suggesting the possibility that there may be coordination between DNA replication and repair. It is interesting to note that while *mec1* and *rad53* mutants show severe defects in S-phase regulation in the presence of MMS, *rad9Δ* mutation confers a far more subtle defect [7]. The basis of these two distinct phenotypes is not understood, and it is equally plausible that *MEC1* (or *RAD53*) and *RAD9* are involved in distinct mechanisms controlling S-phase progression or that they are involved in the same mechanism, with the *MEC1* and *RAD53* mutations showing higher penetrance. Of note, the *mec1 rad9Δ* and *rad53Δ rad9Δ* double mutants are more sensitive to MMS then any of the single mutants [7], indicating that the survival-promoting functions of *MEC1* and *RAD53* do not lie completely within the same pathway as that for *RAD9*.

Elegant work by Tercero and Diffley [42] investigated the underlying mechanism of S-phase slowing in the presence of MMS, and the effects of mutations in *RAD53* and *MEC1*. They showed that exposure to MMS reduces the rate of DNA replication fork progression to about 300 base pairs per minute, 5–10 times lower than fork rates in the absence of MMS [46,47]. However, they found that the slow fork rate progression does not require *RAD53* or *MEC1*, indicating that the accelerated S-phase is primarily a consequence of inappropriate initiation events observed in these mutants. Furthermore, the cytotoxicity of MMS in checkpoint mutants occurs specifically when cells are allowed to enter S-phase with damage, at which time replication forks in checkpoint mutants collapse irreversibly at high rates. Hence, preventing damage-induced replication fork catastrophe seems to be a primary mechanism by which the *MEC1*-dependent checkpoint preserves viability in the face of DNA alkylation. (Of note, these studies were all performed in the presence of 0.033% MMS.)

The mechanism underlying the *RAD9*-dependent slowing of S-phase progression in response to MMS has not been investigated,

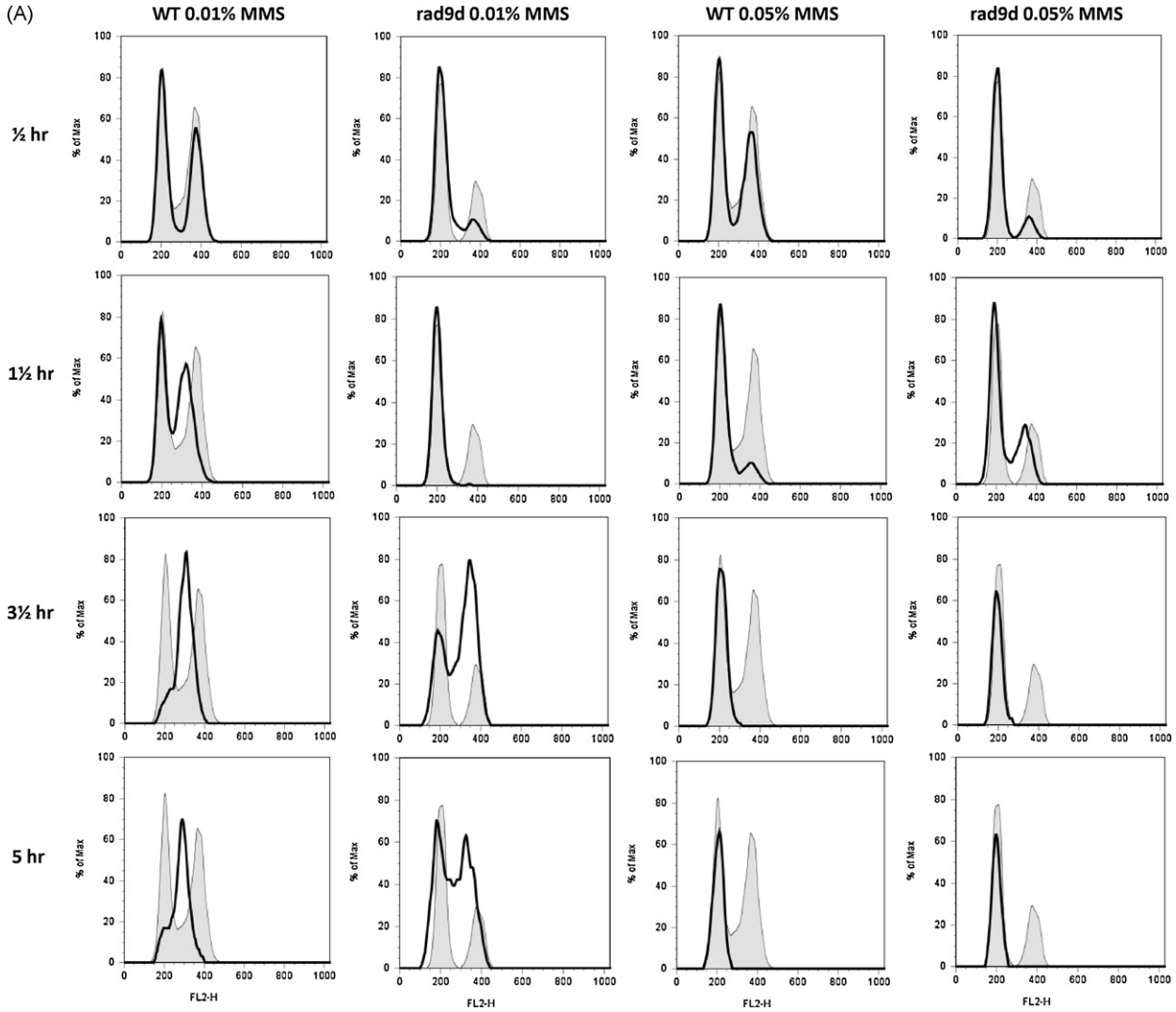

Fig. 3. Relationship between the hypermutability phenotype and cell cycle distribution. (A) Cell cycle redistribution following continuous exposure of asynchronous populations of wild type (yMP10381) or *rad9Δ* (yMP11030) cells to 0.01% and 0.05% MMS. At indicated times of exposure, samples were removed and analyzed by flow cytometry. Each panel contains two histograms. Shaded histograms represent the cell cycle distribution of the asynchronous culture, before addition of MMS. Overlaid histograms represent the cell cycle distribution at various times after addition of MMS. (B) Percentage of unbudded cells at the indicated time during MMS exposure in liquid cultures for wild type and *rad9Δ* cells. (C) Multiple intra-S-phase checkpoint-defective strains show hypermutability in 0.01% MMS. Wild type (yMP10381), *rad9Δ* (yMP11030), *rad17Δ* (yMP11089), and *rad24Δ* (yMP11006) cells were tested for survival, mutation to Can^R and SCE after exposure to 0.01% MMS for 5 h, as above. The survival rates for wild type, *rad9Δ*, *rad17Δ*, and *rad24Δ* cells were 66 ± 8%, 3.5 ± 0.3%, 4.1 ± 0.2% and 1.7 ± 0.2%, respectively. Each strain was tested in triplicate, and the error bars represent standard deviations.

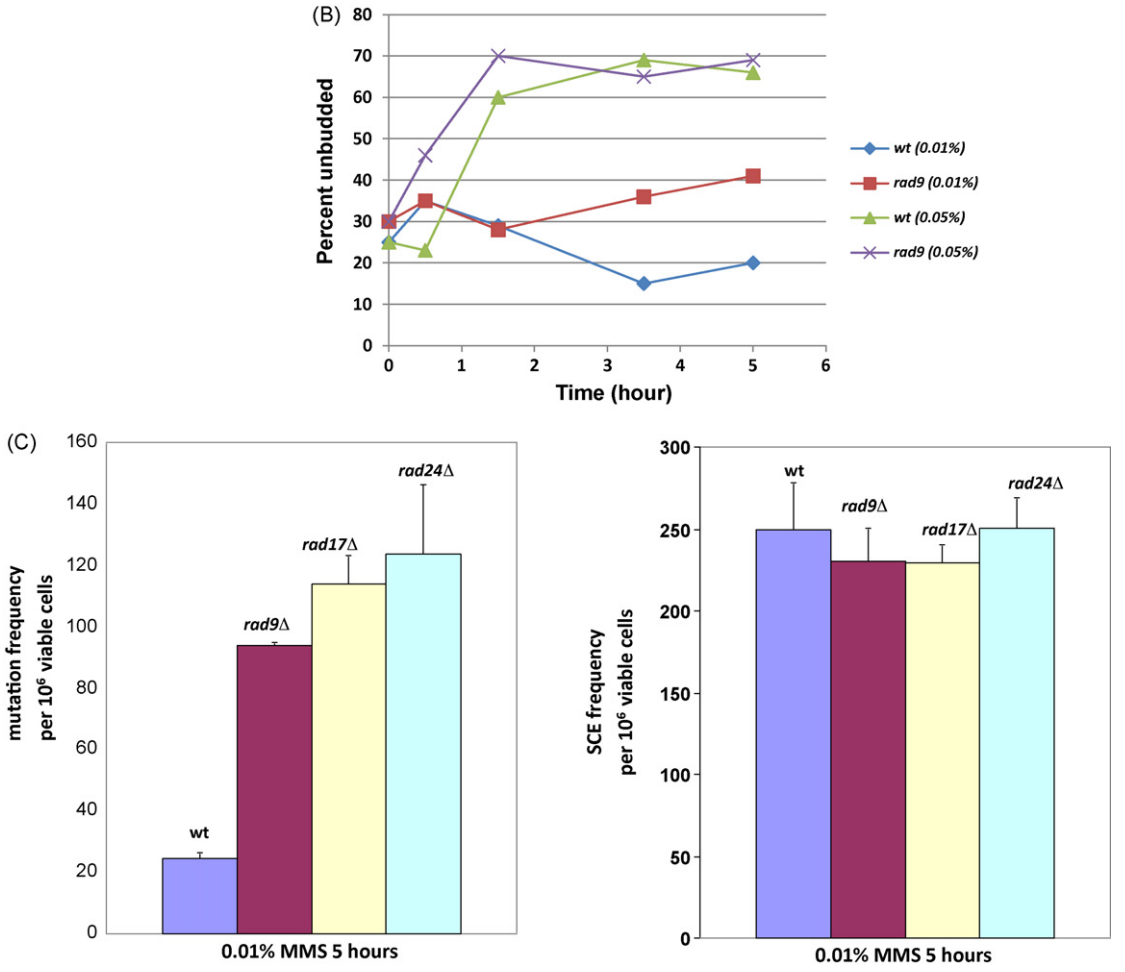

Fig. 3. (*Continued*).

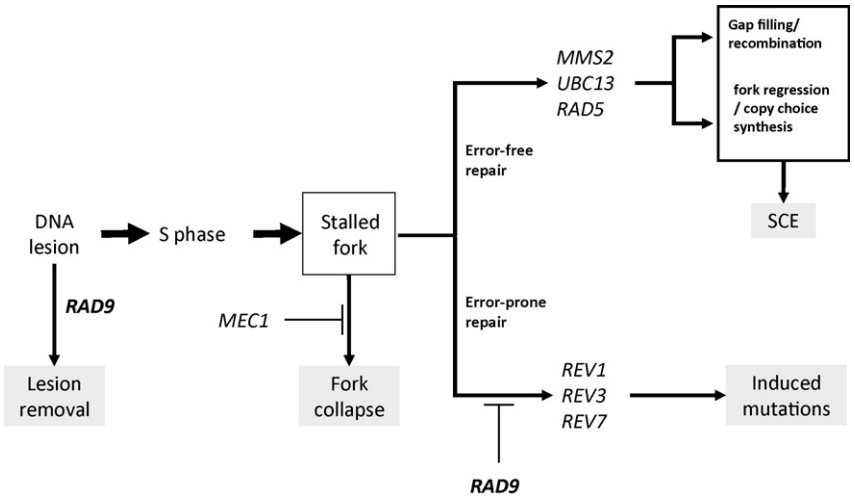

Fig. 4. One model proposing a role for *RAD9* in regulating how lesions are channeled at the replication fork. Under the model, in the presence of MMS, *RAD9* activity would strongly and *actively promote* use of non-mutagenic base excision repair (and/or alkylation reversal), while it would *actively suppress* mutagenic translesion synthesis. Hence, loss of *RAD9* function would reduce the efficacy of base excision repair, thereby increasing the reliance of cells on template switching and translesion synthesis for survival; this would explain the synergy observed between the *rad9Δ* and both the *mms2* and *rev3* mutants. Additionally, loss of *RAD9* function would result in derepression of translesion synthesis, resulting in the hypermutable phenotype observed in our experiments. Hence, under this model, *RAD9* stabilizes the genome by maximizing the cell's ability to employ non-mutagenic mechanisms (base excision repair and template switching) of repairing or tolerating lesions, while suppressing mutagenic translesion synthesis. As discussed in the text, a second alternative model is that *RAD9* acts to promote continuous DNA synthesis, potentially by limiting re-priming of stalled forks at MMS lesions. In this model, the observed hypermutability in MMS-treated *rad9Δ* cells may be due to an increased reliance on PRR to repair large ssDNA gaps resulting from discontinuous synthesis, which would explain the synergy between *rad9Δ* and both the *MMS2* and *REV3* branches of PRR.

nor have fork elongation rates been measured in the *rad9Δ* mutant in the presence of low dose MMS (i.e. 0.01% MMS during active S-phase). Hence, while the Tercero and Diffley [42] data eliminate the possibility of *MEC1*-dependent control of replication fork elongation (at least in 0.033% MMS), their data do not eliminate the possibility that fork elongation rate is controlled in a *MEC1*-independent mechanism. Hence, although speculative, it remains formally possible that slowing of S-phase in response to MMS is due both to control of origin firing (*MEC1*-dependent) and control of elongation, and we hypothesize that control of elongation may be *RAD9*-dependent and required for efficient removal of alkylation damage, via a mechanism potentially analogous to transcription-repair coupling [48].

4.2. Model for RAD9's facilitating the repair or tolerance of DNA damage by regulating the replication fork

Barbour et al. proposed that because *rad9Δ* is synergistic to both *mms2* and *rev3* with respect to killing by MMS, *RAD9* likely functions as a separate branch of post-replication repair, independent of the *REV3*- and *MMS2*-associated branches and downstream of *RAD18*. Our observation that *rad9Δ* cells are hypermutable in 0.01% MMS is consistent with this model, in that loss of a parallel post-replication repair pathway could shuttle a higher percentage of DNA lesions into the mutagenic, *REV3*-dependent translesion synthesis pathway. There are alternative models.

One alternative model is that the *RAD9* adapter acts at the replication fork at sites of damage to regulate how DNA damage is channeled through the various repair and tolerance pathways during the S-phase so as to minimize genetic instability (Fig. 4). Ill-described biochemical acrobatics must occur at the fork to elicit polymerase switching or template switching when DNA damage tolerance mechanisms are employed, and the mechanism of these switches is unclear [49]. Under this alternative model, in the presence of MMS, *RAD9* activity would strongly and *actively promote* use of non-mutagenic base excision repair (and/or alkylation reversal), while it would *actively suppress* mutagenic translesion synthesis. Hence, loss of *RAD9* function would reduce the efficacy of base excision repair (Fig. 4), thereby increasing the reliance of cells on template switching and translesion synthesis for survival; this would explain the synergy observed between the *rad9Δ* and both the *mms2Δ* and *rev3Δ* mutants, without evoking the need of a novel post-replication repair pathway. Additionally, loss of *RAD9* function would result in derepression of translesion synthesis (Fig. 4), leading to the hypermutable phenotype observed in our experiments. Hence, under this alternative model, *RAD9* does not participate in a third branch of DNA damage tolerance, but rather it stabilizes the genome by maximizing the cell's ability to employ non-mutagenic mechanisms (base excision repair and template switching) of repairing or tolerating lesions, while suppressing mutagenic translesion synthesis.

A second alternative model is that *RAD9* acts to promote continuous DNA synthesis, potentially by limiting re-priming of stalled forks at MMS lesions. In this model, the observed hypermutability in MMS-treated *rad9Δ* cells may be due to an increased reliance on PRR to repair large ssDNA gaps resulting from discontinuous synthesis, which would explain the synergy between *rad9Δ* and both the *MMS2* and *REV3* branches of PRR.

Interactions between *rad9Δ* and HR repair genes are consistent with both models. In the first model, loss of *RAD9* function would result in a higher frequency of fork stalling at unrepaired lesions, leading to an elevated probability of fork collapse and repair by HR genes [41,50]. In the second model, a number of these HR genes (*SGS1*, *MUS81*, *MMS4* and members of the *RAD52* group) have been shown to promote gap repair and are epistatic to genes in the error-free branch of PRR [51,52,56]. Their synergy with *rad9Δ* may indicate an inability to repair large ssDNA gaps in *rad9Δ* cells. Recent work has shown that the choice among homologous recombination, translesion synthesis, and Rad52-related gap repair is dependent on a complex interplay between ubiquitination and sumoylation of PCNA [53]. The role, if any, that *RAD9* might play in mediating these signaling events is an intriguing avenue for further study.

4.3. Implications for human disease

BRCA1, one putative mammalian homolog of *RAD9*, also plays an important role in S-phase checkpoint regulation and genome stability [54]. It is tempting to speculate that BRCA1 may also have synergistic interactions with homologs of PRR genes characterized in this study. If such synergistic interactions are evident in human cells, such genes may be modifiers of cancer penetrance for *BRCA1* cases. Moreover, inhibition of PRR pathways may serve as an effective treatment mechanism for BRCA1 −/− tumors, comparable to the growing use of poly(ADP-ribose) polymerase (PARP) inhibitors, now in clinical trials for treating BRCA-deficient tumors [55].

Conflict of interest

The authors declare that there are no conflicts of interest.

Acknowledgments

We thank Jef Boeke for the diploid deletion library pool and Sean Wang for help with statistical analyses. We thank our anonymous reviewers for their insightful comments and suggestions. B.D.P. was supported by the FHCRC Dual Mentor Program and a U.S. Department of Defense Breast Cancer Research Program predoctoral fellowship. This work was supported by NIH grant R01 CA 129604.

Appendix A. Supplementary data

Supplementary data associated with this article can be found, in the online version, at doi:10.1016/j.dnarep.2010.04.007.

References

[1] T.A. Weinert, L.H. Hartwell, The RAD9 gene controls the cell cycle response to DNA damage in *Saccharomyces cerevisiae*, Science 241 (1988) 317–322.
[2] W. Siede, A.S. Friedberg, E.C. Friedberg, RAD9-dependent G1 arrest defines a second checkpoint for damaged DNA in the cell cycle of *Saccharomyces cerevisiae*, Proc. Natl. Acad. Sci. U.S.A. 90 (1993) 7985–7989.
[3] A.G. Paulovich, L.H. Hartwell, A checkpoint regulates the rate of progression through S phase in *S. cerevisiae* in response to DNA damage, Cell 82 (1995) 841–847.
[4] T. Walsh, M.C. King, Ten genes for inherited breast cancer, Cancer Cell 11 (2007) 103–105.
[5] E.C. Friedberg, E.C. Friedberg, DNA Repair and Mutagenesis, ASM Press, Washington, DC, 2006.
[6] W. Xiao, B.L. Chow, L. Rathgeber, The repair of DNA methylation damage in *Saccharomyces cerevisiae*, Curr. Genet. 30 (1996) 461–468.
[7] A.G. Paulovich, R.U. Margulies, B.M. Garvik, L.H. Hartwell, RAD9, RAD17, and RAD24 are required for S phase regulation in *Saccharomyces cerevisiae* in response to DNA damage, Genetics 145 (1997) 45–62.
[8] M.P. Longhese, R. Fraschini, P. Plevani, G. Lucchini, Yeast pip3/mec3 mutants fail to delay entry into S phase and to slow DNA replication in response to DNA damage, and they define a functional link between Mec3 and DNA primase, Mol. Cell. Biol. 16 (1996) 3235–3244.
[9] M.P. Longhese, V. Paciotti, R. Fraschini, R. Zaccarini, P. Plevani, G. Lucchini, The novel DNA damage checkpoint protein ddc1p is phosphorylated periodically during the cell cycle and in response to DNA damage in budding yeast, EMBO J. 16 (1997) 5216–5226.
[10] X.J. Yang, Multisite protein modification and intramolecular signaling, Oncogene 24 (2005) 1653–1662.
[11] F. Conde, E. Refolio, V. Cordon-Preciado, F. Cortes-Ledesma, L. Aragon, A. Aguilera, P.A. San-Segundo, The Dot1 histone methyltransferase and the Rad9 checkpoint adaptor contribute to cohesin-dependent double-strand break

repair by sister chromatid recombination in *Saccharomyces cerevisiae*, Genetics 182 (2009) 437–446.
[12] J.E. Vialard, C.S. Gilbert, C.M. Green, N.F. Lowndes, The budding yeast Rad9 checkpoint protein is subjected to Mec1/Tel1-dependent hyperphosphorylation and interacts with Rad53 after DNA damage, EMBO J. 17 (1998) 5679–5688.
[13] A. Emili, MEC1-dependent phosphorylation of Rad9p in response to DNA damage, Mol. Cell 2 (1998) 183–189.
[14] J. Soulier, N.F. Lowndes, The BRCT domain of the *S. cerevisiae* checkpoint protein Rad9 mediates a Rad9–Rad9 interaction after DNA damage, Curr. Biol. 9 (1999) 551–554.
[15] M.F. Schwartz, J.K. Duong, Z. Sun, J.S. Morrow, D. Pradhan, D.F. Stern, Rad9 phosphorylation sites couple Rad53 to the *Saccharomyces cerevisiae* DNA damage checkpoint, Mol. Cell 9 (2002) 1055–1065.
[16] A.M. Carr, DNA structure dependent checkpoints as regulators of DNA repair, DNA Repair (Amst) 1 (2002) 983–994.
[17] T. Usui, S.S. Foster, J.H. Petrini, Maintenance of the DNA-damage checkpoint requires DNA-damage-induced mediator protein oligomerization, Mol. Cell 33 (2009) 147–159.
[18] C.S. Gilbert, C.M. Green, N.F. Lowndes, Budding yeast Rad9 is an ATP-dependent Rad53 activating machine, Mol. Cell 8 (2001) 129–136.
[19] F.D. Sweeney, F. Yang, A. Chi, J. Shabanowitz, D.F. Hunt, D. Durocher, *Saccharomyces cerevisiae* Rad9 acts as a Mec1 adaptor to allow Rad53 activation, Curr. Biol. 15 (2005) 1364–1375.
[20] J. Majka, P.M. Burgers, Yeast Rad17/Mec3/Ddc1: a sliding clamp for the DNA damage checkpoint, Proc. Natl. Acad. Sci. U.S.A. 100 (2003) 2249–2254.
[21] C.Y. Bonilla, J.A. Melo, D.P. Toczyski, Colocalization of sensors is sufficient to activate the DNA damage checkpoint in the absence of damage, Mol. Cell 30 (2008) 267–276.
[22] S. Sabbioneda, B.K. Minesinger, M. Giannattasio, P. Plevani, M. Muzi-Falconi, S. Jinks-Robertson, The 9-1-1 checkpoint clamp physically interacts with polzeta and is partially required for spontaneous polzeta-dependent mutagenesis in *Saccharomyces cerevisiae*, J. Biol. Chem. 280 (2005) 38657–38665.
[23] A.G. Paulovich, D.P. Toczyski, L.H. Hartwell, When checkpoints fail, Cell 88 (1997) 315–321.
[24] P.L. Andersen, F. Xu, W. Xiao, Eukaryotic DNA damage tolerance and translesion synthesis through covalent modifications of PCNA, Cell Res. 18 (2008) 162–173.
[25] J.R. Nelson, C.W. Lawrence, D.C. Hinkle, Thymine–thymine dimer bypass by yeast DNA polymerase zeta, Science 272 (1996) 1646–1649.
[26] A. Blastyak, L. Pinter, I. Unk, L. Prakash, S. Prakash, L. Haracska, Yeast Rad5 protein required for postreplication repair has a DNA helicase activity specific for replication fork regression, Mol. Cell 28 (2007) 167–175.
[27] M.A. Resnick, The repair of double-strand breaks in chromosomal DNA of yeast, Basic Life Sci. 5B (1975) 549–556.
[28] L. Barbour, L.G. Ball, K. Zhang, W. Xiao, DNA damage checkpoints are involved in postreplication repair, Genetics 174 (2006) 1789–1800.
[29] D.C. Amberg, D.J. Burke, J.N. Strathern, Methods in Yeast Genetics: A Cold Spring Harbor Laboratory Course Manual, Cold Spring Harbor Laboratory Press, NY, 2005.
[30] X. Pan, D.S. Yuan, S.L. Ooi, X. Wang, S. Sookhai-Mahadeo, P. Meluh, J.D. Boeke, dSLAM analysis of genome-wide genetic interactions in *Saccharomyces cerevisiae*, Methods 41 (2007) 206–221.
[31] C.B. Brachmann, A. Davies, G.J. Cost, E. Caputo, J. Li, P. Hieter, J.D. Boeke, Designer deletion strains derived from *Saccharomyces cerevisiae* S288C: a useful set of strains and plasmids for PCR-mediated gene disruption and other applications, Yeast 14 (1998) 115–132.
[32] X. Pan, D.S. Yuan, D. Xiang, X. Wang, S. Sookhai-Mahadeo, J.S. Bader, P. Hieter, F. Spencer, J.D. Boeke, A robust toolkit for functional profiling of the yeast genome, Mol. Cell 16 (2004) 487–496.
[33] E.A. Winzeler, D.D. Shoemaker, A. Astromoff, H. Liang, K. Anderson, B. Andre, R. Bangham, R. Benito, J.D. Boeke, H. Bussey, A.M. Chu, C. Connelly, K. Davis, F. Dietrich, S.W. Dow, M. El-Bakkoury, F. Foury, S.H. Friend, E. Gentalen, G. Giaever, J.H. Hegemann, T. Jones, M. Laub, H. Liao, N. Liebundguth, D.J. Lockhart, A. Lucau-Danila, M. Lussier, N. M'Rabet, P. Menard, M. Mittmann, C. Pai, C. Rebischung, J.L. Revuelta, L. Riles, C.J. Roberts, P. Ross-MacDonald, B. Scherens, M. Snyder, S. Sookhai-Mahadeo, R.K. Storms, S. Veronneau, M. Voet, G. Volckaert, T.R. Ward, R. Wysocki, G.S. Yen, K. Yu, K. Zimmermann, P. Philippsen, M. Johnston, R.W. Davis, Functional characterization of the *S. cerevisiae* genome by gene deletion and parallel analysis, Science 285 (1999) 901–906.
[34] G. Giaever, A.M. Chu, L. Ni, C. Connelly, L. Riles, S. Veronneau, S. Dow, A. Lucau-Danila, K. Anderson, B. Andre, A.P. Arkin, A. Astromoff, M. El-Bakkoury, R. Bangham, R. Benito, S. Brachat, S. Campanaro, M. Curtiss, K. Davis, A. Deutschbauer, K.D. Entian, P. Flaherty, F. Foury, D.J. Garfinkel, M. Gerstein, D. Gotte, U. Guldener, J.H. Hegemann, S. Hempel, Z. Herman, D.F. Jaramillo, D.E. Kelly, S.L. Kelly, P. Kotter, D. LaBonte, D.C. Lamb, N. Lan, H. Liang, H. Liao, L. Liu, C. Luo, M. Lussier, R. Mao, P. Menard, S.L. Ooi, J.L. Revuelta, C.J. Roberts, M. Rose, P. Ross-Macdonald, B. Scherens, G. Schimmack, B. Shafer, D.D. Shoemaker, S. Sookhai-Mahadeo, R.K. Storms, J.N. Strathern, G. Valle, M. Voet, G. Volckaert, C.Y. Wang, T.R. Ward, J. Wilhelmy, E.A. Winzeler, Y. Yang, G. Yen, E. Youngman, K. Yu, H. Bussey, J.D. Boeke, M. Snyder, P. Philippsen, R.W. Davis, M. Johnston, Functional profiling of the *Saccharomyces cerevisiae* genome, Nature 418 (2002) 387–391.
[35] A.G. Paulovich, C.D. Armour, L.H. Hartwell, The *Saccharomyces cerevisiae* RAD9, RAD17, RAD24 and MEC3 genes are required for tolerating irreparable, ultraviolet-induced DNA damage, Genetics 150 (1998) 75–93.
[36] L.C. Kadyk, L.H. Hartwell, Replication-dependent sister chromatid recombination in rad1 mutants of *Saccharomyces cerevisiae*, Genetics 133 (1993) 469–487.
[37] L.C. Kadyk, L.H. Hartwell, Sister chromatids are preferred over homologs as substrates for recombinational repair in *Saccharomyces cerevisiae*, Genetics 132 (1992) 387–402.
[38] C. Boone, H. Bussey, B.J. Andrews, Exploring genetic interactions and networks with yeast, Nat. Rev. Genet. 8 (2007) 437–449.
[39] M. Kai, K. Furuya, F. Paderi, A.M. Carr, T.S. Wang, Rad3-dependent phosphorylation of the checkpoint clamp regulates repair-pathway choice, Nat. Cell Biol. 9 (2007) 691–697.
[40] R.M. Ostroff, R.A. Sclafani, Cell cycle regulation of induced mutagenesis in yeast, Mutat. Res. 329 (1995) 143–152.
[41] S. Lambert, A. Watson, D.M. Sheedy, B. Martin, A.M. Carr, Gross chromosomal rearrangements and elevated recombination at an inducible site-specific replication fork barrier, Cell 121 (2005) 689–702.
[42] J.A. Tercero, J.F. Diffley, Regulation of DNA replication fork progression through damaged DNA by the Mec1/Rad53 checkpoint, Nature 412 (2001) 553–557.
[43] N.M. Al-Moghrabi, I.S. Al-Sharif, A. Aboussekhra, The *Saccharomyces cerevisiae* RAD9 cell cycle checkpoint gene is required for optimal repair of UV-induced pyrimidine dimers in both G(1) and G(2)/M phases of the cell cycle, Nucleic Acids Res. 29 (2001) 2020–2025.
[44] S. Yu, Y. Teng, N.F. Lowndes, R. Waters, RAD9, RAD24, RAD16 and RAD26 are required for the inducible nucleotide excision repair of UV-induced cyclobutane pyrimidine dimers from the transcribed and non-transcribed regions of the *Saccharomyces cerevisiae* MFA2 gene, Mutat. Res. 485 (2001) 229–236.
[45] N.M. Al-Moghrabi, I.S. Al-Sharif, A. Aboussekhra, The RAD9-dependent gene trans-activation is required for excision repair of active genes but not for repair of non-transcribed DNA, Mutat. Res. 663 (2009) 60–68.
[46] A.E. Reynolds, R.M. McCarroll, C.S. Newlon, W.L. Fangman, Time of replication of ARS elements along yeast chromosome III, Mol. Cell. Biol. 9 (1989) 4488–4494.
[47] C.J. Rivin, W.L. Fangman, Replication fork rate and origin activation during the S phase of *Saccharomyces cerevisiae*, J. Cell Biol. 85 (1980) 108–115.
[48] P.C. Hanawalt, G. Spivak, Transcription-coupled DNA repair: two decades of progress and surprises, Nat. Rev. Mol. Cell Biol. 9 (2008) 958–970.
[49] D.J. Chang, K.A. Cimprich, DNA damage tolerance: when it's OK to make mistakes, Nat. Chem. Biol. 5 (2009) 82–90.
[50] L.S. Symington, Role of RAD52 epistasis group genes in homologous recombination and double-strand break repair, Microbiol. Mol. Biol. Rev. 66 (2002) 630–670, table of contents.
[51] F. Fabre, A. Chan, W.D. Heyer, S. Gangloff, Alternate pathways involving Sgs1/Top3, Mus81/Mms4, and Srs2 prevent formation of toxic recombination intermediates from single-stranded gaps created by DNA replication, Proc. Natl. Acad. Sci. U.S.A. 99 (2002) 16887–16892.
[52] V. Gangavarapu, S. Prakash, L. Prakash, Requirement of RAD52 group genes for postreplication repair of UV-damaged DNA in *Saccharomyces cerevisiae*, Mol. Cell. Biol. 27 (2007) 7758–7764.
[53] D. Branzei, F. Vanoli, M. Foiani, SUMOylation regulates Rad18-mediated template switch, Nature 456 (2008) 915–920.
[54] C.X. Deng, BRCA1: cell cycle checkpoint, genetic instability, DNA damage response and cancer evolution, Nucleic Acids Res. 34 (2006) 1416–1426.
[55] P.C. Fong, D.S. Boss, T.A. Yap, A. Tutt, P. Wu, M. Mergui-Roelvink, P. Mortimer, H. Swaisland, A. Lau, M.J. O'Connor, A. Ashworth, J. Carmichael, S.B. Kaye, J.H. Schellens, J.S. de Bono, Inhibition of poly(ADP-ribose) polymerase in tumors from BRCA mutation carriers, N. Engl. J. Med. 361 (2009) 123–134.
[56] L.G. Ball, K. Zhang, J.A. Cobb, C. Boone, W. Xiao, The yeast shu complex couples error-free post-replication repair to homologous recombination, Mol. Microbiol. 73 (2009) 89–102.